Root and soil hydraulic traits controlling plant water status under drought

Doctoral Thesis

submitted to obtain the academic degree of Doctor of Natural Sciences

(Dr. rer. nat.)

of the Bayreuth Graduate School of Mathematical and Natural Sciences

(BayNAT)

of the University of Bayreuth

Mohanned Abdalla Ali Abdalla

from Khartoum, Sudan

Bayreuth, 2022

ii

This doctoral thesis was prepared at the Chair of Soil Physics at the University of Bayreuth from April, 2018 until January, 2022 and was supervised by Prof. Dr. Andrea Carminati.

This is a full reprint of the thesis submitted to obtain the academic degree of Doctor of Natural Sciences (Dr. rer. nat.) and approved by the Bayreuth Graduate School of Mathematical and Natural Sciences (BayNAT) of the University of Bayreuth.

Date of submission: 10.01.2022

Date of defence: 24.06.2022

Acting director: Prof. Dr. Hans Keppler

Doctoral committee:

Prof. Dr. Andrea Carminati   (reviewer)

Prof. Dr. Eva Lehndorff   (reviewer)

Prof. Dr. Johanna Pausch   (chair)

Prof. Dr. Steven Higgins

Dedication

Alhamdulillah!

I dedicate this dissertation to my parents

may Allah endow them with health and strength

Acknowledgments

I would like to express my gratitude to everyone who supported and inspired me over my PhD and had direct or indirect contribution to the presented thesis.

I owe indescribable gratitude to my supervisor Prof. Dr. Andrea Carminati. I have been privileged to join his lab and to complete under his supervision. His constant support, scientific discussions, and inspirations helped me navigate throughout the PhD journey. I would like to express my grateful thank to Dr. Mutez Ali Ahmed for his extensive support in achieving the PhD and beyond. I would like to extend my thank to Prof. Dr. Michaela Dippold for kindly joining my supervision committee.

I would like to thank all my corporation partners who contributed to improving and expanding this work. I thank Prof. Dr. Mathieu Javaux, Dr. Mohsen Zare, and Dr. Gaochao Cai for sharing their knowledge generously. I would like to thank Dr. Nimrod Schwartz, Prof. Dr. Johanna Pausch, and Prof. Dr. Scott McAdam for kindly gifting the seeds of various plant genotypes used during experimental campaigns.

My sincere thank goes to my colleagues in the Chair of Soil Physics, University of Bayreuth, and in the Department of Physics of Soils and Terrestrial Ecosystems, ETH, Zurich, for their help and pleasant working environment. Special thank goes to my office mates, Dr. Gaochao Cai and Dr. Faisal Hayat, for their friendship and memorable times. I highly acknowledge the help from Fabian Wankmüller, Anna Sauer, Asegid Akale, and Osman Mustafa (Göttingen) during the last section of this thesis. A special thank goes to Andreas Kolb for his precious technical assistance. I would like to thank Dr. Pascal Benard, Patrick Duddek, Tina Köhler, Andreas Cramer, Bahar Hosseini and Ruth Adamczewski for their great help throughout different occasions.

This work was supported by the German Academic Exchange Service (DAAD), within the funding program: Research Grants – Doctoral Programs in Germany (57381412). I benefited from joining the Graduate School of the University of Bayreuth and the corresponding qualification program.

I was fortunate to have my beloved wife Safaa, my wonderful daughters by my side throughout this journey and beyond. You deserve special gratitude that no words can express. Finally, I

am forever indebted to my parents, Nabiyha and Abdalla, and my siblings, Rasha, Abeer, Ahmed, and Amjed, for their continuous support and prayers for my success.

Mohanned Abdalla

Bayreuth, December 2021

Summary

Plants are expected to experience intense and extended periods of drought in many regions worldwide. Stomatal regulation, which governs water loss and hence plant water use, has been proposed as a key feature facilitating plant adaptation to water-limited environments. Nevertheless, the fundamental question as to what triggers stomatal closure during soil drying remains disputed.

Recent soil–plant models proposed that the loss in hydraulic conductivities is the driver of stomatal closure, stomata responding to non-linearity in the relationship between transpiration rate (E) and leaf water potential (ψ_{leaf}). However, the primary hydraulic constraint along the soil–plant system, being in the soil or an element of the plants, remains without consensus. The overall objective of my thesis was to investigate how below-ground biophysical processes impact stomatal regulation and plant water status, especially in drying soils.

This thesis comprises six chapters: chapter one introduces the state-of-the-art, summarizes the main findings, and provides an outlook. I asked the following questions: do stomata close when the $E(\psi_{\text{leaf}})$-relation becomes non-linear? And what is the primary hydraulic limitation along the soil–plant system (chapter two)? Would differences in the root system impact the relationships between stomatal conductance, E, and ψ_{leaf} during soil drying (chapter three)? What is the role of abscisic acid (ABA) in stomatal response to non-linearity (chapter four)? What is the impact of salt accumulation at the root surface on plant response to water stress (chapter five)? Do arbuscular mycorrhiza fungi (AMF) impact the gradients in water potential around roots and hence the soil–plant hydraulic conductance during soil drying (Chapter six)? To answer these questions, I combined novel experiments and a soil–plant hydraulic model to shed light on the role of below-ground processes on plant response to edaphic and atmospheric drought. The main hypotheses were: 1) stomata close at the onset of hydraulic non-linearity; 2) the loss in below-ground hydraulic conductances (namely soil, root and/or their interface) represent the primary driver of stomatal closure; 3) ABA plays a central role in plant response hydraulic non-linearity; 4) salt accumulation at the root surface limits transpiration by creating an osmotic gradient, especially as the soil dries; 5) AMF attenuate the drop in matric potential across the rhizosphere and hence enhance soil–plant hydraulic conductance under water stress.

In chapter two, I combined a novel root pressure chamber system and a soil–plant hydraulic model to investigate the primary driver of stomatal closure in tomato during soil drying. The method accurately measures the $E(\psi_{\mathrm{leaf}})$-relation in intact plants. Additionally, I have measured E and ψ_{leaf} without plant pressurization. The $E(\psi_{\mathrm{leaf}})$-relation was linear in wet soil and non-linear as the soil dried. The comparison of pressurized and unpressurized plants revealed no decline in xylem hydraulic conductance, and the primary hydraulic limitation to E occurred within root-soil continuum, which proves the hypothesis that stomata close to obviate the non-linear drop in ψ_{leaf}. Thus, I conclude that, in tomatoes, a decline in root-soil hydraulic conductance was the primary driver of stomatal closure in drying soil.

To investigate the impacts of below-ground hydraulics, namely root system, on stomatal regulation, I grafted tomato plants, having identical shoots and two contrasting roots, a short and a long one. The $E(\psi_{\mathrm{leaf}})$-relation varied between the two root systems, i.e., short-rooted plant exhibited a marked non-linearity. Stomatal closure matched the onset of hydraulic non-linearity and was significantly different between root systems. This proves there is no unique relationship between E and ψ_{leaf} and below-ground hydraulics play a pivotal role in plant response to soil drying.

The role of ABA in stomatal response to hydraulic non-linearity was explored in chapter four. I used two tomato genotypes: ABA-deficient mutant and its parental line. The latter showed linear $E(\psi_{\mathrm{leaf}})$-relation, while the mutant exhibited non-linear relation already in wet soil. This initial finding proposes ABA as a potential mechanism allowing stomata to obviate hydraulic non-linearity.

Salinity has an adverse effect on water availability. Such effects are highly dynamic, as they depend on soil moisture gradients, diffusion and convection, and are difficult to predict. Thus, in chapter five, I have demonstrated how salt accumulation at the root surface induces an osmotic stress which dictates a more negative leaf water potential in the predawn and successively throughout the daytime.

AMF symbiosis plays a positive role in plant water status under drought. In chapter six, I have elucidated that AMF enhance plant water status by increasing soil-root hydraulic conductance during soil drying. These findings together suggest root-soil interface as a crucial biological hotspot that plays a major role in controlling plant water status.

These findings disclose the tied link between stomatal regulation and below-ground hydraulics, and call for reconciling soil and root hydraulics and rhizosphere biophysical processes to fully understand and optimally predict plant behavior and adaptation to future climate change.

Zusammenfassung

Es ist zu erwarten, dass Pflanzen in Zukunft verstärkt durch Trockenperioden betroffen sind. Die Regulation der Spaltöffnungen, welche den Wasserverlust und damit die Effizienz der Wassernutzung durch Pflanzen entscheidend beeinflusst repräsentiert einen Schlüsselmechanismus zur Anpassung an durch Wasserverfügbarkeit limitierte Umweltbedingungen. Die grundlegende Frage, welche Faktoren ein Schließen der Spaltöffnungen auslöst bleibt umstritten.

Aktuelle Boden-Pflanzen Modelle begründen das Schließen der Stomata mit einer Abnahme der hydraulischen Leitfähigkeit. Spaltöffnungen reagieren demnach auf das nichtlineare Verhältnis zwischen Transpirationsrate (E) und Blattwasserpotential (ψ_{leaf}). Ungeachtet dieses Zusammenhangs bleibt ungeklärt, an welcher Stelle entlang des Fließpfades zwischen Bodenwasser und Atmosphäre die Hauptursache für den beobachteten Mechanismus zu findet ist. In dieser Arbeit galt es zu klären, inwieweit biophysikalische Prozesse des Bodens die Regulation der Spaltöffnungen und damit den Zustand des Pflanzenwassers beeinflussen. Insbesondere galt es dabei den Einfluss des trocknenden Bodens zu klären.

Diese Doktorarbeit besteht aus sechs Kapiteln. Kapitel eins beschreibt den aktuellen Stand der Wissenschaft, fasst die wichtigsten Ergebnisse dieser Arbeit zusammen und gibt einen Ausblick auf potenzielle Forschungsschwerpunkte. Im Detail stellten sich die folgenden Fragen: Wird das Schließen der Spaltöffnungen ausgelöst, sobald das Verhältnis zwischen E und ψ_{leaf} nichtlinear wird? Wo befindet sich der Auslöser oder die hydraulische Limitierung entlang des Boden-Pflanzen Systems (Kapitel zwei)? Wirken sich Unterschiede im Aufbau des Wurzelsystems auf das Verhältnis zwischen E und ψ_{leaf} in trocknenden Böden aus (Kapitel drei)? Welche Rolle spielt dabei Abscisinsäure (ABA) (Kapitel vier)? Welchen Einfluss hat die Anreicherung von Salz an der Wurzeloberfläche auf die Reaktion von Pflanzen auf Trockenstress (Kapitel fünf)? Beeinflussen arbuskuläre Mykorrhizapilze (AMF) den Gradienten im Wasserpotenzial im Boden um die Wurzeln und damit die hydraulische Leitfähigkeit zwischen Boden und Pflanzen im trocknenden Boden (Kapitel sechs)? Um diese Fragen zu beantworten, wurden neuartige Experimente mit einem hydraulischen Modell des Boden-Pflanze Kontinuums durchgeführt. Folgende Hypothesen wurden aufgestellt: 1) Stomata schließen mit dem Einsetzen nichtlinearer hydraulischer Bedingungen; 2) der Verlust

x

in hydraulischer Leitfähigkeit zwischen Boden und Wurzeloberfläche ist die Hauptursache für das Schließen der Spaltöffnungen; 3) ABA spielt eine entscheidende Rolle mit Bezug auf die Reaktion von Pflanzen auf diese nichtlinearen Bedingungen; 4) die Anreicherung von Salz an der Wurzeloberfläche, während der Boden trocknet verringert die Transpiration aufgrund des zunehmenden osmotischen Gradienten; 5) AMF verringern den Gradienten im Matrixpotential in der Rhizosphäre und verbessern damit die effektive hydraulische Leitfähigkeit des Bodens bei Trockenstress.

Im zweiten Kapitel wird mithilfe einer neuartigen Wurzeldruckkammer und einem hydraulischen Modell des Pflanze-Boden Kontinuums der Einfluss verschiedener Faktoren auf die Schließung der Spaltöffnungen anhand von Tomaten in trocknenden Böden untersucht. Mit der angewendeten Methode lässt sich E und ψ_{leaf} in intakten Pflanzen quantifizieren. Zusätzlich wurde das Verhältnis ohne Anpassung des Drucks bestimmt um den Einfluss der Methode abzuschätzen. Das Verhältnis zwischen E und ψ_{leaf} war linear in feuchtem Boden und nichtlinear in trocknendem Boden. Der Vergleich zwischen Messungen unter Druck und ohne Anpassung des Drucks zeigte keine Veränderung in der hydraulischen Leitfähigkeit des Xylems und die Hauptursache für eine hydraulische Limitierung von E trat im Wurzel-Boden Kontinuum auf. Dies bestätigt die Hypothese, dass Stomata schließen, um eine nichtlineare Abnahme des ψ_{leaf} zu vermeiden. Auf dieser Grundlage folgere ich, dass eine Abnahme in der hydraulischen Leitfähigkeit in der Rhizosphäre im Falle von Tomaten die Hauptursache für das Verschließen der Spaltöffnungen darstellt.

Um den Einfluss der Wurzeleigenschaften auf die Regulation der Stomata zu untersuchen wurden Tomaten mit gleichem Spross auf unterschiedliche Wurzelstöcke aufgepfropft. Ein kurzes und ein langes Wurzelsystem wurden dabei verglichen. Das Verhältnis zwischen E und ψ_{leaf} variierte zwischen den Wurzelsystemen, wobei das kurze Wurzelsystem ein markantes nichtlineares Verhältnis zur Folge hatte. Die Schließung der Stomata war zwischen den beiden Wurzelsystemen signifikant unterschiedlich und folgte auf das nicht-lineare Verhältnis zwischen E und ψ_{leaf}. Diese Ergebnisse beweisen, dass die Beziehung zwischen E und ψ_{leaf} nicht vorgegeben ist, sondern entscheidend durch bodenhydraulische Eigenschaften beeinflusst wird.

Die Rolle von ABA in diesem Prozess wurde in Kapitel vier untersucht. Zwei Genotypen der Tomate, einer mit einem Defizit in ABA Produktion und die nicht-defizitäre Stammlinie wurden dabei verglichen. Während die ursprüngliche Linie (nicht-defizitär) einen linearen Zusammenhang zwischen E und ψ_{leaf} zeigte, wurde für die defizitäre Mutante bereits in relativ feuchtem Boden ein nichtlinearer Zusammenhang beobachtet. Diese ersten Ergebnisse deuten auf die fundamentale Rolle von ABA zur Vermeidung des nichtlinearen Bereiches in der Abnahme des Blattwasserpotentials hin.

Ein erhöhter Salzgehalt reduziert das pflanzenverfügbare Volumen des Bodenwassers. Dieser Effekt ist dynamisch, da er sowohl durch den Gradienten in der Bodenfeuchte als auch durch Diffusion und Konvektion beeinflusst wird. Entsprechend schwer gestalteten sich vorhersagen in diesem Zusammenhang. Aufgrund dessen wurde in Kapitel fünf der Einfluss der Akkumulation von Salz an der Wurzeloberfläche auf den daraus resultierenden osmotischen Gradienten untersucht. Ein erhöhter Salzgehalt hatte ein verringertes Blattwasserpotenzial von Beginn der Morgendämmerung zur Folge.

Die Symbiose von Pflanzen und AMF hat einen positiven Effekt auf die Wasseraufnahme während Trockenheit. In Kapitel Sechs wird der Einfluss von AMF auf die hydraulische Leitfähigkeit zwischen Wurzeln und Boden untersucht. Die Ergebnisse weisen auf eine entscheidende Rolle der Grenzfläche zwischen Wurzeln und Boden zur Kontrolle des Pflanzenwassers hin.

Diese Arbeit zeigt die Abhängigkeit zwischen der Regulation der Spaltöffnungen und bodenhydraulischen Parametern. Die hydraulischen Eigenschaften von Böden und Wuzeln, sowie biophysikalische Prozesse in der Rhizosphäre bedürfen einer ganzheitlichen Betrachtung, um die Reaktion von Pflanzen zu verstehen und vorherzusagen. Von besonderer Bedeutung erscheint diese Aufgabe vor dem Hintergrund der Anpassung an ein im zügigen Wandel befindliches Klima.

List of manuscripts

1- Stomatal closure of tomato under drought is driven by an increase in soil–root hydraulic resistance.

Mohanned Abdalla, Andrea Carminati, Gaochao Cai, Mathieu Javaux, and Mutez Ali Ahmed (2021) *Plant, Cell and Environment* 44 (2), 425 – 431

https://doi.org/10.1111/pce.13939

2- Stomatal closure during soill water deficit is controlled by below-ground hydraulics.

Mohanned Abdalla, Mutez Ali Ahmed, Gaochao Cai, Fabian Wankmüller, Nimrod Schwartz, Or Litig, Mathieu Javaux, and Andrea Carminati (2021) *Annals of Botany* 129 (2), 161 – 170

https://doi.org/10.1093/aob/mcab141

3- Coupled effects of soil drying and salinity on soil–plant hydraulics.

Mohanned Abdalla, Mutez Ali Ahmed, Gaochao Cai, Mohsen Zarebanadkauki, and Andrea Carminati (2022) *Plant Physiology* 190 (2) 1228 – 1241

https://doi.org/10.1093/plphys/kiac229

4- Arbuscular mycorrhiza symbiosis enhances water status and soil–plant hydraulic conductance under drought

Mohanned Abdalla and Mutez Ali Ahmed (2021) *Frontiers in Plant Science*, 12 (722954)

https://doi.org/10.3389/fpls.2021.722954

5- The role of ABA in stomatal response to hydraulic non-linearity

<u>**Mohanned Abdalla**</u> and Mutez Ali Ahmed (2022) *In Prep*.

Table of content

List of figures

xxiii

Glossary

ABA	Abscisic acid
AMF	Arbuscular Mycorrhiza Fungi
C_w	Concentration of NaCl in the soil solution
DAI	Day after last irrigation
D_0	Self-diffusion coefficient of Na in free water
$D(\theta)$	Diffusion coefficient of Na in the soil solution
E	Transpiration rate
g_c	Canopy conductance
g_s	Stomatal conductance
K_p	Plant hydraulic conductance
K_{plant}	Plant hydraulic conductance
K_{root}	Root hydraulic conductance
K_s	Soil hydraulic conductance
K_{sat}	Soil saturated hydraulic conductivity
K_{sp}	Soil–plant hydraulic conductance
K_x	Xylem hydraulic conductance
LED	Light emitting diodes
LI	Light Intensity
MUT	Mutant
NaCl	Sodium chloride
P	Balancing pressure

PPFD	Photosynthetic photon flux density
PVC	Polyvinyl chloride
q	Water flux
RPCS	Root pressure chamber system
RH	Root hair
RMC	Reduced mycorrhiza colonization
R_{root}	Root hydraulic resistance
r	Radial distance
r_0	Root radius
r_b	Soil radius around the root
SOL	Stress onset limit
TDR	Time-domain refractometer
VPD	Vapor pressure deficit
WT	Wild-type
ψ_{leaf}	Leaf water potential
ψ_{leaf-x}	Leaf xylem water potential
$\psi_{leaf-x\ PD}$	Leaf xylem water potential at the predawn
ψ_{π}	Leaf osmotic potential
ψ_{soil}	Soil matric potential
ψ_0	Soil air entry value
ψ_{0x}	Xylem air entry value
ϕ	Soil porosity (Chapter five)
Φ	Matric flux potential

θ	Volumetric water content
τ	fitting parameter for soil unsaturated conductivity
τ_x	fitting parameter for xylem conductivity
ω	Osmotic coefficient

1   Chapter One: Synopsis

1.1   Introduction

Terrestrial vegetation is progressively exposed to episodes of edaphic and atmospheric water deficits impacting global productivity, photosynthesis and yield. These increasing drought episodes threaten future agricultural and food productions and drive widespread tree mortality (Madadgar *et al.*, 2017; Choat *et al.*, 2018; Brodribb *et al.*, 2020). Soil drying diminishes the water pool available for plants, hence, limits root water uptake and transpiration fluxes. Simultaneously, vapor pressure deficit (VPD) drives transpiration that causes continuous decrease in the leaf water potential that propagates through the xylem vessels down to the roots and the soil. A recent study, employing mathematical modeling, decoupled the impacts of VPD and soil moisture on terrestrial vegetation, and demonstrated that soil moisture dominates the dryness stress on ecosystem production globally (Liu *et al.*, 2020). Although transpiration dominates terrestrial water fluxes (Jasechko et al., 2013), and climate change is expected to influence global transpiration (López et al., 2021), the mechanistic understanding of how edaphic water deficit impacts leaf water potential, stomatal conductance, and transpiration rate remains obscure. Filling this knowledge gap is essential to improve the current understanding and future predictions of plant responses to environmental changes (Bartlett *et al.*, 2016; Martin-StPaul *et al.*, 2017; Buckley, 2019).

Stomata, microscopic bio-valves formed by guard cells, are present in aerial surfaces of most land plants 400 million years ago (Edwards *et al.*, 1998; Peterson *et al.*, 2010). Stomata play a pivotal role in regulating the exchange of carbon and water between the atmosphere and terrestrial vegetation (Hetherington and Woodward, 2003; Wolz *et al.*, 2017; Buckley, 2019; Deans *et al.*, 2020). Stomatal regulation makes it possible for plants to promptly respond to intrinsic and extrinsic environments to sustain plant water status, and thus adaptability to water scarcity in the soil and the atmosphere. The fundamental understanding of how stomata function under stress conditions will facilitate an improved prediction of plant behavior under stress conditions. Furthermore, understanding stomatal behavior under water deficit conditions will facilitate predicting plant behavior under other co-occurring stresses, e.g., salinity, and interactions with plant microbiome, e.g., arbuscular mycorrhiza fungi. Gaining this knowledge

is instrumental for future breeding programs and improvements of crops that are resilient in the face of climate change and capable of supplying the increasing food demand.

Various concepts have been proposed to understand and predict stomatal behavior. Carbon optimization theory, a pioneering concept predicting stomatal responses, posits stomata maximize carbon gain for a penalty of water loss (Cowan and Farquhar, 1977; Wang *et al.*, 2020). Another approach suggest stomatal regulation to respond to decline in leaf water potential in two ways, hydro-active and hydro-passive mechanisms (Brodribb and McAdam, 2011; Buckley, 2019). Following the hydro-passive hypothesis, stomata close in response to declining leaf water potential (Buckley *et al.*, 2003). While the hydro-active path postulated that stomatal regulation is actively controlled by the abscisic acid (ABA) under stress conditions (Brodribb and McAdam, 2011; Merilo *et al.*, 2018; Buckley, 2019). Combining chemical and hydraulic signal was suggested to fully understand stomatal regulation (Buckley, 2019). The proposition of these various hypotheses indicates the challenges on understanding how stomata detect and react to their intrinsic and extrinsic environment while maintaining plant water status (Brodribb and McAdam, 2011; Buckley, 2019).

Even though the underpinning mechanisms controlling stomatal regulation at the mechanistic and molecular levels are yet to be fully revealed (Buckley, 2005, 2019), recent studies have demonstrated that we still could anticipate stomatal response to soil and atmospheric drought from its emergent hydraulic properties (Sperry *et al.*, 2016). A hydraulic framework was proposed to predict stomatal closure based on a 'supply-demand' function to understand the physical constraints on transpiration (Sperry and Love, 2015). In this concept, stomatal regulation obviates excessive (non-linear) drop in leaf water potential by responding to disproportionality between transpiration rate and leaf water potential (Sperry and Love, 2015). The non-linearity and the trigger of stomatal closure have been presumed to be coordinated with xylem vulnerability (Sperry and Love, 2015; Anderegg *et al.*, 2017). This hydraulic-based framework has been utilized in other models. For instance, Stomata optimization models were shown to exhibit improved predictions skills when based on hydraulics (Wolf *et al.*, 2016; Eller *et al.*, 2020; Wang *et al.*, 2020). The primary hydraulic limitation among soil–plant continuum remains controversial. Modeling approaches has been used to identify the greater hydraulic limitation along the soil-plant-atmosphere continuum. For instance, Sperry *et al.*

(2002) argued that either xylem or rhizosphere are primary hydraulic limitations to transpiration. Afterward, Sperry and Love (2015) suggested xylem as the main hydraulic constraint to transpiration, neglecting below-ground components. Carminati and Javaux (2020) proposed declining soil hydraulic conductance as the driver of stomatal closure. The authors, utilizing meta-analysis, validated their concept among different plant species and soil types (Carminati and Javaux, 2020). Although there is no consensus regarding the primary hydraulic limitation, either above- or below-ground, both models argue that stomata respond to the hydraulic non-linearity between transpiration rate and leaf water potential (Sperry and Love, 2015; Carminati and Javaux, 2020). These fascinating conceptual models are an excellent reminder that despite mathematical models are approximation to reality, they are essentially valuable to interpret and predict experimental outcomes and, more still, to direct future research (Blatt, 2021).

Experimental studies endeavored to understand the primary hydraulic limitation triggering stomatal closure. Numerous studies have associated stomatal closure to xylem capability to transport water under tension (e.g. Scoffoni *et al.*, 2014; Brodribb *et al.*, 2016, 2017). Occurrence of other hydraulic limitations along the soil–plant continuum, apart from xylem vulnerability, has been experimentally investigated. For instance, Corso *et al.* (2020) investigated the loss in hydraulic conductance in the vascular system during plant dehydration, and concluded that neither xylem cavitation nor a decrease in leaf conductance drives stomatal closure (Corso *et al.*, 2020). The authors showed that, in wheat, stomata close before embolism propagation (Corso *et al.*, 2020). Similarly, Lamarque *et al.* (2020) demonstrated that stomatal closure occur well before xylem cavitation in tomato. Recent studies applied novel methods to evaluate reduction in below-ground hydraulics *in situ*. Rodriguez-Dominguez and Brodribb (2020) used rehydration kinetic technique in olive trees and showed that root-soil interface represents the primary hydraulic resistance to water flow in water-stressed plants. The authors observed a sharp decline in root hydraulic conductance (including soil-root interface) happening during the same range of water potentials as stomatal closure, which was far higher above those needed to initiate xylem cavitation (Rodriguez-Dominguez and Brodribb, 2020). The rehydration technique was recently applied to woody and herbaceous species (Bourbia *et al.*, 2021). The authors showed that stomata close concomitantly with the decline in root hydraulic conductivity in both herbaceous and woody species (Bourbia *et al.*, 2021).

Collectively, these experimental studies have presented below-ground hydraulic conductance as the potential primary hydraulic constraint to transpiration. This conclusion implicitly proposes reducing below-ground hydraulics, rather than xylem, as a potential source in initiating hydraulic non-linearity between transpiration rate and leaf water potential. Although the linkage between declining below-ground hydraulics and the onset of hydraulic non-linearity is logical, it remains, as yet, without experimental support. Because there is a lack of systematic experimentations that directly measure the incidence of hydraulic non-linearity and stomatal closure. Furthermore, the influence of different below-ground hydraulic traits (e.g. root length) on the onset of hydraulic non-linearity and stomatal closure, to the best of my knowledge, has never been investigated so far.

The hydraulic framework suggests stomata close at the onset of hydraulic non-linearity. However, this concept does not provide what helps stomata optimally respond to non-linearity. A potential mechanism might be through a chemical signal that mediates stomatal closure. Mounting evidence established the inverse relation between ABA and stomatal conductance (Davies and Zhang, 1991; Schurr *et al.*, 1992; Dodd, 2005; Brodribb and McAdam, 2011; McAdam and Brodribb, 2018). Earlier studies suggested a cross-talk between root and shoot under stress conditions (Dodd, 2005). Roots were suggested to produce ABA that is transferred to the shoot and induces stomatal closure (Davies and Zhang, 1991; Dodd, 2005). However, root-sourced ABA has been shown to play no role in stomatal closure in tomato (see the seminal work by Holbrook *et al.* (2002)). Recent studies demonstrated that ABA is *de novo* synthesized in leaf mesophyll and initiates stomatal closure (McAdam and Brodribb, 2018). Although these studies together indicate a little consensus regarding the location of ABA production, they do emphasize ABA essentiality to guard cells movement. The fact that ABA initiates stomatal closure suggests a potential correlation between ABA abundance/synthesis and the onset of hydraulic non-linearity (Wankmüller and Carminati, 2021). Thus the urgent question is: what is the role of ABA in stomatal response to the hydraulic non-linearity?

The relation between transpiration rate and leaf water potential might be affected by factors impacting root-soil interface. As transpiration demand drives water stream from soil to root, it is worth noting that the water in the soil is never chemically pure. The liquid phase in the soil encompasses considerable amounts of solutes, Na^+ and Cl^- in saline soils, for instance. High

salt concentrations in the soil impede root water uptake and reduce the maximum transpiration rate. Indeed, soil salinity is a considerable bottleneck limiting crop growth and productivity, which might coincide with drought conditions, especially in arid and semi-arid zones (Munns, 2002; Fricke *et al.*, 2004; Munns and Tester, 2008; Chaves *et al.*, 2009). High salt concentration in soil limits plants' ability to take up water (Munns and Tester, 2008), similarly to the impact of soil drying (Munns, 2002). Numerous studies showed that salinity triggers stomatal closure, subsequently impacting photosynthesis, plant growth and development (Munns, 2002; Fricke *et al.*, 2004; Munns and Tester, 2008; Chaves *et al.*, 2009). Salt accumulation in the soil hinders plant's capabilities in two actions: reducing water availability and inducing toxic effects of sodium and chlorine ions (Munns and Tester, 2008; van Zelm *et al.*, 2020; Zhang *et al.*, 2021). Munns *et al.* (2020) suggested that, in saline soils, plants must eliminate 98% of both Cl^- and Na^+ while taking up water to evade high ion concentrations inside plant tissues (Munns and Gilliham, 2015; Munns *et al.*, 2020). Consequently, salts might build up around roots and possibly induce osmotic stress at the root-soil interface (Stirzaker and Passioura, 1996). The follow-up question is how salt accumulation at the root-soil interface impacts plant hydraulics during soil drying?

Another open question is regarding plant microbiome impacting root-soil hydraulic conductance during soil drying. Root-soil interface is a biological hot spot and is occupied by plant microbiome, which may impact plant water status, possibly by influencing the hydraulics of the rhizosphere (Bitterlich *et al.*, 2018a; Benard *et al.*, 2019; Trivedi *et al.*, 2020; Pauwels *et al.*, 2020). For instance, Arbuscular mycorrhiza fungi (AMF) symbiosis, which occurs naturally between fungi and most plant species, is documented to play a positive role in plant water relations, especially under water stress conditions (Augé, 2001; Augé *et al.*, 2015; Ouledali *et al.*, 2018). Earlier studies showed that AMF facilitates higher transpiration rate in dry soils in tomato (Bitterlich *et al.*, 2018b). Similarly, AMF was reported to enhance tomato performance under water stress and improve plant biomass and water use efficiency (Chitarra *et al.*, 2016). In maize, Quiroga *et al.*, (2019) demonstrated that AMF enable higher stomatal conductance during soil drying. Moreover, AMF was suggested to increase root hydraulic conductivity (Aroca *et al.*, 2007; Quiroga *et al.*, 2019) and amend soil hydraulic properties (Bitterlich *et al.*, 2018a; Pauwels *et al.*, 2020). However, the impact of AMF on soil–plant hydraulic conductance, especially during soil drying, remains obscure. This would be crucial

to improving our current understanding of plant responses to drought (Carminati *et al.*, 2020; Hayat *et al.*, 2020; Rodriguez-Dominguez and Brodribb, 2020). Therefore, investigating the influences of AMF on soil–plant hydraulic conductance during soil drying is a research priority.

1.2 Objectives and thesis outlines

The ultimate objective of this thesis was to utilize a hydraulic framework to mechanistically understand how soil drying affects plant response to drought. In other words, understanding the mechanisms by which declining soil water potential impact stomatal conductance and soil–plant hydraulics. And to define what are the hydraulic limitations to transpiration. Additionally, understanding the coupled effects of other co-occurring factors impacting root-soil interface.

Do stomata close at the point when the hydraulic conductance starts to decrease? The hypothesis is that stomata respond to a decline in soil–plant hydraulic conductance and hence close at the onset of hydraulic non-linearity. Testing this hypothesis requires a method that not only measures transpiration rate and leaf water potential but also explores the non-linear part of the relation. This is achievable by the root pressure chamber apparatus (Passioura 1980; Cai *et al.*, 2020). By pressurizing the soil and thus maintaining the leaf turgid, plant explores the non-linear part of the relationship. Furthermore, pressurization prevents cavitation (Passioura and Munns, 1984). Yet, below-ground conductances are not affected by pressurization, including the potential shrinkage of the root cortex and the loss of contact with the soil. Therefore, this method accurately evaluates the changes in below-ground hydraulic conductance occurring at a given transpiration rate and a soil water status (Passioura, 1980; Carminati *et al.*, 2017). In parallel, I measured the decrease of transpiration rate and leaf water potential in unpressurized plants. By comparing leaf water potential in pressurized and unpressurized plants at the same transpiration rate and a soil water status, we obtain information on the decrease in shoot hydraulic conductance and xylem cavitation (both prevented in pressurized plants). Additionally, by comparing pressurized and unpressurized experiments, we tested the hypothesis that stomata close at the onset of hydraulic limitation. I applied this method to tomato plants growing in a sandy-loam soil. The data were interpreted using the conceptual and numerical soil–plant hydraulic model of Carminati and Javaux (2020).

Do differences in below-ground traits (i.e. contrasting root system) impact the relation between transpiration rate and leaf water potential during soil drying? At a given transpiration rate, water fluxes at root surface will be affected by the root length. I expect that short root system would require a larger water flow per root surface, and thus larger gradients in soil matric potential. Therefore, plants with shorter root system should exhibit a more marked hydraulic non-linearity and should close stomata at less negative leaf water potential.

Does ABA make it possible for plant to avoid hydraulic non-linearity? Answering this question requires measuring transpiration rate and leaf water potential in ABA-deficient mutant and its wild-type counterpart using the above-mentioned method. The hypothesis is that ABA-deficient mutant might not respond to non-linearity and show limited stomatal regulation, which would require higher water fluxes at the root surface, causing a steep drop in matric potential in the vicinity around the root. This in turn would entail a more negative water potential in leaves of ABA-deficient plants, and consequently, incidence of the non-linearity, which might possibly occur in a combination of wet soil conditions and high transpiration rates.

Investigating these fundamental question highlights the significant importance of soil–plant hydraulic conductance and how it may be affected by other factors. Salinity might cause an accumulation of salts at root surface and impact root water uptake. To test this hypothesis, I have investigated the coupled effects of salinity and soil drying on soil–plant hydraulics using the similar method. Additionally, AMF was proposed to enhance soil-root contact and improve soil-root hydraulic conductance. I hypothesize that AMF limit the drop in matric potential across the rhizosphere and hence enhance soil–plant hydraulic conductance under edaphic water stress.

The specific objectives were:

- To investigate whether stomata close at the onset of hydraulic non-linearity and to identify the main hydraulic limitation, along the soil–plant continuum, that limits transpiration (**Chapter Two**).
- To investigate whether differences in below-ground traits (i.e., contrasting root system) impact the $E(\psi_{leaf})$-relation and the onset of hydraulic non-linearity during soil drying (**Chapter Three**).

- To assess the impacts of root hydraulic capacitance on the onset of hydraulic non-linearity. Further, to evaluate the differences in root water contents vs. differences in soil water content on the onset of non-linearity (**Chapter Three**).
- To investigate the potential role of the phytohormone abscisic acid on stomatal response to hydraulic non-linearity (**Chapter Four**).
- To explain how salinity impedes root water uptake and the consequences on stomatal regulation and soil–plant hydraulics, particularly under water stress conditions, implementing hydraulic framework. Furthermore, whether salinity generates additional below-ground resistance to water fluxes, namely in the rhizosphere, impacting stomatal regulation (**Chapter Five**).
- To quantify the osmotic stress at the root surface under soil drying and salinity conditions (**Chapter Five**).
- To elucidate the role of AMF on below-ground hydraulic conductance and whether AMF attenuate the drop in matric potential around roots hence sustaining an improving plant water status (**Chapter Six**).

The thesis encompasses six chapters. The first chapter is an extended summary of the work that had been done. The following chapters represent research articles, three are published, and two are undergoing peer-review. I have added three additional abstracts of manuscripts where I have co-authored and they are intimately linked to this doctoral work.

1.3   Materials and methods

1.3.1   Plant material

Various tomato genotypes were used during the experimental campaigns. *Solanum lycopersicum* L. was used to investigate what triggers stomatal closure during soil drying, while its wild relatives, i.e., *Lycopersicon hirsutum* and a hybrid of both *L. hirsutum* and *L. pimpinellifolium* were used as rootstocks to investigate how differences in below-ground hydraulics will impact the onset of hydraulic non-linearity and stomatal closure. Additionally, *L. hirsutum* was used as rootstock to study the coupled effects of salinity and soil drying on soil–plant hydraulics (Chapter five), where I treated half of the plant population with 100 mM NaCl before the drying cycle. The tomato variety *M82* was used as a scion in the second and

third studies to have identical shoots growing onto different root systems. The tomato variety *76R* and its reduced mycorrhiza colonization (RMC) mutant were used for investigating the influences of AMF on plant water status and soil–plant hydraulic conductance during soil drying. The tomato variety *sitiens* and its parent line *Reinlands ruhm* were used for studying the interplay between ABA and soil–plant hydraulics. Grafting technique was used in the second and third studies to combine the desired root and shoot traits.

Seeds were sown in polyvinyl chloride (PVC) columns with 30 cm in height and 10 cm in diameter. The columns had five holes with a diameter of 5 mm on the side to facilitate soil moisture content measurements. For plant pressurization experiments, the PVC columns were topped (using a silicon rubber glue; Teroson, Henkeln, Germany) with a 0.8-cm-thick aluminum plate that had a centered-hole of 1.4 cm in diameter (Supplementary Data Figure S1). The plants were grown in climate-controlled chamber under ample water conditions. Measurements took place during drying cycles, where irrigation was withheld and parameters were collected.

1.3.2 Transpiration and leaf xylem water pressure measurements

I used a root pressure chamber system (RPCS; Figure 1.1) to measure transpiration rate and leaf xylem water potential simultaneously within an intact plant (Passioura, 1980; Cai *et al.*, 2020a). The assembly and calibration of RPCS was recently described in Cai *et al.* (2020b), see also figure 1.1. Succinctly, RPCS is composed of a pressure chamber topped with a cuvette and a control unit. Four groups of light-emitting diodes (LED) were vertically attached to the cuvette to provide photosynthetic photon flux density (PPFD), which ranged from 0 to 1000 μmol m^{-2} s^{-1}. Transpiration rate was increased by amplifying PPFD, and the latter was measured via a fixed radiometric sensor (Gamma Scientific, San Diego, USA). A constant airflow passed through the cuvette (8.25 L min^{-1}) and a fan was used to stir the air inside. Combined temperature-humidity sensors (Galltec-Mela, Bondorf, Germany) continuously measured the temperature and the relative humidity of the inward and the outward air. Transpiration rate was obtained by multiplying the airflow by the difference between the outward and the inward humidity.
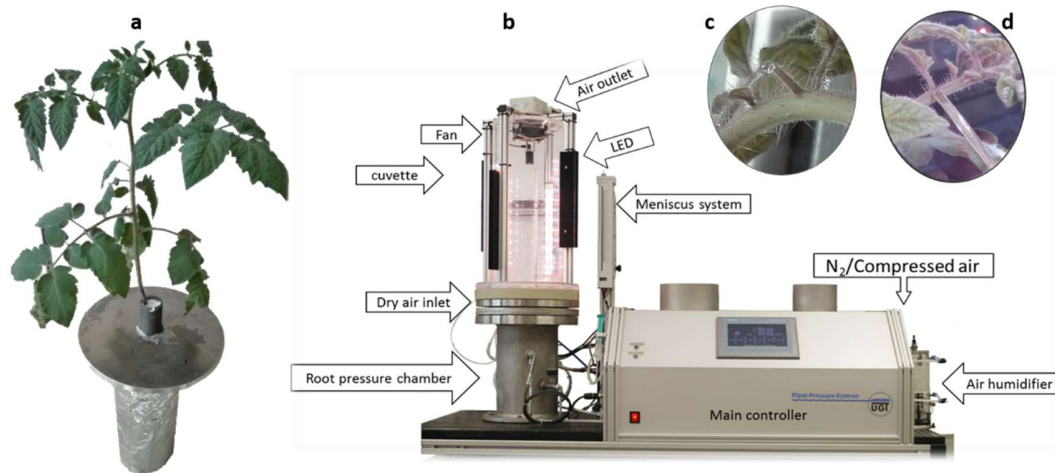
Figure 1.1 *Root pressure chamber system*

a) Tomato plant prepared for pressurization. b) Root pressure chamber system components. c) Droplet emerging from leaf cut when applying balancing pressure. d) Leaf cut connected to meniscus system with a capillary tube.

Additionally, transpiration and leaf water potential were measured without plant pressurization. Transpiration rate was measured gravimetrically using wireless balances that automatically record the changes in plant weight. Transpiration rate was obtained by calculating the difference in weight over time (Chapter five). Leaf water potential of unpressurized plant was measured using a leaf pressure chamber (Soil Moisture Equipment Corp., Santa Barbara, Ca., USA) as described in Scholander *et al.* (1965).

1.3.3 Soil hydraulic properties

The hydraulic properties of the soils used in these studies were measured via the evaporative method implemented in the Hyprop (Meter Group, Munich, Germany). Soil samples were packed into a Hyprop sample holder (area of 50 cm^2 and height of 5 cm) at the same bulk density as the one achieved in the cylinders used for plant growth. The samples were let dry from the top via evaporation, and the changes in soil water content, matric potential at two depths (-1.25 and -3.75 cm) were recorded over time. Water retention curves and unsaturated hydraulic conductivity curves were parameterized according to the PDI (Peter-Durner-Iden) model (Peters *et al.*, 2015). The parameters were estimated by fitting the obtained measurements and solving the Richards equation.

1.3.4 Soil–plant hydraulic model

I used the soil–plant hydraulic model of Carminati and Javaux (2020) to reproduce and interpret the measurements. The model simulates water flow in the soil–plant continuum. The series of resistances across the bulk soil, across soil–root interface, and through the root to the leaf xylem were considered in the model. A detailed description of the model was presented in Carminati and Javaux (2020), as well as in chapters three and four. Briefly, the model calculates the gradient in water potential through the soil and along the plant till the leaf. Soil water flow is simulated assuming a radial geometry and a steady-state root water uptake into a fraction of the total root length. The water flow in the plant is calculated assuming a proportionality between the plant hydraulic conductance and the difference in water potential between the root-soil interface and the leaf. Xylem cavitation was considered by allowing plant hydraulic conductance to drop according to a power law at a given xylem water potential (which is the point at which the xylem starts to cavitate). Plant hydraulic conductance is given by the harmonic mean of the root hydraulic conductance and the xylem conductance.

The onset of hydraulic limitation (stress onset limit; SOL) was defined as the point at which the slope of the relation reaches 70 % of its maximum value at a given soil water potential. Note that the value of 70 % is somehow arbitrary. I used it because it indicates a significant change of the conductance. According to Wankmüller and Carminati (2021), SOL gives a similar shape within a range of 50 %, (i.e., between 75 % and 25 %), although SOL was slightly shifted. To reproduce the measurements, I inversely modeled the data by varying plant hydraulic conductance and the root length that is active in water uptake.

The assumption regarding steady-state water flow was examined in Chapter three by including root hydraulic capacitance into the model. Thus, this made it possible to investigate the influence of root hydraulic capacitance on the onset of hydraulic non-linearity (Chapter three).

The soil–plant hydraulic model was modified to include solute transport processes. Hence, the model simulated the effects of salt accumulation at the root surface and the dynamics of soil water content within the rhizosphere. The model simulated NaCl transport and concentration in the soil solution to include the effects of the osmotic potential on leaf xylem water potential (Chapter four).

1.4 Summary of main outcomes

1.4.1 What trigger stomatal closure during soil drying (chapter two)?

The main objectives of chapter two were (1) to define the primary hydraulic limitation to transpiration and (2) to investigate whether stomata close at the onset of hydraulic non-linearity. The relation between transpiration rate and leaf water potential was linear in wet soil and non-linear as soil progressively dried (Figure 1.2). The slope of the relation, depicting soil–plant hydraulic conductance, was nearly constant in wet soil and decreased as soil dried. Maximum transpiration was measured in unpressurized plants, and interestingly matched the onset of hydraulic non-linearity (Figure 1.2).
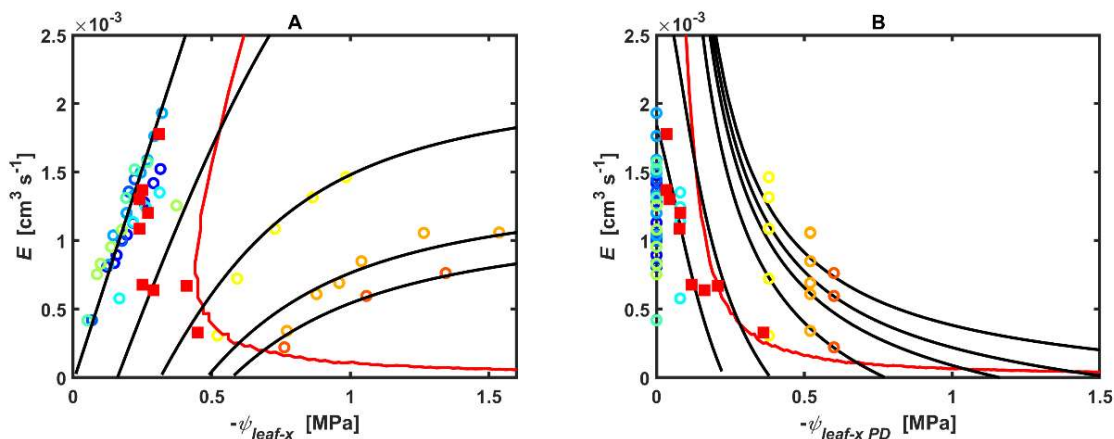
Figure 1.2 *Relation between A) leaf xylem water potential (ψ_{leaf-x}) and transpiration (E) and B) predawn leaf xylem water potential ($\psi_{leaf-x\ PD}$) and E, for different soil water contents (θ; cm³ cm⁻³). The measurements (open symbols) were well reproduced by the model (solid lines). Stomatal closure of unpressurized plants (red squares) matched the onset of non-linearity (SOL; red line) from both leaf view (A) and soil view (B).*

Leaf xylem water potential in pressurized and unpressurized plants was similar under the same soil water content and transpiration rate, with values close to the 1:1 line ($r^2 = 0.7$) (Figure 1.3). This indicates that the plant hydraulic conductance was not altered by plant pressurization. Thus, there was no significant decrease in the conductivities of shoot and xylem vessels during soil drying. Thus, the main hydraulic limitation was below-ground (chapter two).

Soil–plant hydraulic model reproduced the measurements and predicted stomatal closure based on disproportionality between transpiration rate and leaf water potential. These results confirm that, during soil drying, stomata respond to decrease in soil–plant hydraulic conductance and hence close at the onset of hydraulic non-linearity. In summary, stomata closure obviates non-linear decline in leaf water potential caused by the decrease in soil-root hydraulic conductance.
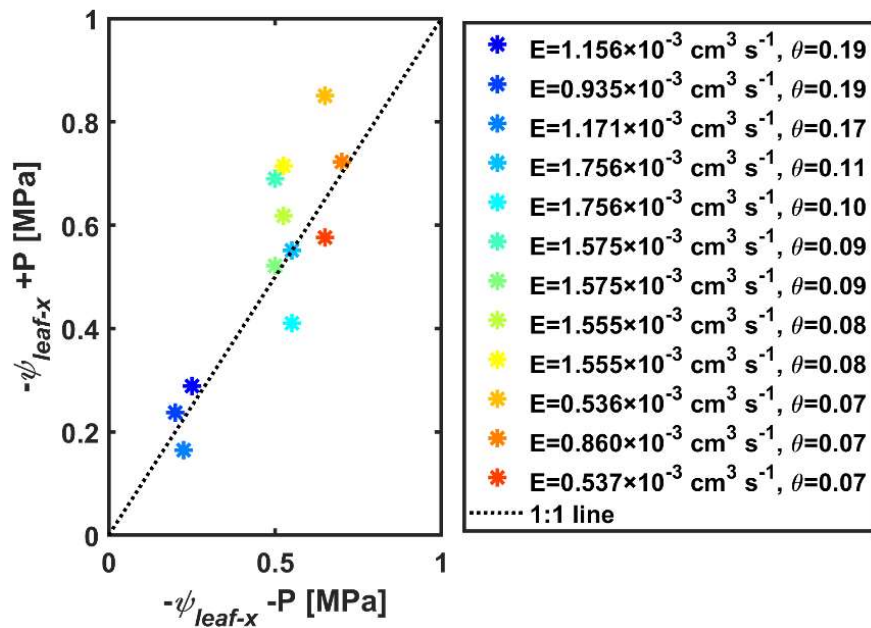
Figure 1.3 *Comparison of leaf xylem water potential (ψ_{leaf-x}) in pressurized (+P) and unpressurized (-P) plants at the same soil water content (θ; cm^3 cm^{-3}) and transpiration rate (E; cm^2 s^{-1}). $r^2 = 0.7$.*

1.4.2 Below-ground hydraulics control stomatal closure

The main objective of chapter three was to investigate whether differences in below-ground traits (i.e., contrasting root system) impact the $E(\psi_{leaf})$-relation and the onset of hydraulic non-linearity during soil drying. Tomato plants were grafted on two contrasting root systems to evaluate the impacts of different below-ground hydraulics on stomatal regulation during soil drying. For the short root system, maintaining similar transpiration rate would require a larger water flow per root surface, and thus larger gradients in soil matric potential compare to the long root. The length of the two root systems differed by a factor of 3 (*p-value* < 0.05), whereas root diameter and leaf area were similar (*p-value* > 0.05).

The relationship between transpiration rates and leaf xylem water potential varied between the two root systems (Figure 1.4). The long root system sustained higher transpiration rate during soil drying, while a more marked non-linearity in the relation appeared in the short root system at relatively high leaf xylem water potential and soil water content. Longer roots ensured the linearity of the relation for a broader range of transpiration rate and soil water content.
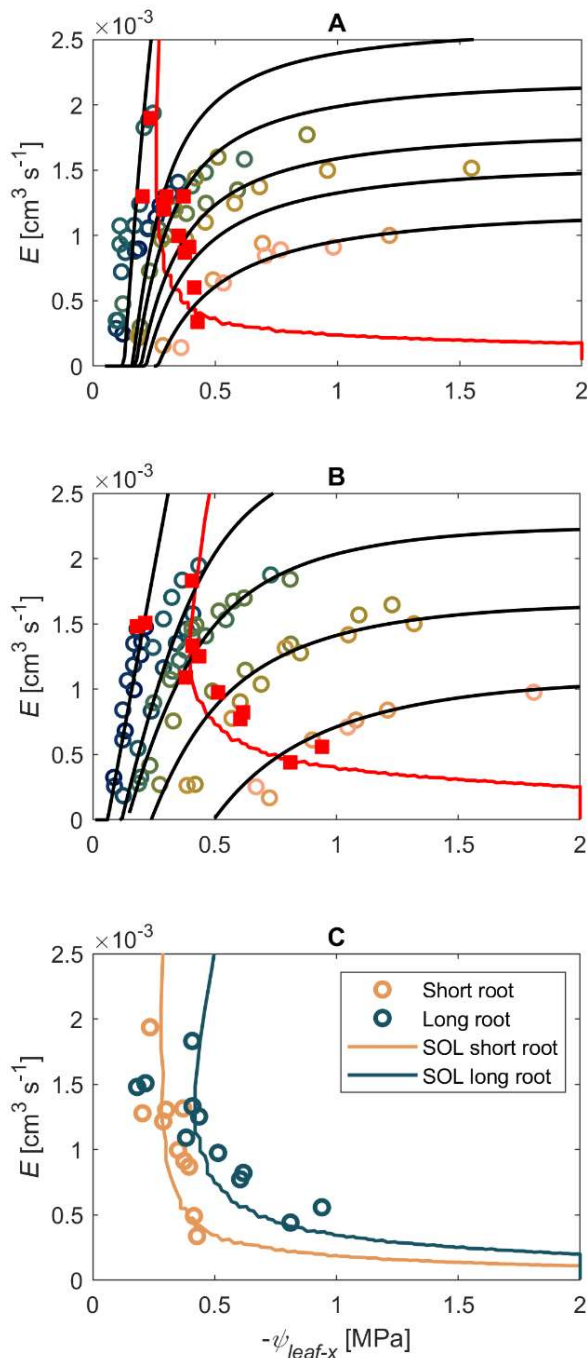
Figure 1.4 *Relation between transpiration rate and leaf xylem water potential for tomato grafted onto short (**A**) and long (**B**) root systems. The measurements (open symbols) were well reproduced by the model (black lines) at different soil water contents (different colors). The red squares are the measured transpiration rates during soil drying in unpressurized plants, which matched the onset of non-linearity (SOL; red line) for both roots (short root system, $r^2 = 0.74$; long root system, $r^2 = 0.82$, respectively).* *C) The reduction in transpiration of long and short rooted plants is significantly different (p-value < 0.001).*

The onset of hydraulic non-linearity (SOL) matched the transpiration rate of unpressurized plants of both roots. This supports the earlier hypothesis that stomata close when the relation between transpiration rate and leaf water potential becomes non-linear. The measured relation

between transpiration rate and leaf xylem water potential as well as the SOL of the long and short root systems were discrete. Analysis of covariance shows that stomatal closure was significantly different between the two root systems without pressurization (*p-value* < 0.001). Plants with the short root system reached 50 % transpiration at ψ_{leaf-x} = -0.3 MPa compared to ψ_{leaf-x} = -0.5 MPa with the long root system.

The measurements show that a decrease in root length induces an earlier non-linearity in the soil–plant hydraulic conductance and triggers an earlier stomatal closure. The relation between stomatal conductance and leaf water potential is affected by root length and below-ground hydraulics, particularly soil hydraulic conductance. This finding has important implications for understanding and predicting the response of transpiration to drought.

1.4.3   The role of ABA in stomatal response to hydraulic non-linearity

In chapter two and three, the results showed that tomato exhibit linear relation between transpiration rate and leaf water potential in wet soils and non-linear only under dry soils. Furthermore, we proved that stomata close at the onset of the hydraulic non-linearity. The mechanism that allows stomata to accomplish such function remains unknown. Thus, I investigated the role of ABA in the onset of hydraulic non-linearity using ABA-deficient mutant and its parental line. The relation between transpiration rate and leaf water potential in the wild type was linear (Figure 1.5). However, ABA-deficient mutant exhibited non-linearity in wet soil, where leaf water potential abruptly declined in response to a tiny increment in transpiration rate (Figure 1.5). This result supports the hypothesis that ABA facilitated earlier stomatal closure that reduced transpiration rates allowing a proportional decline in leaf water potential, as observed in wild type (Figure 1.5). Furthermore, ABA-deficient mutant showed higher transpiration rates, which required higher water fluxes at the root surface, causing a steep drop of matric potential in the vicinity around the root and, consequently, more negative leaf water potential.
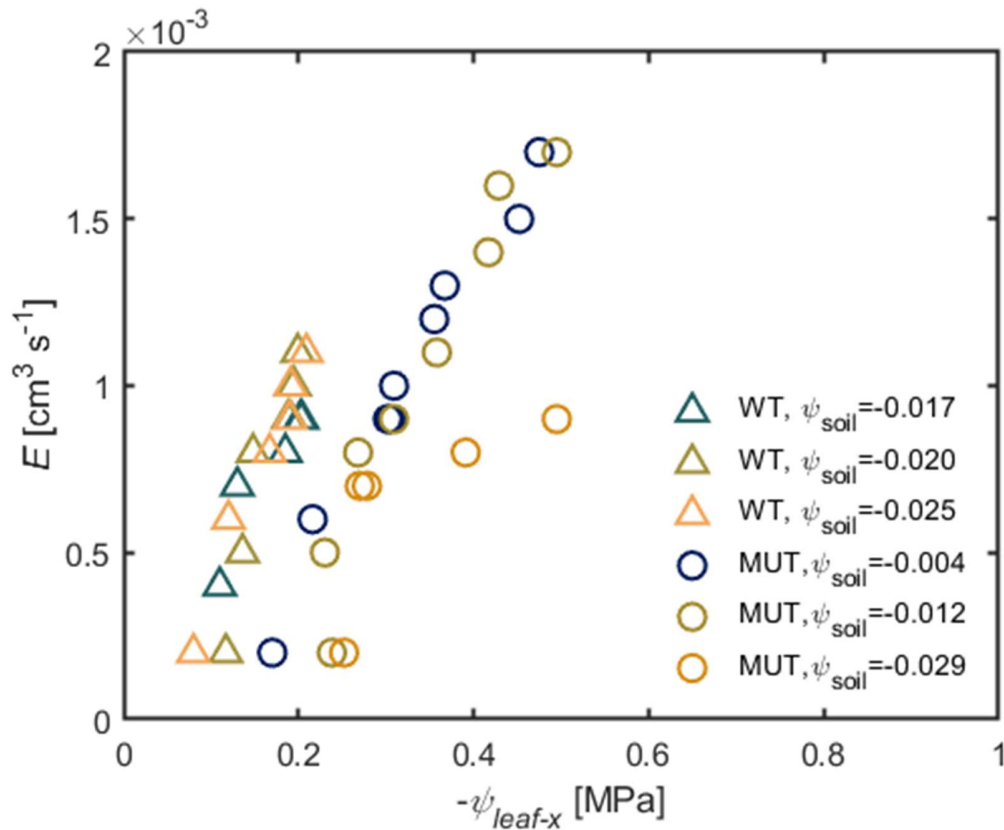
Figure 1.5 *Relation between transpiration rate (E) and leaf xylem water potential ($\psi_{leaf\text{-}x}$) in wet soil conditions (soil water potential: ψ_{soil} [MPa]). Wild type (WT; triangles) exhibited linear relation between E and $\psi_{leaf\text{-}x}$, while ABA-deficient mutant (MUT; open symbols) shows non-linear relation, even in wet soils.*

1.4.4 Coupled effects of soil drying and salinity on soil–plant hydraulics

Here I used the non-invasive root pressure chamber system to evaluate the consequences of salt accumulation at root surface on the relation between transpiration rate and leaf xylem water potential during soil drying. I used the tomato genotypes described above. Soil–plant hydraulic model was modified to include the effect of salt accumulation at the root surface and dynamic soil water content within the rhizosphere.

NaCl treatment (100 mM NaCl) influenced the relation between transpiration rate and leaf xylem water potential during soil drying. In wet conditions, leaf xylem water potential in controlled plants decreased linearly with increasing transpiration rate, while NaCl-treated

16

plants showed non-linearity under relatively wet soil conditions. In dry soils, non-linearity emerged in both treatments and it was more marked under saline conditions (Figure 6, A – B). The soil–plant hydraulic model reproduced the relation between transpiration rate and leaf xylem water potential during soil drying with and without NaCl treatments (Figure 6, A – B).
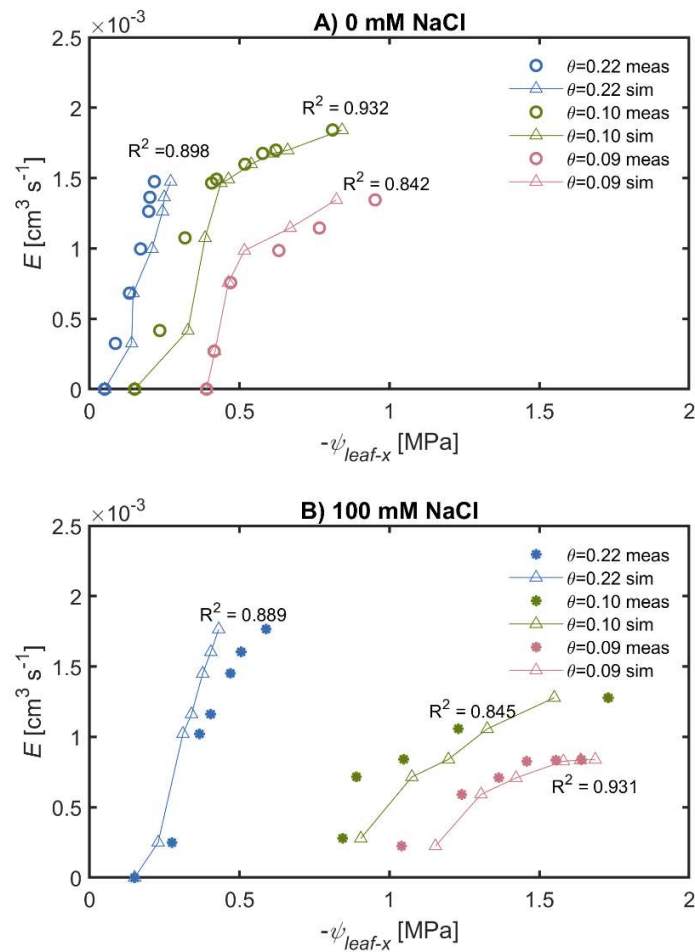
Figure 1.6 *Comparison of transpiration rate (E) and leaf xylem water potential (ψ_{leaf-x}) between non-saline and saline conditions. The relationship between E and ψ_{leaf-x} was reproduced by the soil-plant hydraulic model for **A)** non-saline and **B)** saline-treated plants during soil drying. Water stress level was represented at three soil water contents (θ = 0.22, 0.10 and 0.09 cm³ cm⁻³) for both non-saline and saline-treated plants (meas: measured; sim: simulated).*

The modeling results showed that salt treatment induced a rapid decline in leaf xylem water potential compared to control (Figure 1.7, A – B). The decline in leaf xylem water potential was accelerated during soil drying. The modeling results showed that, in dry and saline conditions, the salt concentration at root surface increased by a factor of three within one day of measurements (Figure 1.7, C and D), which was less evident in controlled conditions (Figure 1.7, C). These results revealed that salts have accumulated at the root surface under dry and saline soil conditions. The decline in leaf xylem water potential temporally followed the accumulation of NaCl at the root surface, particularly with salt treatment (Figure 1.7, A – D).

Osmotic potential (ψ_π) around roots was lower (more negative) after NaCl treatment (Figure 1.8). The decline in ψ_π was more pronounced near the root surface after several hours of transpiration (Figure 1.8, A – D). In wet soils, although the decrease of ψ_π was negligible in controlled plants, it declined to -0.24 MPa in salinity conditions (Figure 1.8, A and B). In dry soils, ψ_π at the root surface was -0.2 MPa in controlled plants and dropped to -0.8 MPa after salt treatment (Figure 1.8, E – F).

The decreases in water potentials across the soil-plant continuum were estimated from modeling the experimental results and are shown at the maximum transpiration rates for three exemplary soil water contents. In wet conditions (soil water content = 0.22), the decrease of the potential in non-saline treatment occurred mainly in the plant due to the resistance to water flow (-0.17 MPa). Under saline conditions, the decrease in the osmotic potential was important (-0.24 MPa). In dry soil conditions (soil water content = 0.10, 0.09), water potential dissipation in the bulk soil and the rhizosphere were greater than the loss inside the plant. The loss in osmotic potential at the root surface was the preeminent component of the total loss under saline-dry conditions (-0.83 MPa).
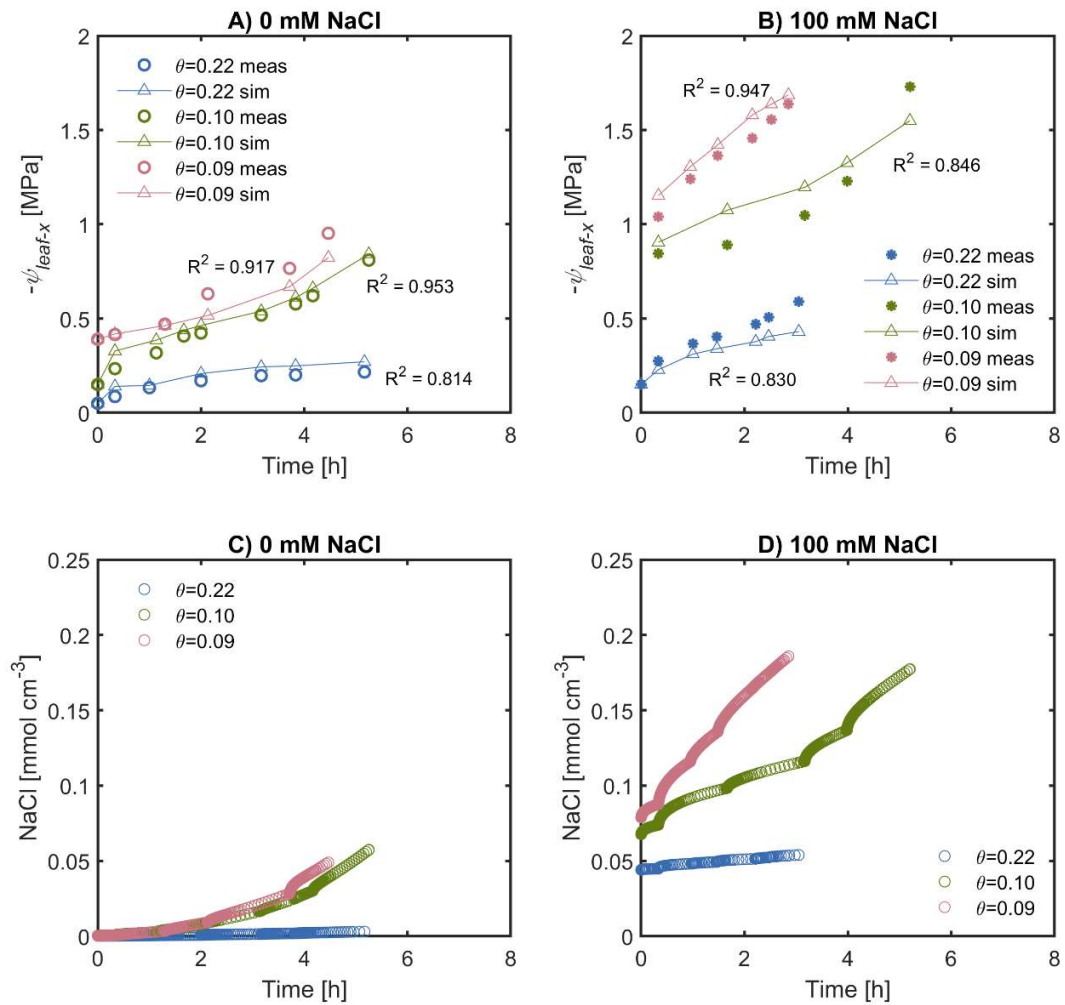
Figure 1.7 *Changes in leaf xylem water potential ($\psi_{leaf\text{-}x}$) and NaCl over time. The dynamics of $\psi_{leaf\text{-}x}$ over time (**A** and **B**) follow salt accumulation at root surface for the corresponding time periods (**C** and **D**). Open symbols and asterisks denote measurements of non-saline and 100 mM NaCl treatment, respectively (**A** – **B**). Connected triangles stand for the simulated values (**A** – **B**; meas: measured; sim: simulated). Salt accumulation was simulated by the soil-plant model in non-saline (**C**), and saline conditions (**D**).*

19
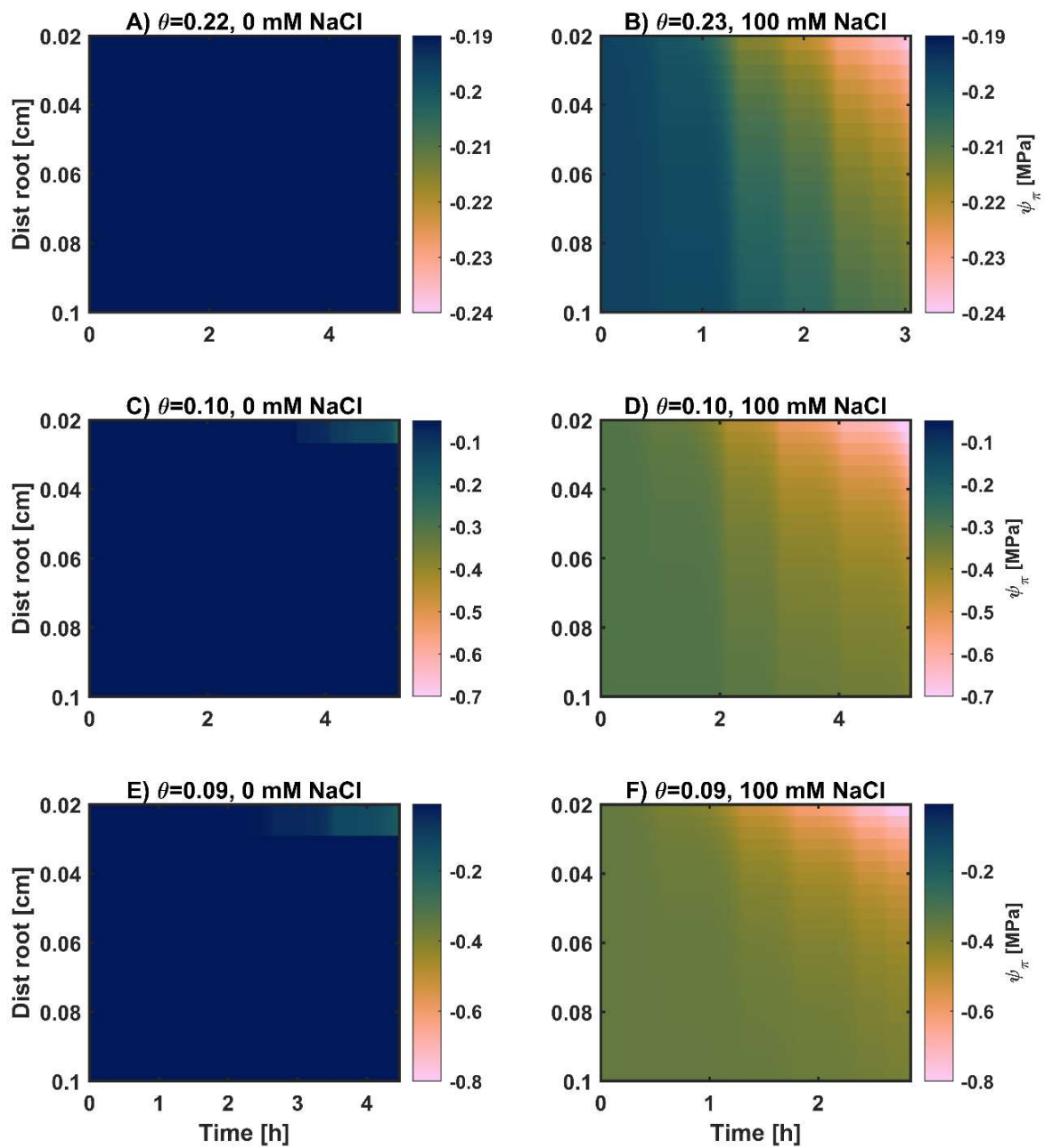
Figure 1.8 *Spatiotemporal distribution of soil osmotic potential ($\psi\pi$; MPa) toward the root surface for different soil water contents (θ; cm^3 cm^{-3}). Salt treatments induced additional osmotic stress at the root surface. Color bars stand for ψ_π gradients.*

1.4.5 Arbuscular mycorrhiza symbiosis enhances soil–plant hydraulics under water stress

I have also investigated the impact of AMF on plant water status and soil–plant hydraulic conductance in two tomato genotypes, reduced mycorrhiza colonization (RMC) and its wild type (WT) counterpart. Leaf water potential of the WT plants did not drop below -0.8 MPa six days after withholding irrigation, while leaf water potential of the RMC dropped below -1.0 MPa already after four days (*p-value* < 0.01). Transpiration declined in both treatments as a consequence of water deficit. During soil drying, we observed, surprisingly, no differences in transpiration rate between the two genotypes (*p-value* = 0.5).

During soil drying, the relation between transpiration and leaf water potential was affected by AMF colonization (Figure 1.9). In wet conditions, i.e., day one, both genotypes showed high transpiration and leaf water potential (Figure 1.9). As soil progressively dried, RMC showed relatively lower transpiration and more negative leaf water potential than the WT (Figure 1.9). This decoupling in the relation between transpiration and leaf water potential reveals that it is not unique but depends on below-ground hydraulics.

I conclude that AMF extend the effective root radius hereby reducing the water fluxes at the root-soil interface and attenuating the drop in matric potential across the rhizosphere. This would result in an enhanced soil-plant hydraulic conductance and plant water status in drying soil. Further research is needed to directly measure the effects of AMF on water fluxes under contrasting soil textures and nutrient availabilities among different AMF species and plant genotypes.
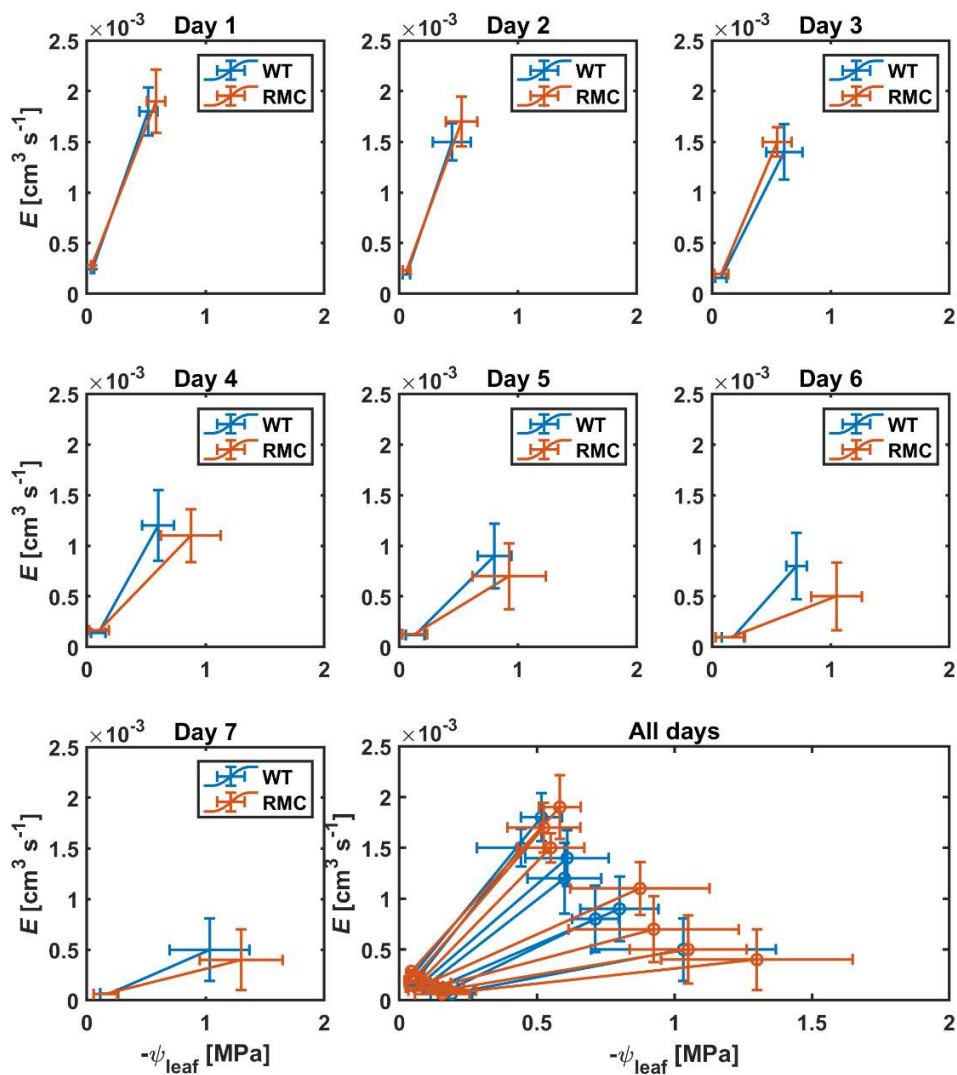
Figure 1.9 *Relation between transpiration rate (E) and leaf water potential (ψ_{leaf}) during soil drying. Subplots show the relation on daily basis after last irrigation. As soil progressively dried, the reduced mycorrhiza colonization (RMC) plants showed lower E and more negative ψ_{leaf} on the same day compare to wild type (WT).*

1.5 Concluding remarks and future outlook

This research has provided new fundamental knowledge concerning the links between soil hydraulics and stomatal regulation. The work focuses on measurements and simulations of stomatal response to soil drying, and partitioning above- and below-ground hydraulic conductivities. Significant results on understanding stomatal regulation during soil drying are obtained. Yet, several questions were raised opening new avenues for research.

1.5.1 Hydraulic limitations governing stomatal regulation

In chapter two and three, I found that stomata do close at the onset of hydraulic non-linearity. Although this concept was hypothesized by theoretical models (Sperry and Love, 2015, Carminati and Javaux, 2020), the findings here have finally validated these hypotheses, and provided the first experimental proof of stomatal closure at hydraulic non-linearity to avoid excessive decrease in leaf water potential. Even though current research trends focus on the coordination between stomatal closure and xylem vulnerability (Scoffoni *et al.*, 2014; Brodribb *et al.*, 2016; Wolf *et al.*, 2016; Anderegg *et al.*, 2017; Henry *et al.*, 2019; Eller *et al.*, 2020), this doctoral work suggests that, in tomato, there is no apparent reduction in xylem hydraulic conductance during soil drying. Interestingly, stomatal closure is rather coordinated to decline in soil-root hydraulic conductance. Furthermore, to properly predict stomatal closure and understand its relation to soil–plant hydraulics, the knowledge of below-ground conductivities are essential. The results show a tied link between soil hydraulic conductivity, active root length and stomatal conductance, and the coordination between these parameters is central in predicting the ability of plants to cope with water shortage.

The follow-up question raised, in chapter four, was what allows stomata to respond to the onset of hydraulic non-linearity and reduced below-ground hydraulics (Wankmüller and Carminati, 2021). Thus, I investigated the role of ABA in the onset of hydraulic non-linearity. This doctoral work has demonstrated that ABA synthesis could be a mechanism that allows plants to close stomata (even though PPFD increased) to avoid the incidence of hydraulic non-linearity in the relation between transpiration rate and leaf water potential (Wankmüller and Carminati, 2021).

1.5.2 Impacts of salinity on soil–plant hydraulics

Within the experimental campaigns, this work investigates the coupled effects of salinity and soil drying on plant water relations. Salinity induced a more negative leaf water potential at predawn and successively throughout the daytime. It has significantly reduced maximum transpiration rate. One of the conclusions is that osmotic stress at the root surface causes a large drop in leaf water potential of plants growing in dry and saline soils, which eventually suppress high transpiration rates.

1.5.3 AMF impacting soil–plant hydraulic conductance

This research additionally investigates the interplay between AMF and soil drying, using a reduced mycorrhiza colonization mutant and the corresponding wild-type. The results show that AMF enhance plant water status during soil drying by improving soil–plant hydraulic conductance. The results suggest that AMF could play an essential role in achieving sustainable agricultural production with greater importance in regions faced by water scarcity conditions worldwide.

1.5.4 Outlooks

The link between below-ground hydraulics and stomatal regulation during soil drying has been elucidated in this thesis. In the following, a number of final recommendations are made to work which could follow-on or complement the developments and the outcomes presented in this doctoral thesis:

- This work demonstrates the significance of below-ground hydraulics in controlling stomatal regulation in dry soils. An addition to this work, to overcome the limitations of the novel root pressure chamber system, would be to experimentally partition below-ground hydraulic conductivities, namely, soil, root, and their interface in intact plant during soil drying. The aim would be to measure water potential dissipation within each of below-ground components. This will make it possible to identify which of these components represents the primary hydraulic limitation to transpiration. Owing to the fact that tomato was used as a model plant in these studies, it will be beneficial to apply

this concept on diverse herbaceous and woody species growing in contrasting soil textures and climatic conditions (Chapters two and three).

- The findings regarding the role of ABA in stomatal response to hydraulic non-linearity were observed in wet soil conditions. Therefore, additional experiments can be done in dry soil conditions using similar genotypes to explore the role of ABA on the onset of the non-linearity (Chapter four).

- Concerning salinity stress quantification, experimental setup can be developed to directly measure solute concentrations at the root surface together with transpiration rate and water potential across soil–plant continuum with high temporal resolution, particularly under saline conditions, in different plant species (Chapter five).

- Although limited transpiration rate was proposed as plant mechanism to save water under saline conditions, this study demonstrates that, in tomato, it is rather a consequence of altered below-ground biophysical processes. Therefore, one would anticipate that a successful mechanism may include means of rhizosphere modulation (Chapter five).

- The impacts of NaCl solution on unsaturated soil hydraulic conductivity was not apparent in this study. However, it can be explored in undisturbed and aggregated soils that contains elevated clay content (Chapter five).

- Another conclusion regarding the influence of AMF on the soil-root interface of tomato is that AMF impacted water fluxes across the rhizosphere. Further work is needed to directly measure the effects of AMF on water fluxes under contrasting soil textures using a combination of isotopes and neutron imaging using various species of plants and AMF (Chapter six).

- Direct measurements of AMF root-soil contact, water potential at the root surface in presence/absence of AMF, together with transpiration rate during soil drying will shed light on the underlying mechanisms (Chapter six).

The fundamental findings presented in this doctoral work call for reconciling soil and root biophysical processes to fully understand plant water relation under water deficit. Further investigations are needed to reveal the interplay between ABA, leaf water potential, stomatal conductance, and carbon assimilation rate in different plant species and soil types to fully

understand plant responses to edaphic and atmospheric water stress. The results have been obtained on plant scale, thus, it is urgently needed to project these findings to larger scales. The high influence of soil hydraulic properties on ecosystem sensitivity to water stress is under-discussed in the literature concerning ecosystem drought stress responses.

1.6 Contribution to the included publications

1.6.1 Manuscripts

1- Stomatal closure of tomato under drought is driven by an increase in soil–root hydraulic resistance.

Mohanned Abdalla, Andrea Carminati, Gaochao Cai, Mathieu Javaux, and Mutez Ali Ahmed (2021) *Plant, Cell and Environment* 44 (2), 425 – 431

https://doi.org/10.1111/pce.13939

Authors contributions: Al authors conceptualized the study. MA conducted the experiments and wrote the manuscript with the contribution of AC, GC, MJ, and MAA.

2- Stomatal closure during soil water deficit is controlled by below-ground hydraulics.

Mohanned Abdalla, Mutez Ali Ahmed, Gaochao Cai, Fabian Wankmüller, Nimrod Schwartz, Or Litig, Mathieu Javaux, and Andrea Carminati (2021) *Annals of Botany,* 129 (2), 161 – 170

https://doi.org/10.1093/aob/mcab141

Authors contributions: MA, MAA, GC and AC designed the experiments. MA performed the experiment and wrote the first draft. MA, FW and AC made the simulations. MAA, GC, MJ and AC contributed to the writing. NM and OL provided the seed and contributed to the study design. All authors discussed the results and approved the final version.

3- Coupled effects of soil drying and salinity on soil–plant hydraulics.

Mohanned Abdalla, Mutez Ali Ahmed, Gaochao Cai, Mohsen Zarebanadkauki, and Andrea Carminati (2022) *Plant Physiology* 190 (2) 1228 – 1241

Authors contributions: All authors conceptualized the study. MA performed the experiment and analyzed the data. MA MZ, and AC made the simulations. MA wrote the manuscript with contributions of MAA, GC, MZ and AC.

4- Arbuscular mycorrhiza symbiosis enhances water status and soil–plant hydraulic conductance under drought

Mohanned Abdalla and Mutez Ali Ahmed (2021) *Frontiers in Plant Science*, 12 (722954)

https://doi.org/10.3389/fpls.2021.722954

Authors contributions: MA and MAA designed the study. MA conducted the experiments and analyzed the data. MA and MAA wrote the manuscript.

5- The role of ABA in stomatal response to hydraulic non-linearity

Mohanned Abdalla and Mutez Ali Ahmed (2022) *In Prep*.

Authors contributions: MA and MAA designed the study. MA conducted the experiments and analyzed the data. MA and MAA wrote the manuscript.

1.6.2. Own contribution to main manuscripts

Manuscript No	Conceptualization	Data acquisition	Analyses and figures	Writing
1	70%	100%	90%	75%
2	75%	100%	100%	85%
3	95%	100%	100%	90%
4	95%	90%	100%	85%
5	90%	100%	100%	90%

1.7   References

Anderegg WRL, Wolf A, Arango-Velez A, Choat B, Chmura DJ, Jansen S, Kolb T, Li S, Meinzer F, Pita P, *et al.* **2017**. Plant water potential improves prediction of empirical stomatal models (R Aroca, Ed.). *PLOS ONE* **12**: e0185481.

Aroca R, Porcel R, Ruiz-Lozano JM. **2007**. How does arbuscular mycorrhizal symbiosis regulate root hydraulic properties and plasma membrane aquaporins in Phaseolus vulgaris under drought, cold or salinity stresses? *New Phytologist* **173**: 808–816.

Augé RM. **2001**. Water relations, drought and vesicular-arbuscular mycorrhizal symbiosis. *Mycorrhiza* **11**: 3–42.

Augé RM, Toler HD, Saxton AM. **2015**. Arbuscular mycorrhizal symbiosis alters stomatal conductance of host plants more under drought than under amply watered conditions: a meta-analysis. *Mycorrhiza* **25**: 13–24.

Bitterlich M, Franken P, Graefe J. **2018a**. Arbuscular Mycorrhiza Improves Substrate Hydraulic Conductivity in the Plant Available Moisture Range Under Root Growth Exclusion. *Frontiers in Plant Science* **9**.

Bitterlich M, Sandmann M, Graefe J. **2018b**. Arbuscular Mycorrhiza Alleviates Restrictions to Substrate Water Flow and Delays Transpiration Limitation to Stronger Drought in Tomato. *Frontiers in Plant Science* **9**: 154.

Blatt M. **2021**. Challenging research. *Plant Physiology* **186**: 802–803.

Bourbia I, Pritzkow C, Brodribb TJ. **2021**. Herb and conifer roots show similar high sensitivity to water deficit. *Plant Physiology* **186**: 1908–1918.

Brodribb TJ, McAdam SAM. **2011**. Passive Origins of Stomatal Control in Vascular Plants. *Science* **331**: 582–585.

Brodribb TJ, McAdam SA, Carins Murphy MR. **2017**. Xylem and stomata, coordinated through time and space. *Plant, Cell & Environment* **40**: 872–880.

Brodribb TJ, Powers J, Cochard H, Choat B. **2020**. Hanging by a thread? Forests and drought. *Science* **368**: 261–266.

Brodribb TJ, Skelton RP, McAdam SAM, Bienaimé D, Lucani CJ, Marmottant P. **2016**. Visual quantification of embolism reveals leaf vulnerability to hydraulic failure. *New Phytologist* **209**: 1403–1409.

Buckley TN. **2005**. The control of stomata by water balance. *New Phytologist* **168**: 275–292.

Buckley TN. **2019**. How do stomata respond to water status? *New Phytologist* **224**: 21–36.

Buckley TN, Mott KA, Farquhar GD. **2003**. A hydromechanical and biochemical model of stomatal conductance. *Plant, Cell & Environment* **26**: 1767–1785.

Cai G, Ahmed MA, Dippold MA, Zarebanadkouki M, Carminati A. **2020a**. Linear relation between leaf xylem water potential and transpiration in pearl millet during soil drying. *Plant and Soil* **447**: 565–578.

Cai G, Ahmed MA, Reth S, Reiche M, Kolb A, Carminati A. **2020b**. Measurement of leaf xylem water potential and transpiration during soil drying using a root pressure chamber system. *Acta Horticulturae*: 131–138.

Carminati A, Ahmed MA, Zarebanadkouki M, Cai G, Lovric G, Javaux M. **2020**. Stomatal closure prevents the drop in soil water potential around roots. *New Phytologist* **226**: 1541–1543.

Carminati A, Javaux M. **2020**. Soil Rather Than Xylem Vulnerability Controls Stomatal Response to Drought. *Trends in Plant Science* **25**: 868–880.

Carminati A, Passioura JB, Zarebanadkouki M, Ahmed MA, Ryan PR, Watt M, Delhaize E. **2017**. Root hairs enable high transpiration rates in drying soils. *New Phytologist* **216**: 771–781.

Chaves MM, Flexas J, Pinheiro C. **2009**. Photosynthesis under drought and salt stress: regulation mechanisms from whole plant to cell. *Annals of Botany* **103**: 551–560.

Chitarra W, Pagliarani C, Maserti B, Lumini E, Siciliano I, Cascone P, Schubert A, Gambino G, Balestrini R, Guerrieri E. **2016**. Insights on the Impact of Arbuscular Mycorrhizal Symbiosis on Tomato Tolerance to Water Stress. *Plant Physiology* **171**: 1009–1023.

Choat B, Brodribb TJ, Brodersen CR, Duursma RA, López R, Medlyn BE. 2018. Triggers of tree mortality under drought. *Nature* 558: 531–539.

Corso D, Delzon S, Lamarque LJ, Cochard H, Torres-Ruiz JM, King A, Brodribb T. **2020**. Neither xylem collapse, cavitation, or changing leaf conductance drive stomatal closure in wheat. *Plant, Cell & Environment* **43**: 854–865.

Cowan I, Farquhar G. **1977**. Stomatal function in relation to leaf metabolism and environment: Stomatal function in the regulation of gas exchange. *Symposia of the Society for Experimental Biology* **31**: 471–505.

Davies WJ, Zhang J. **1991**. Root Signals and the Regulation of Growth and Development of Plants in Drying Soil. *Annual Review of Plant Physiology and Plant Molecular Biology* **42**: 55–76.

Deans RM, Brodribb TJ, Busch FA, Farquhar GD. **2020**. Optimization can provide the fundamental link between leaf photosynthesis, gas exchange and water relations. *Nature Plants* **6**: 1116–1125.

Dodd IC. **2005**. Root-To-Shoot Signalling: Assessing The Roles of 'Up' In the Up and Down World of Long-Distance Signalling In Planta. *Plant and Soil* **274**: 251–270.

Edwards D, Kerp H, Hass H. **1998**. Stomata in early land plants: an anatomical and ecophysiological approach. *Journal of Experimental Botany* **49**: 255–278.

Eller CB, Rowland L, Mencuccini M, Rosas T, Williams K, Harper A, Medlyn BE, Wagner Y, Klein T, Teodoro GS, *et al.* **2020**. Stomatal optimization based on xylem hydraulics (SOX) improves land surface model simulation of vegetation responses to climate. *New Phytologist* **226**: 1622–1637.

Fricke W, Akhiyarova G, Veselov D, Kudoyarova G. **2004**. Rapid and tissue-specific changes in ABA and in growth rate in response to salinity in barley leaves. *Journal of Experimental Botany* **55**: 1115–1123.

Hayat F, Ahmed MA, Zarebanadkouki M, Javaux M, Cai G, Carminati A. **2020**. Transpiration Reduction in Maize (Zea mays L) in Response to Soil Drying. *Frontiers in Plant Science* **10**.

Hetherington AM, Woodward FI. **2003**. The role of stomata in sensing and driving environmental change. *Nature* **424**: 901–908.

Holbrook NM, Shashidhar VR, James RA, Munns R. **2002**. Stomatal control in tomato with ABA-deficient roots: response of grafted plants to soil drying. *Journal of Experimental Botany* **53**: 1503–1514.

Jasechko S, Sharp ZD, Gibson JJ, Birks SJ, Yi Y, Fawcett PJ. **2013**. Terrestrial water fluxes dominated by transpiration. *Nature* **496**: 347–350.

Lamarque LJ, Delzon S, Toups H, Gravel A-I, Corso D, Badel E, Burlett R, Charrier G, Cochard H, Jansen S, *et al.* 2020. Over-accumulation of abscisic acid in transgenic tomato plants increases the risk of hydraulic failure. *Plant, Cell & Environment* **43**: 548–562.

Liu L, Gudmundsson L, Hauser M, Qin D, Li S, Seneviratne SI. **2020**. Soil moisture dominates dryness stress on ecosystem production globally. *Nature Communications* **11**: 4892.

López J, Way DA, Sadok W. **2021**. Systemic effects of rising atmospheric vapor pressure deficit on plant physiology and productivity. *Global Change Biology* **27**: 1704–1720.

Madadgar S, AghaKouchak A, Farahmand A, Davis SJ. **2017**. Probabilistic estimates of drought impacts on agricultural production. *Geophysical Research Letters* **44**: 7799–7807.

McAdam SAM, Brodribb TJ. **2018**. Mesophyll Cells Are the Main Site of Abscisic Acid Biosynthesis in Water-Stressed Leaves. *Plant Physiology* **177**: 911–917.

Merilo E, Yarmolinsky D, Jalakas P, Parik H, Tulva I, Rasulov B, Kilk K, Kollist H. **2018**. Stomatal VPD Response: There Is More to the Story Than ABA. *Plant Physiology* **176**: 851–864.

Munns R. **2002**. Comparative physiology of salt and water stress. *Plant, Cell & Environment* **25**: 239–250.

Munns R, Gilliham M. **2015**. Salinity tolerance of crops – what is the cost? *New Phytologist* **208**: 668–673.

Munns R, Passioura JB, Colmer TD, Byrt CS. **2020**. Osmotic adjustment and energy limitations to plant growth in saline soil. *New Phytologist* **225**: 1091–1096.

Munns R, Tester M. **2008**. Mechanisms of Salinity Tolerance. *Annual Review of Plant Biology* **59**: 651–681.

Ouledali S, Ennajeh M, Zrig A, Gianinazzi S, Khemira H. **2018**. Estimating the contribution of arbuscular mycorrhizal fungi to drought tolerance of potted olive trees (Olea europaea). *Acta Physiologiae Plantarum* **40**: 81.

Passioura JB. **1980**. The Transport of Water from Soil to Shoot in Wheat Seedlings. *Journal of Experimental Botany* **31**: 333–345.

Passioura JB, Munns R. **1984**. Hydraulic Resistance of Plants. II. Effects of Rooting Medium, and Time of Day, in Barley and Lupin. *Functional Plant Biology* **11**: 341–350.

Pauwels R, Jansa J, Püschel D, Müller A, Graefe J, Kolb S, Bitterlich M. **2020**. Root growth and presence of Rhizophagus irregularis distinctly alter substrate hydraulic properties in a model system with Medicago truncatula. *Plant and Soil* **457**: 131–151.

Peters A, Iden SC, Durner W. **2015**. Revisiting the simplified evaporation method: Identification of hydraulic functions considering vapor, film and corner flow. *Journal of Hydrology* **527**: 531–542.

Peterson KM, Rychel AL, Torii KU. **2010**. Out of the Mouths of Plants: The Molecular Basis of the Evolution and Diversity of Stomatal Development. *The Plant Cell* **22**: 296–306.

Quiroga G, Erice G, Ding L, Chaumont F, Aroca R, Ruiz-Lozano JM. **2019**. The arbuscular mycorrhizal symbiosis regulates aquaporins activity and improves root cell water permeability in maize plants subjected to water stress. *Plant, Cell & Environment* **42**: 2274–2290.

Rodriguez-Dominguez CM, Brodribb TJ. **2020**. Declining root water transport drives stomatal closure in olive under moderate water stress. *New Phytologist* **225**: 126–134.

Scholander PF, Bradstreet ED, Hemmingsen EA, Hammel HT. **1965**. Sap Pressure in Vascular Plants: Negative hydrostatic pressure can be measured in plants. *Science* **148**: 339–346.

Schurr U, Gollan T, Schulze E-D. **1992**. Stomatal response to drying soil in relation to changes in the xylem sap composition of Helianthus annuus. II. Stomatal sensitivity to abscisic acid imported from the xylem sap. *Plant, Cell & Environment* **15**: 561–567.

Scoffoni C, Vuong C, Diep S, Cochard H, Sack L. **2014**. Leaf Shrinkage with Dehydration: Coordination with Hydraulic Vulnerability and Drought Tolerance. *Plant Physiology* **164**: 1772–1788.

Sperry JS, Hacke UG, Oren R, Comstock JP. **2002**. Water deficits and hydraulic limits to leaf water supply. *Plant, Cell and Environment* **25**: 251–263.

Sperry JS, Love DM. **2015**. What plant hydraulics can tell us about responses to climate-change droughts. *New Phytologist* **207**: 14–27.

Sperry JS, Wang Y, Wolfe BT, Mackay DS, Anderegg WRL, McDowell NG, Pockman WT. **2016**. Pragmatic hydraulic theory predicts stomatal responses to climatic water deficits. *New Phytologist* **212**: 577–589.

Stirzaker RJ, Passioura JB. **1996**. The water relations of the root–soil interface. *Plant, Cell & Environment* **19**: 201–208.

Tardieu F, Davies WJ. **1993**. Integration of hydraulic and chemical signalling in the control of stomatal conductance and water status of droughted plants. *Plant, Cell & Environment* **16**: 341–349.

Wang Y, Sperry JS, Anderegg WRL, Venturas MD, Trugman AT. **2020**. A theoretical and empirical assessment of stomatal optimization modeling. *New Phytologist* **227**: 311–325.

Wolf A, Anderegg WRL, Pacala SW. **2016**. Optimal stomatal behavior with competition for water and risk of hydraulic impairment. *Proceedings of the National Academy of Sciences* **113**: E7222–E7230.

Wolz KJ, Wertin TM, Abordo M, Wang D, Leakey ADB. **2017**. Diversity in stomatal function is integral to modelling plant carbon and water fluxes. *Nature Ecology & Evolution* **1**: 1292–1298.

van Zelm E, Zhang Y, Testerink C. **2020**. Salt Tolerance Mechanisms of Plants. *Annual Review of Plant Biology* **71**: 403–433.

Zhang H, Li X, Wang W, Pivovaroff AL, Li W, Zhang P, Ward ND, Myers-Pigg A, Adams HD, Leff R, *et al.* 2021. Seawater exposure causes hydraulic damage in dying Sitka-spruce trees. *Plant Physiology* 187: 873–885.

2 Chapter two: Stomatal closure of tomato under drought is driven by an increase in soil–root hydraulic resistance

Mohanned Abdalla[1,2], Andrea Carminati[1], Gaochao Cai[1,3], Mathieu Javaux[4,5], and Mutez Ali Ahmed[1,3]

[1]Chair of Soil Physics, Bayreuth Center of Ecology and Environmental Research (BayCEER), University of Bayreuth, Universitätsstraße 30, 95447, Bayreuth, Germany.

[2]Department of Horticulture, Faculty of Agriculture, University of Khartoum, Khartoum North 13314 Shambat, Sudan.

[3]Biogeochemistry of Agroecosystems, University of Göttingen, Göttingen, Germany.

[4]Earth and Life Institute-Environmental Science, Universite Catholique de Louvain, Louvain la Neuve, Belgium.

[5]Agrosphere (IBG-3), Forschungszentrum Juelich GmbH, Juelich, Germany.

2.1 ABSTRACT

The fundamental question as to what triggers stomatal closure during soil drying remains contentious. Thus, we urgently need to improve our understanding of stomatal response to water deficits in soil and atmosphere. Here, we investigated the role of soil–plant hydraulic conductance (K_{sp}) on transpiration (E) and stomatal regulation. We used a root pressure chamber to measure the relation between E, leaf xylem water potential (ψ_{leaf-x}) and soil water potential (ψ_{soil}) in tomato. Additional measurements of ψ_{leaf-x} were performed with unpressurized plants. A soil–plant hydraulic model was used to simulate $E(\psi_{leaf-x})$ for decreasing ψ_{soil}. In wet soils, $E(\psi_{leaf-x})$ had a constant slope while in dry soils the slope decreased, with ψ_{leaf-x} rapidly and non-linearly decreasing for moderate increases in E. The ψ_{leaf-x} measured in pressurized and unpressurized plants matched well, which indicates that the shoot hydraulic conductance did not decrease during soil drying and that the decrease in K_{sp} is caused by a decrease in soil-root conductance. The decrease of E matched well the onset of hydraulic non-linearity. Our findings demonstrate that stomatal closure prevents the drop in ψ_{leaf-x} caused by a decrease in K_{sp} and elucidate a strong correlation between stomatal regulation and below-ground hydraulic limitation.

Keywords: *Solanum lycopersicum*, below-ground hydraulic, hydraulic conductivity, transpiration, leaf water potential, water stress, soil drying.

2.2 INTRODUCTION

What triggers stomatal closure in plants during soil drying? Water flow across the soil-plant-atmosphere continuum is controlled by leaf area, stomatal conductance (g_s [mol m^{-2} s^{-1}]), and atmospheric demand (vapor pressure deficit, VPD [kPa]). Transpiration (E [cm^3 s^{-1}]) causes a decrease in the leaf xylem water potential ($\psi_{\text{leaf-x}}$ [MPa]) that propagates through the xylem vessels down to the roots and the soil. $\psi_{\text{leaf-x}}$ depends on the soil water potential (ψ_{soil} [MPa]), transpiration rate, and the hydraulic conductivities of the elements composing the soil–plant system. It is well accepted that plants continuously adapt to variable atmospheric and soil conditions by altering the hydraulic conductivity of key elements below and above ground, but our understanding of this hydraulic acclimatization is, as yet, incomplete.

Although the underlying mechanisms controlling stomatal regulation at the mechanistic and molecular levels, especially in drying soil, are yet to be fully revealed (Buckley, 2005, 2019), recent studies have demonstrated that we still could anticipate stomatal response to soil drying from its emergent properties (Sperry *et al.*, 2016). Sperry and Love (2015) proposed a "supply-demand" hydraulic framework to understand the physical constraints on transpiration. The premise is that stomatal regulation avoids excessive drop in $\psi_{\text{leaf-x}}$ by responding to non-linearities in the relationship between $\psi_{\text{leaf-x}}$ and E. The non-linearities and the trigger of stomatal closure have been assumed to be closely coordinated with xylem cavitation (Sperry and Love, 2015; Anderegg *et al.*, 2017). However, other elements of the soil–plant continuum can limit the water transport before xylem cavitates. A recent study on wheat (*Triticum aestivum*) concluded that neither xylem cavitation nor a decrease in leaf conductance drives stomatal closure (Corso *et al.*, 2020). Similarly, Rodriguez-Dominguez and Brodribb (2020) found that the drop of hydraulic conductance of the root-soil interface was the main limitation to water transport and hence represented the primary driver of stomatal closure in olive trees (*Olea europea* L).

Carminati and Javaux (2020) re-proposed the hydraulic model of Sperry and Love (2015) highlighting the role of soil hydraulic conductance (K_s). Using a meta-analysis across species they showed that the loss of K_s, more than the xylem, coincides better with the stomatal closure. They visualized the relationship between E, $\psi_{\text{leaf-x}}$, and ψ_{soil} as a surface $E(\psi_{\text{leaf-x}}, \psi_{\text{soil}})$ and hypothesized that stomatal regulation prevents plants to cross the onset of hydraulic non-

linearity. They supported their hypothesis with literature data, which shows a linear relationship between E and the difference between $\psi_{\text{leaf-x}}$ and ψ_{soil}. However, existing data failed to prove that stomata close at the onset of hydraulic non-linearity. In other words, most of the existing evidence indicates that stomata close before the occurrence of hydraulic non-linearity. Reviews and meta-analysis approaches have addressed this question with emphasis on above-ground components (Bartlett *et al.,* 2016; Martin-StPaul *et al.*, 2017*)*, however, there is still a need for systematic experiments to explore the role of below-ground hydraulic processes in stomatal regulation. The question is: do stomata close at the point when the hydraulic conductance starts to decrease?

Answering this question requires a method to explore the non-linear part of the $E(\psi_{\text{leaf-x}})$ relation. This is achievable by the root pressure chamber apparatus (Passioura 1980; Cai *et al.*, 2020a). The method provides accurate and high temporal resolution measurements of $\psi_{\text{leaf-x}}$ and E in intact plants with no (or very limited) stomatal regulation. By pressurizing the soil and thus maintaining the leaf turgid, we explored the non-linear part of the relationship between $\psi_{\text{leaf-x}}$ and E. Furthermore, pressurization prevents cavitation during the increase in E (Passioura and Munns, 1984). Yet, below-ground conductances are not affected by pressurization, including the potential shrinkage of the root cortex and the loss of contact to the soil. Therefore, this method evaluates accurately the changes in below-ground hydraulic conductance occurring at a given E and ψ_{soil} (Passioura, 1980; Carminati *et al.*, 2017). In parallel, we measured the decrease of E and $\psi_{\text{leaf-x}}$ in non-pressurized plants. By comparing $\psi_{\text{leaf-x}}$ in pressurized and unpressurized plants at the same ψ_{soil} and E, we obtain information on the decrease in shoot hydraulic conductance and xylem cavitation (both prevented in pressurized plants). Additionally, by comparing pressurized and not-pressurized experiments, we tested the hypothesis that stomata close at the onset of hydraulic limitation. We applied this method to tomato plants in a sandy-loam soil. The data were interpreted using the conceptual and numerical soil–plant hydraulic model of Carminati and Javaux (2020).

2.3 MATERIALS AND METHODS

2.3.1 Plant and soil

Tomato (*Solanum lycopersicum* L.) seeds were soaked in H_2O_2 solution for 3 minutes and then germinated in Petri dishes for 5 days. Plants were grown in polyvinyl chloride (PVC) columns with 30 cm height, 10 cm outer diameter, and 9.4 cm inner diameter. Five holes, with a diameter of 5 mm, were made on the column's side for soil moisture measurements. The PVC columns were topped with a 0.8-cm-thick aluminum plate with a centered-hole of 1.4 cm in diameter (Supplementary figure S1).

Plants were grown in a climate-controlled room for three weeks, with a day/night temperature of 28/18 °C, relative humidity of 57/65%, and 14 hours as the photoperiod. The light intensity (LI) was 600 µmol m^{-2} s^{-1} (Luxmeter, Meschede, Germany). Plants were watered every 2-3 days to maintain wet soil conditions ($\theta \approx 0.2$ cm^3 cm^{-3}). Preparatory to the experiments, plants were translocated to the laboratory and stems around the collar were glued (UHU, Bühl, Germany) to facilitate the forthcoming root pressurization (Supplementary figure S1).

The substrate consisted of a mixture of quartz sand and loamy soil with a ratio of 3:5. The substrate was dried at 60 ºC for 48 hours and then sieved separately at 1 mm. The water retention and unsaturated hydraulic conductivity curves of the soil mixture are reported in Cai *et al.* (2020a). The soil water content (θ [cm^3 cm^{-3}]) was monitored during the experiment using a time-domain refractometer (TDR) that consists of two rods (length: 6 cm, spacing: 0.5 cm) connected to a data logger (E-Test, Lublin, Poland). Leaves were imaged and analyzed using ImageJ (1.50e http://imagej.nih.gov/ij) to estimate leaf area (Skelton *et al.*, 2017). The roots were washed after the experiments and then scanned (with a scanner Epson STD 4800, at a resolution of 400 dpi) to determine the total root length using WinRhizo (Regent Instruments Inc., Canada).

2.3.2 Leaf xylem water potential measurements via the root pressure chamber system

We used a root pressure chamber to continuously monitor $\psi_{\text{leaf-x}}$ for varying LI which yielded a varying E (after Passioura (1980)). The detailed construction and calibration were recently introduced in Cai *et al.* (2020a). Briefly, it comprises a root pressure chamber (a metallic

cylinder with the dimension of 31.5 cm in height and 17.5 cm in diameter) with a cuvette on top and the main controller unit. The cuvette was equipped with four groups of light-emitting diode (LED) lamps that were attached vertically to the cuvette. LI was measured using a radiometric sensor (Gamma Scientific, San Diego, USA). The airflow passed constantly through the cuvette at a velocity of 8 L min^{-1} and was stirred by a small fan. The temperature and the relative humidity of the inward and outward air were measured with combined temperature-humidity sensors (Galltec-Mela, Bondorf, Germany).

ψ_{leaf-x} was determined by applying sufficient pneumatic pressure to the root pressure chamber to bring the water in a cut leaf to atmospheric pressure. This applied pressure, called the balancing pressure (P [MPa]), is numerically equal to minus the suction in leaf xylem before pressurization at the same transpiration rate E (Passioura, 1980; Carminati *et al.*, 2017; Cai *et al.*, 2020a). A meniscus system that encompasses a capillary tube and an infrared detector was attached to the leaf cut (petiolule) to maintain the hydraulic connection to observe P. ψ_{leaf-x} was determined when the meniscus was stable for at least 10 minutes (Cai *et al.*, 2020a). E was calculated by multiplying the airflow by the difference between the outward and inward humidity.

Experiments were started with positioning the columns inside the pressure chamber and the shoots in the cuvette. E was altered by changing LI from 0 µmol m^{-2} s^{-1} to 200, 400, 600, 800, and 1000 µmol m^{-2} s^{-1}. The corresponding ψ_{leaf-x} was determined at each E. The full cycle of LI was achieved only in wet soils because in dry soils ψ_{leaf-x} could not be sustained at high E.

Additionally, we measured ψ_{leaf-x} and E in unpressurized plants. E was measured using the same cuvette as explained above. ψ_{leaf-x} was measured using a Scholander bomb (Soil Moisture Equipment corp. Santa Barbara, CA., USA).

2.3.3   Soil–plant hydraulic model

We used a simplified model of water flow in the soil–plant continuum. The series of resistances between the bulk soil, soil-root interface, and through the root to the leaf xylem were considered in the soil–plant hydraulic model, assuming that one single root represents all active roots that took up water. A detailed description of the model can be found in Carminati and

Javaux (2020), Cai *et al.* (2020a), Hayat *et al.* (2020) and supplementary note S1 and supplementary table S1.

Briefly, the model calculates the gradient in water potential through the soil and along the plant till the leaf. Soil water flow is simulated assuming a radial geometry and an uniform root water uptake into a fraction of the total root length. The water flow in the plant is calculated assuming a proportionality between the plant hydraulic conductance (K_{plant} [cm^3 s^{-1} MPa^{-1}]) and the difference in water potential between the root-soil interface and the leaf, with K_{plant} dropping according to a power law at a given xylem water potential (which is the point at which the xylem starts to cavitate – Eqn. S5). K_{plant} is given by the harmonic mean of the root conductance K_{root} and the xylem conductance K_x. Solving the flow equation (S2) we obtain the surface $E(\psi_{leaf-x}, \psi_{soil})$. The soil–plant conductance K_{sp} is given by the ratio between E and the difference between ψ_{leaf-x} and ψ_{soil}:

$$K_{sp} = \frac{E}{\psi_{soil} - \psi_{leaf-x}} \qquad \text{(Eqn. 1)}$$

We defined the onset of hydraulic limitation (SOL) as E at which $\left.\frac{\partial E}{\partial \psi_{leaf-x}}\right|_{\psi_{soil}}$ reaches 70 % of its maximum value at a given ψ_{soil} (i.e. at $E = 0$). Note that the value of 70 % is somehow arbitrary. We used it because it indicates a significant change of the conductance. A value between 60 and 80 % would give a similar shape for SOL, although slightly shifted.

To match the measured $E(\psi_{leaf-x}, \psi_{soil})$, we inversely modelled the $E(\psi_{leaf-x}, \psi_{soil})$ relation by varying K_{plant} and the active root length.

2.4   RESULTS

In wet soils ($\theta > 0.114$), the relation between leaf xylem water potential (ψ_{leaf-x}) and transpiration (E) had a constant slope (Figure 2.1). As the soil progressively dried, $E(\psi_{leaf-x})$ became non-linear, with ψ_{leaf-x} rapidly and non-linearly decreasing for small increases in E. The slope of the $E(\psi_{leaf-x})$ relation was nearly constant in wet soils, with the slope being equal to K_{plant} (6.25×10^{-7} cm^3 s^{-1} MPa^{-1}), and decreased as the soil dried, indicating a decrease in K_{sp}.
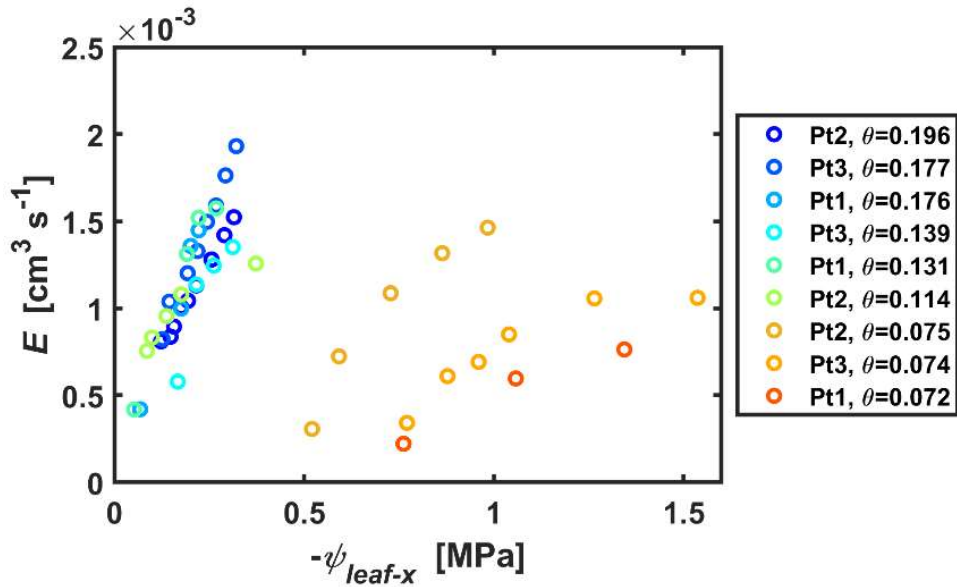
Figure 2.1 *Relation between leaf xylem water potential ($\psi_{leaf\text{-}x}$) and transpiration (E) for different soil water contents (θ: cm^3 cm^{-3}). The relation shifts from linear to non-linear during soil drying. Pt: plant number, n=3.*
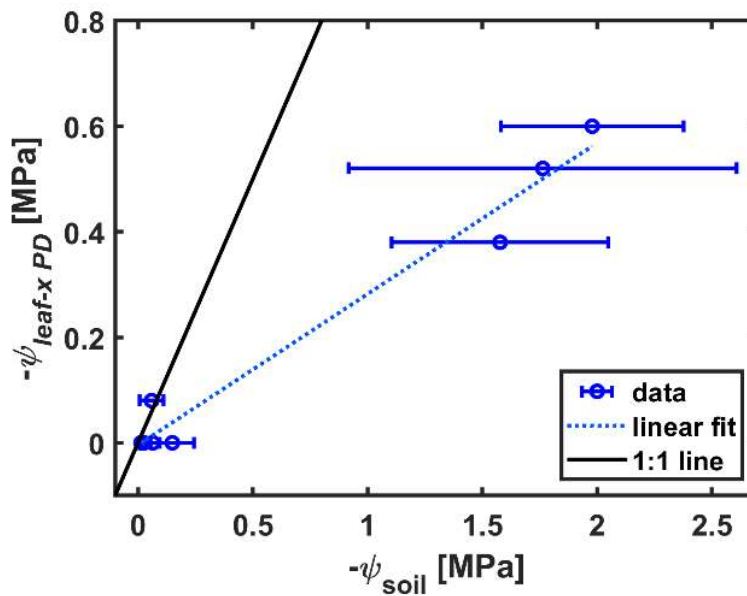
Figure 2.2 *Predawn leaf water potential ($\psi_{leaf\text{-}x\ PD}$), obtained from the intercept of E($\psi_{leaf\text{-}x}$) with E = 0, against the soil matric potential (ψ_{soil}) obtained from the measured soil water contents (θ) and the water retention curve. The dashed line is the best linear fit. The solid line is 1:1 line. In each sample, θ was measured five times and ψ_{soil} was calculated from each of them.*

The intercept of the $E(\psi_{\text{leaf-x}})$ relation with the axis $E = 0$, here defined as the predawn leaf xylem water potential ($\psi_{\text{leaf-x PD}}$), deviated from the soil matric potential (ψ_{soil}) estimated from the measured θ and the retention curve (Figure 2.2). Note that $\psi_{\text{leaf-x PD}}$ is not simply expected to be equal to the averaged ψ_{soil} but to a ψ_{soil} that is weighted according to root length distribution (Couvreur *et al.* 2012). Here, we also neglected the gravitational potential, which for our sample size is justified for pressure differences above 0.01 MPa. We come back to the difference between $\psi_{\text{leaf-x PD}}$ and ψ_{soil} in the discussion.

E decreased as the soil dried in both pressurized and non-pressurized plants, but in non-pressurized plants, the decrease was much more marked (Figure 2.3). E slightly decreased also in pressurized plants despite water in the leaf xylem was kept at atmospheric pressure. However, the difference is not significant.
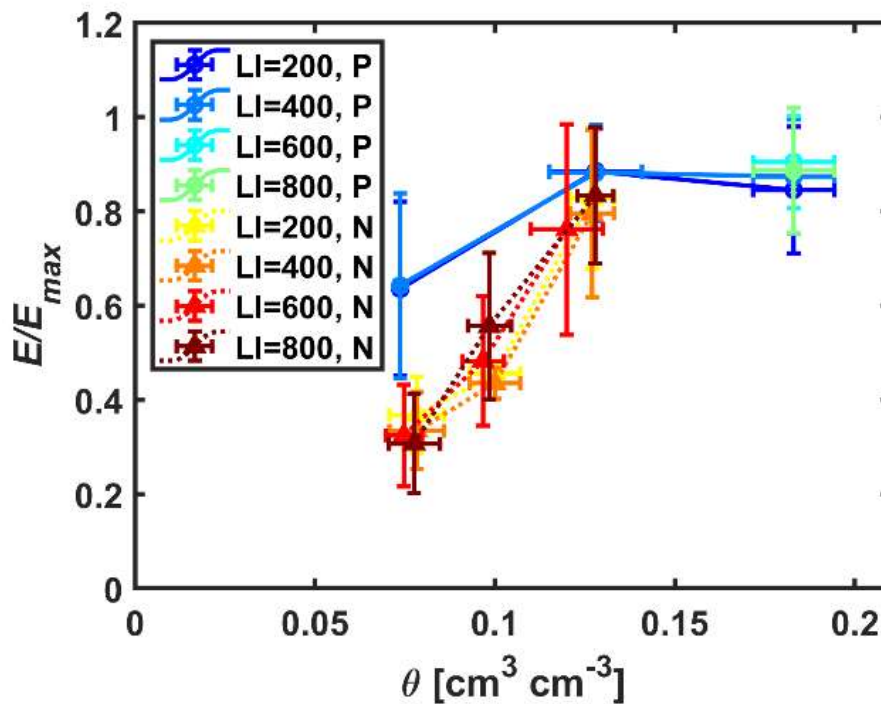
Figure 2.3 *Normalized transpiration rate (E/E$_{max}$) during soil drying (θ: soil water content) under different light intensities (LI: μmol m^{-2} s^{-1}) for pressurized plants (P) and non-pressurized plants (N). Each point is the mean of three plants.*

The $\psi_{\text{leaf-x}}$ in pressurized and unpressurized plants was similar under the same E and θ, with values close to the 1:1 line ($r^2 = 0.7$) (Figure 2.4). This means that the plant conductance (K_{plant})

did not change under plant pressurization. This implies that there was no significant decrease in the conductivities of shoot and xylem vessels during soil drying. We will come back to this important point in the discussion.

The soil–plant hydraulic model was able to reproduce the observed $E(\psi_{\text{leaf-x}})$ relation. To match the measurements, the active root length was reduced to 20 m, while the measured one was 75.4 ±1.3 m ($n = 3$). The water retention curve and soil hydraulic conductivity used in the model are shown in Figure 2.5. The Brooks-Corey parameterization, used in the soil–plant model (blue line), fits well the measured hydraulic properties (red line) in the range of soil water contents and soil water potential relevant for the experiments (blue solid line) (Brooks and Corey, 1966).
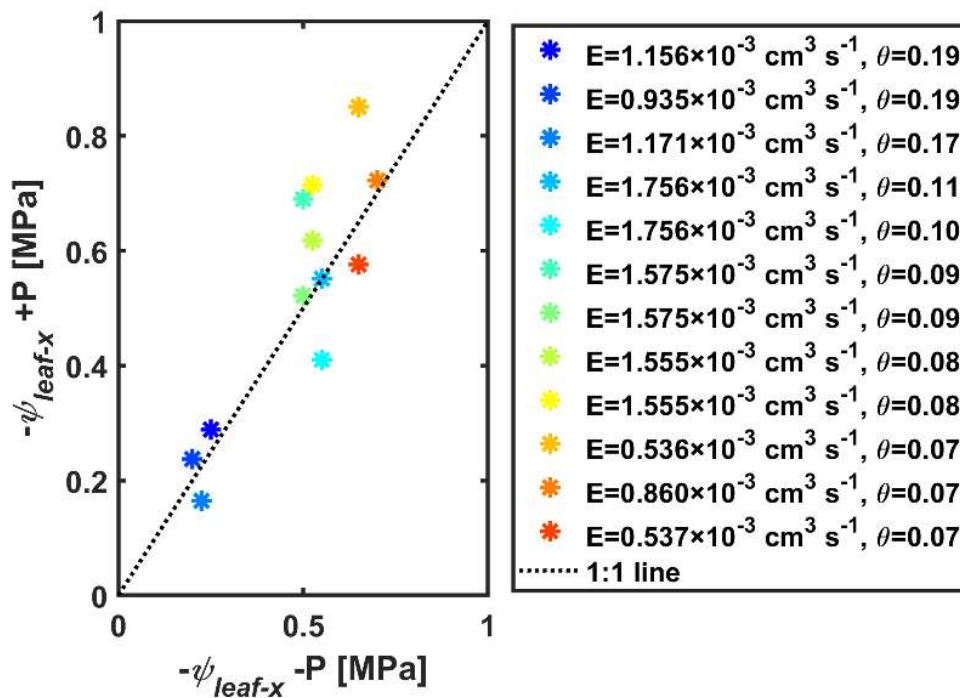
Figure 2.4 *Comparison of leaf water potential (ψ_{leaf-x}) in pressurized (+P) and unpressurized (-P) plants at the same soil water content (θ [cm³ cm⁻³]) and transpiration (E [cm² s⁻¹]). r2 = 0.7. ψ_{leaf-x} of pressurized plant was measured by the root pressure chamber system, while ψ_{leaf-x} of unpressurized plants was measured by the Scholander leaf pressure chamber.*

46

The same set of parameters was used to fit the three plants at all water contents. The onset of hydraulic limitation was defined when $\left.\frac{\partial E}{\partial \psi_{leaf-x}}\right|_{\psi_{soil}}$ reached 70 % of its maximum value and it is plotted as a red line in Figure 1.6, A and B.

The model allows to reconstruct the surface $E(\psi_{leaf-x}, \psi_{soil})$ and to plot E as a function of ψ_{soil} (Figure 2.6). In Figure 2.6B, we used $\psi_{leaf-x\ PD}$ instead of ψ_{soil} estimated from the TDR and the water retention curve. The reasons are discussed later in the discussion section. In Figure 2.6, we included E and ψ_{leaf-x} measured in unpressurized plants at the maximum LI of 800 µmol m^{-2} s^{-1} (red squares obtained from three plants at three water contents – same data as those shown in Figure 2.4). The decrease in E for decreasing leaf and soil water potentials matches well with the onset of hydraulic limitation (red line), showing a strong correlation ($r^2 = 0.6$) between stomatal closure and hydraulic limitation. Note, that we do not claim that stomatal closure is always at the onset of hydraulic limitations, but rather that stomatal conductance does not cross the hydraulic limitation represented by the SOL line.
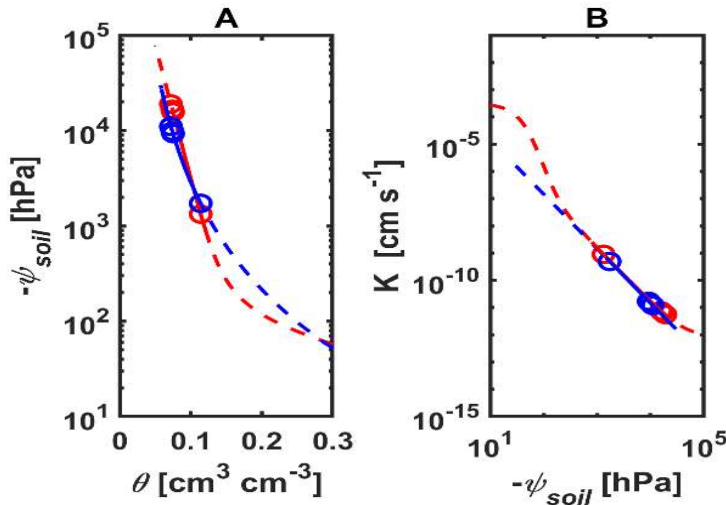
Figure 2.5 (A) Soil water retention curve as fitted with the van Genuchten parameterization (red) and Brooks and Corey model (blue). The solid part of the lines shows the range of water content (θ) relevant for the experiment. (B) Unsaturated hydraulic conductivities (K) fitted with the Peters-Durner-Iden parameterization (red) and with a power-law relation (Eqn. S5, blue).
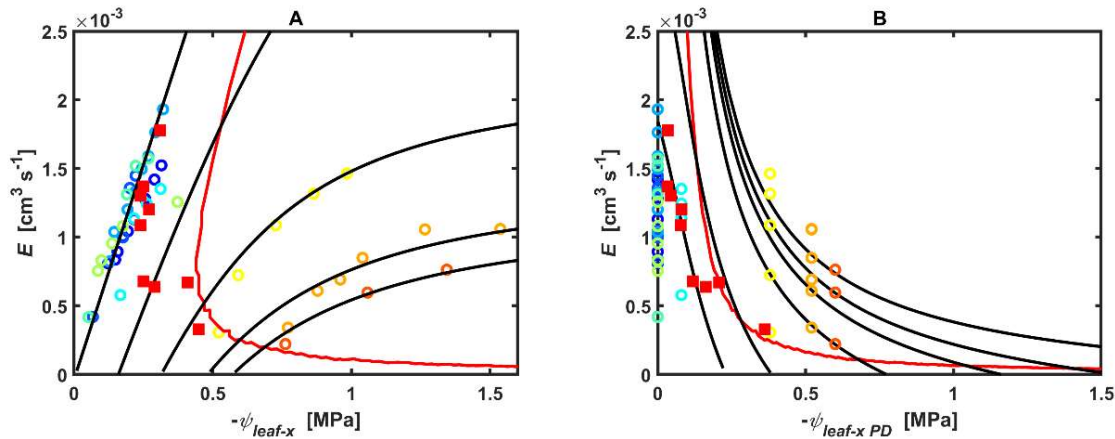
Figure 2.6 *Measured (open circles) and fitted (black lines) relationship between transpiration rate (E), leaf xylem water potential ($\psi_{leaf\text{-}x}$), and soil water potential (here replaced by the pre-dawn leaf water potential; $\psi_{leaf\text{-}x\,PD}$). The relation is plotted as (**A**) the plant view $E(\psi_{leaf\text{-}x})$ and as (**B**) the soil view $E(\psi_{leaf\text{-}x\,PD})$. The point at which the slope of $E(\psi_{leaf\text{-}x})$ reaches 70% of its maximum value is marked by the red line (onset of hydraulic limitation) in both (**A**) and (**B**). The transpiration rates and leaf water potentials of unpressurized plants during soil drying are shown as red squares (3 plants at 3 soil water contents).*

Figure 2.7 shows an additional way to compare the decrease of E to the soil–plant hydraulic limitation. K_{sp} was normalized by the highest K_{sp} (K_{sp_max}) at the highest θ. E was normalized by the highest E at the same light intensity. E was measured in unpressurized plants while K_{sp} was obtained from pressurized plants. The results are plotted for different soil water contents. The decline in normalized K_{sp} matched very well the reduction in normalized E ($r^2 = 0.9$). This shows that stomatal closure corresponds to a decrease in K_{sp}.

2.5 DISCUSSION

In tomato, $E(\psi_{leaf\text{-}x})$ was linear in wet soils, which is in line with the studies on wheat (Passioura 1980; Deery *et al.* 2013) barley (Carminati *et al.*, 2017), maize (Hayat *et al.*, 2020), pearl millet (Cai *et al.*, 2020a) and lupin (Hayat *et al.* 2019). The linearity is explained by the fact that in wet soils the plant hydraulic conductance is constant and lower than that of the soil, thereby controlling the water flow. As the soil dried, its conductivity decreased by several orders of magnitude and the $E(\psi_{leaf\text{-}x})$ relation became non-linear which is in line with previous studies on wheat, barley, and maize (Passioura, 1980; Carminati *et al.*, 2017; Hayat *et al.*, 2020).

The non-linearity of $E(\psi_{\text{leaf-x}})$ and the associated decline in K_{sp} were concomitant with stomatal closure. This is shown by the good match between the onset of hydraulic limitation and independent measurements of transpiration response to soil drying (Figure 2.6), as well as by parallel responses of E and K_{sp} to decreasing soil water content. These results support the hypothesis by Sperry and Love (2015) and Carminati and Javaux (2020) that stomatal closure is triggered by a drop in K_{sp}.
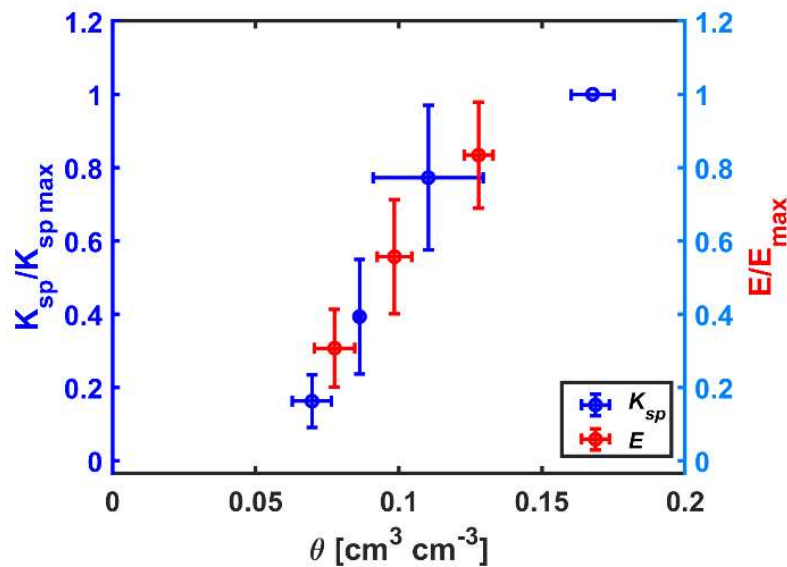
Figure 2.7 *The drop in soil–plant hydraulic conductance (K_{sp}) matches the reduction in transpiration (E) during soil drying (θ: soil water content, cm³ cm⁻³). K_{sp} was determined at the maximum measured E of the pressurized plants. E was obtained at the light intensity of 800 μmol m⁻² s⁻¹ without pressurization.*

K_{sp} decreased at relatively high leaf xylem water potential (the maximum value of the red line is -0.39 MPa in Figure 2.6) compared to the value of -1.0 MPa that was recently reported to cause an embolism in tomato (Skelton *et al.*, 2017). In our model, the water potential at which the xylem cavitates was set to -1.5 MPa (ψ_{0x} in Eqn. S9), which is in the most negative range of leaf xylem water potentials that we simulated, which means that we could have chosen a more negative value without affecting the results. As the water in the leaf xylem was maintained at atmospheric pressure during the measurements of $E(\psi_{\text{leaf-x}})$, the risk of cavitation was reduced (Passioura and Munns, 1984). Moreover, K_{sp} was not substantially affected by pressurization, which is shown by the high correlation ($r^2 = 0.7$) between the measurements of

leaf xylem water potential of pressurized and unpressurized plants (Figure 2.4). The fact that K_{sp} was identical in pressurized and unpressurized plants suggests that its decline in drying soils took place below-ground, as neither the xylem nor the shoot were affected by a decline in water pressure.

The decline in K_{sp} at a relatively high ψ_{leaf-x} indicates a marked vulnerability to soil drying (Figure 2.6). The root length density was relatively small (2.5 cm cm^{-3}) compared to the value of 13.5 cm cm^{-3} measured in pearl millet (Cai *et al.*, 2020a). This might explain the drop in K_{sp} at a relatively high ψ_{leaf-x}. This result could be reproduced by the model imposing a root length of 20 m, which corresponds to *ca.* 25 % of the measured root length (75.4 m ±1.3). The simulations support the hypothesis that the hydraulic decline was caused by water potential dissipation in the soil (Eqn. S7). An additional cause of the hydraulic decline is root shrinkage and the formation of air-filled gaps at the root-soil interface (Carminati *et al.*, 2013; Rodriguez-Dominguez and Brodribb, 2020). Plants developed strategies, e.g. root hairs and mucilage exudation, to bridge gaps and hence softening the drop of the matric potential at the root-soil interface (Carminati *et al.* 2016; Ahmed, Passioura and Carminati 2018). However, tomato has been reported to have short root hairs (*ca.* 120 µm; Guo *et al.* 2009), which might hinder their ability to bridge the hydraulic break between soil and roots and prevent the drop in the matric potential across the rhizosphere. Our data do not allow to conclude on what is the main limitation on water flow to the root. So, it is not clear whether the main limitation to water uptake is in the soil or across the root-soil interface. Additional research is needed to investigate the effects of root shrinkage on water fluxes.

Pressurization increased E at low soil water content ($\theta < 0.12$), as it maintained leaf turgidity. This finding is in line with previous studies in wheat, sunflower (Gollan *et al.* 1986), maize (Hayat *et al.*, 2020), and pearl millet (Cai *et al.*, 2020a). Still, a trend in stomatal closure under severe drying (see the reduced E at $\theta < 0.07$; Figures 2.1, 2.3 and 2.6) is visible even in pressurized plants, as previously shown in Gollan et al. (1986), Holbrook et al. (2002) and Cai et al. (2020a). At such negative soil water potentials, a root signal might be responsible for the moderate stomatal closure despite the leaves being turgid (Dodd, 2005). However, it might also be that during the measurements the increase in suction could not be instantaneously balanced by the applied pressure inducing a temporary loss of turgidity in the leaves.

Additionally, as plants were not pressurized throughout the whole period of soil drying (which took some days), it might be that ABA produced before plant pressurization was still present in the plant tissues.

In terms of soil water potential, transpiration decreased to *ca.* its 50 % value at $\psi_{\text{leaf-x PD}}$ of -0.2 MPa, which was less negative than the expected ψ_{soil} (Figure 2.2). The deviations could be caused by a more negative osmotic potential in the xylem than in the soil (Carminati *et al.*, 2017; Cai *et al.*, 2020a) which would cause the suction in the xylem to be lower than that expected based on the soil matric potential. Note that we measured only the pressure component of the $\psi_{\text{leaf-x}}$ (neglecting the osmotic ones). Another reason is the inaccuracy of estimating ψ_{soil} based on measurements of soil water content and water retention curve. First, the water retention curve was measured in unplanted pots, and root growth might have impacted the water retention curve. Second, averaging the soil water content through the column and assigning it to a water potential is not an obvious operation and it is likely to differ from the average soil water potential felt by the plant. The fact that $\psi_{\text{leaf-x PD}}$ was less negative that ψ_{soil} might indicate that roots were radially more conductive in the wettest soil layers. Accurate measurements of water content (or/and water potential) distribution in the root zone will be needed to better resolve the question on the deviation of $\psi_{\text{leaf-x PD}}$ from ψ_{soil}.

In summary, we have shown that, as the soil dried, the relation between leaf xylem water potential and transpiration rate became markedly non-linear, indicating a drop in K_{sp}. The loss of K_{sp} was primarily explained by a decrease in the soil-root conductance. The decrease in soil-root conductance was concomitant with the reduction in transpiration. This confirms the hypothesis that stomata respond to a decrease in soil–plant hydraulic conductance during soil drying. This stomatal regulation is needed to allow plants to cope with the inherent non-linearity of the soil–plant hydraulics.

ACKNOWLEDGMENTS

AUTHOR CONTRIBUTIONS

Al authors conceptualized the study. MA conducted the experiments and wrote the manuscript with the contribution of AC, GC, MJ, and MAA.

2.6   REFERENCES

Ahmed M.A., Passioura J. & Carminati A. (2018) Hydraulic processes in roots and the rhizosphere pertinent to increasing yield of water-limited grain crops: a critical review. *Journal of Experimental Botany* **69**, 3255–3265.

Anderegg W.R.L., Wolf A., Arango-Velez A., Choat B., Chmura D.J., Jansen S., … Pacala S. (2017) Plant water potential improves prediction of empirical stomatal models. *PLOS ONE* 12, e0185481.

Bartlett M.K., Klein T., Jansen S., Choat B. & Sack L. (2016) The correlations and sequence of plant stomatal, hydraulic, and wilting responses to drought. *Proceedings of the National Academy of Sciences* **113**, 13098–13103.

Brooks R.H. & Corey A.T. (1966) Properties of porous media affecting fluid flow. *Journal of the Irrigation and Drainage Division* **92**, 61–90.

Buckley T.N. (2005) The control of stomata by water balance. *New Phytologist* **168**, 275–292.

Buckley T.N. (2019) How do stomata respond to water status? *New Phytologist* **224**, 21–36.

Cai G., Ahmed M.A., Dippold M.A., Zarebanadkouki M. & Carminati A. (2020) Linear relation between leaf xylem water potential and transpiration in pearl millet during soil drying. *Plant and Soil*.

Cai G., Ahmed M.A., Reth S., Reiche M., Kolb A. & Carminati A. (In Press) Measurement of leaf xylem water potential and transpiration during soil drying using a root pressure chamber system. *Acta Horticulturae*.

Carminati A. & Javaux M. (2020) Soil Rather Than Xylem Vulnerability Controls Stomatal Response to Drought. *Trends in Plant Science* **25**, 868–880.

Carminati A., Passioura J.B., Zarebanadkouki M., Ahmed M.A., Ryan P.R., Watt M. & Delhaize E. (2017) Root hairs enable high transpiration rates in drying soils. *New Phytologist* 216, 771–781.

Carminati A., Vetterlein D., Koebernick N., Blaser S., Weller U. & Vogel H.-J. (2013) Do roots mind the gap? *Plant and Soil* 367, 651–661.

Carminati A., Zarebanadkouki M., Kroener E., Ahmed M.A. & Holz M. (2016) Biophysical rhizosphere processes affecting root water uptake. *Annals of Botany* **118**, 561–571.

Corso D., Delzon S., Lamarque L.J., Cochard H., Torres-Ruiz J.M., King A. & Brodribb T. (2020) Neither xylem collapse, cavitation or changing leaf conductance drive stomatal closure in wheat. *Plant, Cell & Environment.*

Couvreur V., Vanderborght J. & Javaux M. (2012) A simple three-dimensional macroscopic root water uptake model based on the hydraulic architecture approach. *Hydrology and Earth System Sciences* **16**, 2957–2971.

Deery D.M., Passioura J.B., Condon J.R. & Katupitiya A. (2013) Uptake of water from a Kandosol subsoil. II. Control of water uptake by roots. *Plant and Soil* **368**, 649–667.

Dodd I.C. (2005) Root-To-Shoot Signalling: Assessing The Roles of 'Up' In the Up and Down World of Long-Distance Signalling In Planta. *Plant and Soil* **274**, 251–270.

Genuchten M.T. van (1980) A Closed-form Equation for Predicting the Hydraulic Conductivity of Unsaturated Soils. *Soil Science Society of America Journal* **44**, 892–898.

Gollan T., Passioura J.B. & Munns R. (1986) Soil water status affects the stomatal conductance of fully turgid wheat and sunflower leaves. *Australian Journal of Plant Physiology* **13**, 459–464.

Guo K., Kong W.W. & Yang Z.M. (2009) Carbon monoxide promotes root hair development in tomato. *Plant, Cell & Environment* **32**, 1033–1045.

Hayat F., Ahmed M.A., Zarebanadkouki M., Cai G. & Carminati A. (2019) Measurements and simulation of leaf xylem water potential and root water uptake in heterogeneous soil water contents. *Advances in Water Resources* **124**, 96–105.

Hayat F., Ahmed M.A., Zarebanadkouki M., Javaux M., Cai G. & Carminati A. (2020) Transpiration Reduction in Maize (Zea mays L) in Response to Soil Drying. *Frontiers in Plant Science* **10**.

Holbrook N.M., Shashidhar V.R., James R.A. & Munns R. (2002) Stomatal control in tomato with ABA-deficient roots: response of grafted plants to soil drying. *Journal of Experimental Botany* **53**, 1503–1514.

Martin-StPaul N., Delzon S. & Cochard H. (2017) Plant resistance to drought depends on timely stomatal closure. *Ecology Letters* **20**, 1437–1447.

Passioura J.B. (1980) The Transport of Water from Soil to Shoot in Wheat Seedlings. *Journal of Experimental Botany* **31**, 333–345.

Passioura J.B. & Munns R. (1984) Hydraulic Resistance of Plants. II. Effects of Rooting Medium, and Time of Day, in Barley and Lupin. *Functional Plant Biology* **11**, 341–350.

Peters A., Iden S.C. & Durner W. (2015) Revisiting the simplified evaporation method: Identification of hydraulic functions considering vapor, film and corner flow. *Journal of Hydrology* **527**, 531–542.

Rodriguez-Dominguez C.M. & Brodribb T.J. (2020) Declining root water transport drives stomatal closure in olive under moderate water stress. *New Phytologist* **225**, 126–134.

Skelton R.P., Brodribb T.J. & Choat B. (2017) Casting light on xylem vulnerability in an herbaceous species reveals a lack of segmentation. *New Phytologist* **214**, 561–569.

Sperry J.S. & Love D.M. (2015) What plant hydraulics can tell us about responses to climate-change droughts. *New Phytologist* **207**, 14–27.

Sperry J.S., Wang Y., Wolfe B.T., Mackay D.S., Anderegg W.R.L., McDowell N.G. & Pockman W.T. (2016) Pragmatic hydraulic theory predicts stomatal responses to climatic water deficits. *New Phytologist* **212**, 577–589.

2.7 Supplementary materials of the first manuscript:

Supplementary figure S1: *Tomato plant is prepared for pressurization.*

Supplementary figure S2: *Direct measurements of transpiration (E), balancing pressure (P), Meniscus height (M), and the applied plant active radiation (PAR) at a deficit soil water content ($\theta = 0.075$ cm³ cm⁻³).*
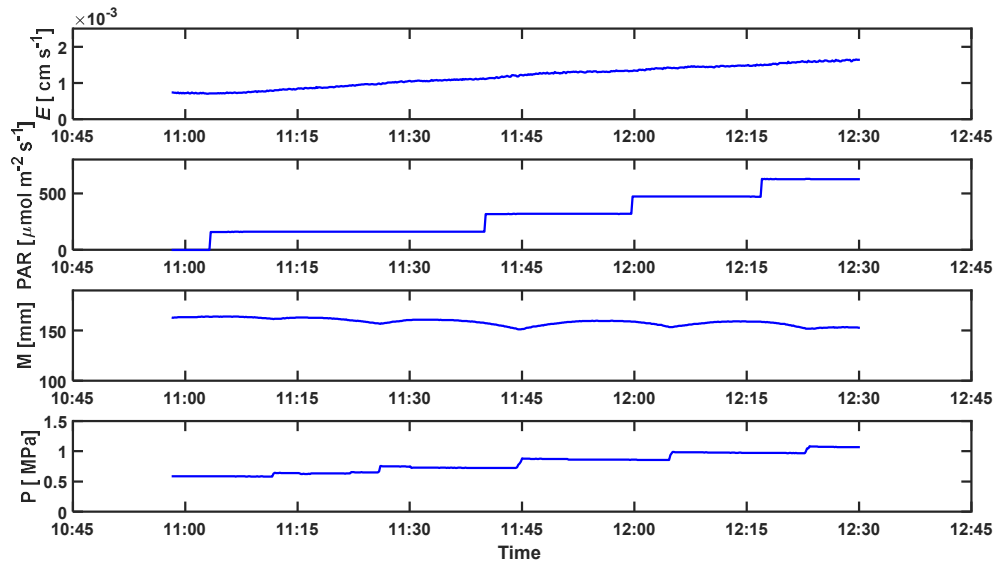
Supplementary note 1: Soil plant hydraulic model

We used a simplified model to reproduce the measurements of the water flow in the soil–plant continuum. The series of resistances between the bulk soil, soil-root interface, and through the root to the leaf xylem were considered in the soil–plant hydraulic model, assuming that one single root represents all active roots that took up water. Water flow in the soil follows Darcy's low:

$$q = -k_s(\psi_{soil}) \frac{\partial \psi}{\partial r} \qquad \text{(Eqn. S1)}$$

Where q is the water flux (cm s^{-1}), K_s is the soil conductivity (cm^2 s^{-1} hPa^{-1}), which is the function of the matric potential ψ (hPa, 1 hPa $\approx$ 1 cm), r is the radial distance (cm), and $\frac{\partial \psi}{\partial r}$ is the gradient in the matric potential. Note that K_s has units of (cm s^{-1}) when the soil matric potential is expressed in unit heads and we used this unit throughout the text.

The boundary conditions were expressed as follows:

$$q(r_0) = \frac{E}{2\pi r_0 L} \qquad \text{(Eqn. S2)}$$

$$q(r_b) = 0 \qquad \text{(Eqn. S3)}$$

Where r_0 and r_b are the root radius and the exterior radius of soil around the root (cm), E is the transpiration rate (cm^3 s^{-1}), L is the active root length in water uptake (cm). r_b is determined by L and V, the volume of the column (cm^3), according to:

$$r_b = \sqrt{\frac{V}{\pi L}} \qquad \text{(Eqn. S4)}$$

The soil hydraulic conductivity was determined according to the Brooks and Corey model, which expressed as follows:

$$K_s(\Psi) = K_{sat} \left(\frac{\psi_{soil}}{\psi_0}\right)^\tau \qquad \text{(Eqn. S5)}$$

Where K_{sat} is the saturated hydraulic conductivity of the soil (cm s^{-1}), ψ_0 is the soil air entry value (hPa), and τ is a fitting parameter (-). From matching the PDI model and Brooks and

Corey model for the experimentally-measured series of potentials we obtained the parameters for Eqn. S5. According to de Jong van Lier *et al.* (2008), and assuming a steady-rate behavior for the water flow in the soil, Eqn. S1 was reformulated using the matric flux potential (Φ, cm^2 s^{-1}):

$$\Phi (\psi) = \int_{-\infty}^{\psi} K(x)dx \qquad \text{(Eqn. S6)}$$

Combining Eqn. 5, Eqn. 6, and the radial Richards equation we obtain the flux boundary condition at the soil-root interface, $\psi_{root\text{-}soil}$, according to Schröder *et. al.*, (2009):

$$\Phi_{root\_soil} = -\frac{E}{2\pi L}\left(\frac{1}{2} - r_b^2\ \frac{\ln(r_b/r_0)}{r_b^2 - r_0^2}\right) + \Phi_{soil} \qquad \text{(Eqn. S7)}$$

Where Φ_{root_soil} is the matric flux potential at the root-soil interface (cm^2 s^{-1}), and Φ_{soil} is the matric flux potential in the bulk soil (cm^2 s^{-1}). Φ_{root_soil} is obtained calculating Eqn. S5 and S6.

The water flow in the root system is given by

$$E = -K_{root}\left(\psi_{root\_xylem} - \psi_{root\_soil}\right) \qquad \text{(Eqn. S8)}$$

where ψ_{root_xylem} and ψ_{root_soil} are the water potential at the root-soil interface and at the xylem collar and K_{root} (cm^3 s^{-1} MPa^{-1}) is the root conductance (assumed to be constant).

The xylem conductance is given by:

$$K_x = K_{root}\left(\frac{\psi}{\psi_{0x}}\right)^{-\tau x} \qquad \text{(Eqn. S9)}$$

which includes the effect of cavitation.

The plant conductance K_{plant} is given by the harmonic mean of K_{root} and K_x:

$$\frac{1}{K_{plant}} = \frac{1}{K_{root}} + \frac{1}{K_x} \qquad \text{(Eqn. S10)}$$

The leaf matric flux potential is calculated as

$$\Phi_{leaf} = -E + \Phi_{root\_xylem} \qquad \text{(Eqn. S11)}$$

and the leaf water potential ψ_{leaf} (which here is defined as the water potential in the leaf xylem) is calculated inserting K_x into Eqn. S6.

The onset of hydraulic limitation is defined as the point at which the slope of $E(\psi_{\text{leaf}})$ reaches 70 % of its maximum.

Supplementary table 1. The parameters used in the model

Parameter	Symbol	value	Unit
Soil saturated conductivity	K_{sat}	2.1×10^{-5}	cm s^{-1}
Fitting parameter for the unsaturated conductivity	τ	2	-
Root conductance	K_{root}	6.25×10^{-11}	cm^3 s^{-1} MPa^{-1}
Soil air entry value	ψ_0	-8.33×10^{-4}	MPa
Xylem air entry value	ψ_{0x}	-1.5	MPa
Fitting parameter for xylem conductivity	τ_{x}	5	-
Active root length in water uptake	L	2000	cm
Root radius	r$_0$	0.05	cm
Soil radius around the root	r$_{\text{b}}$	1	cm
The volume of the column	V	2047	cm^3

BIBLIOGRAPHY

de Jong van Lier Q., van Dam J.C., Metselaar K., de Jong R. & Duijnisveld W.H.M. (2008) Macroscopic Root Water Uptake Distribution Using a Matric Flux Potential Approach. *Vadose Zone Journal* **7**, 1065–1078.

Schröder T., Javaux M., Vanderborght J., Körfgen B. & Vereecken H. (2009) Implementation of a Microscopic Soil–Root Hydraulic Conductivity Drop Function in a Three-Dimensional Soil–Root Architecture Water Transfer Model. *Vadose Zone Journal* **8**, 783–792.

3 Chapter three: Stomatal closure during water deficit is controlled by below-ground hydraulics

Mohanned Abdalla[1,2], Mutez Ali Ahmed[1], Gaochao Cai[1], Fabian Wankmüller[3], Nimrod Schwartz[4], Or Litig[4], Mathieu Javaux[5,6], and Andrea Carminati[3]

[1]Chair of Soil Physics, Bayreuth Center of Ecology and Environmental Research (BayCEER), University of Bayreuth, Bayreuth, Germany.

[2]Department of Horticulture, Faculty of Agriculture, University of Khartoum, Khartoum North, Sudan.

[3]Physics of Soils and Terrestrial Ecosystems, Department of Environmental Systems Science, ETH Zürich, Zürich, Switzerland.

[4]Department of Soil and Water Science, The Hebrew University of Jerusalem, Rehovot, Israel.

[5]Earth and Life Institute-Environmental Science, Universite catholique de Louvain, Louvain-la-Neuve, Belgium.

[6]Agrosphere (IBG-3), Forschungszentrum Juelich GmbH, Juelich, Germany.

3.1 ABSTRACT

Background and Aims: Stomatal closure allows plants to promptly respond to water shortage. Although the coordination between stomatal regulation, leaf and xylem hydraulics has been extensively investigated, the impact of below-ground hydraulics on stomatal regulation remains unknown.

Methods: We used a novel root pressure chamber to measure, during soil drying, the relation between transpiration rate (E) and leaf xylem water pressure ($\psi_{\text{leaf-x}}$) in tomato shoots grafted onto two contrasting rootstocks, a long and a short one. In parallel, we also measured the $E(\psi_{\text{leaf-x}})$ relation without pressurization. A soil–plant hydraulic model was used to reproduce the measurements. We hypothesize that (1) stomata close when the $E(\psi_{\text{leaf-x}})$ relation becomes non-linear and (2) non-linearity occurs at higher soil water contents and lower transpiration rates in short-rooted plants.

Key Results: The $E(\psi_{\text{leaf-x}})$ relation was linear in wet conditions and became non-linear as the soil dried. Changing below-ground traits (i.e. root system) significantly affected the $E(\psi_{\text{leaf-x}})$ relation during soil drying. Plants with shorter root systems required larger gradients in soil water pressure to sustain the same transpiration rate and exhibited an earlier non-linearity and stomatal closure.

Conclusions: We conclude that, during soil drying, stomatal regulation is controlled by below-ground hydraulics in a predictable way. The model suggests that the loss of hydraulic conductivity occurred in soil. These results prove that stomatal regulation is intimately tied to root and soil hydraulic conductances.

Keywords: *Solanum lycopersicum*, water stress, hydraulic signal, modelling, root system, hydraulic limitations.

3.2 INTRODUCTION

Stomata regulate the exchange of carbon and water between the atmosphere and vegetation (Hetherington and Woodward, 2003; Wolz *et al.*, 2017; Buckley, 2019; Deans *et al.*, 2020). Stomatal regulation provides a key survival feature to terrestrial vegetation under unfavorable conditions, preventing an excessive drop in water pressure and minimizing the risk of xylem cavitation upon drought (Martin-StPaul *et al.*, 2017; Choat *et al.*, 2018; Grossiord *et al.*, 2020). Despite the importance of this regulation, the mechanisms by which edaphic stress impacts transpiration and stomatal regulation remain elusive.

Stomatal regulation has been extensively studied in relation to xylem vulnerability (Scoffoni *et al.*, 2014; Sperry and Love, 2015; Bartlett *et al.*, 2016; Wolf *et al.*, 2016; Anderegg *et al.*, 2017; Henry *et al.*, 2019; Eller *et al.*, 2020). However, other hydraulic limitations occur along the soil–plant continuum before xylem cavitation (Scoffoni *et al.*, 2017; Huber *et al.*, 2019; Corso *et al.*, 2020; Albuquerque *et al.*, 2020), especially below-ground (Rodriguez-Dominguez and Brodribb, 2020; Carminati and Javaux, 2020; Abdalla *et al.*, 2021). For instance, Rodriguez-Dominguez and Brodribb (2020) have recently shown that, in olive trees, the root–soil interface represented the largest hydraulic resistance to water flow. In a follow-up study, Bourbia *et al.* (2021) showed that stomata close concomitantly with the decline in root hydraulic conductivity in both herbaceous and woody species. Abdalla *et al.* (2021) demonstrated that an increase in soil–root hydraulic resistance was the main driver of stomatal closure in tomato. Carminati and Javaux (2020), by means of a soil–plant hydraulic model and a meta-analysis, showed that the loss of soil conductivity, rather than xylem, constrains transpiration. They proposed that stomata close at the onset of hydraulic limitation – i.e. when the relation between transpiration and leaf water potential becomes non-linear (Sperry and Love, 2015; Carminati and Javaux, 2020; see Figure 3.1 for details of the main hypothesis). In other words, the loss in soil hydraulic conductance entails severe gradients in soil matric potential around roots, which cause an excessive drop in leaf water pressure to sustain a tiny increment in transpiration. Hence, the relation between stomatal conductance and leaf water potential should be soil- and root-specific (Carminati and Javaux, 2020).

Despite the advances in conceptual and modelling work linking stomatal regulation to soil–plant hydraulics (Sperry and Love, 2015; Wang *et al.*, 2020), there is no conclusive

experimental proof that stomatal closure is driven by the loss in below-ground hydraulic conductances (i.e. contrasting root system or soil textures). Previous modelling studies explained midday stomatal closure by the reduction in below-ground hydraulic conductance (Williams *et al.*, 2001; Fisher *et al.*, 2006; Lier *et al.*, 2013). However, these modelling exercises still require experimental validations. Gollan *et al.* (1985, 1986) compared stomatal behavior of pressurized and unpressurized plants, and showed that stomata close in dry soil conditions even though the shoots were kept turgid. However, Gollan and co-authors did not attempt to link stomatal closure to the onset of the hydraulic non-linearity. We have recently provided the first systematic experimentation to test stomatal sensitivity to the hydraulic non-linearity (Abdalla *et al.*, 2021). We showed that stomatal closure was concomitant with the onset of the non-linearity in $E(\psi_{leaf-x})$-relation (Abdalla *et al.*, 2021). In this study, we ask the following question: do differences in below-ground traits (i.e. contrasting root system) impact the *$E(\psi_{leaf-x})$*-relation during soil drying?

We experimentally tested the hypothesis that below-ground hydraulics, i.e. soil, root and/or their interface, determine the relation between stomatal conductance and leaf water potential. We measured leaf xylem water pressure (ψ_{leaf-x}) and transpiration rate (E) in tomato shoots grafted onto two contrasting rootstocks, a short and a long one. To sustain the same transpiration rate, the short root system would require a larger water flow per root surface, and thus larger gradients in soil matric potential (Figure 3.1). Therefore, plants with shorter root system should exhibit a more marked non-linearity in the *$E(\psi_{leaf-x})$* relation and should close stomata at less negative leaf water pressures (Figure 3.1). Alternatively, the larger root system might attenuate the drop in leaf water pressure because of its larger hydraulic capacitance; i.e. not only the ability to conduct water but also the capacity to store water might affect stomatal regulation.

We employed a root pressure chamber designed by Passioura (1980) and implemented by Gollan *et al.* (1986) and recently by Cai *et al.* (2020a) to measure the soil–plant hydraulic conductance during soil drying. This method makes it possible to explore the non-linear part of the *$E(\psi_{leaf-x})$* relation. Additionally, we measured transpiration, leaf water pressure (refers to the hydrostatic component of leaf water potential) and root water content during soil drying.

66

The soil–plant hydraulic model of Carminati and Javaux (2020) was used to reproduce and interpret the data.
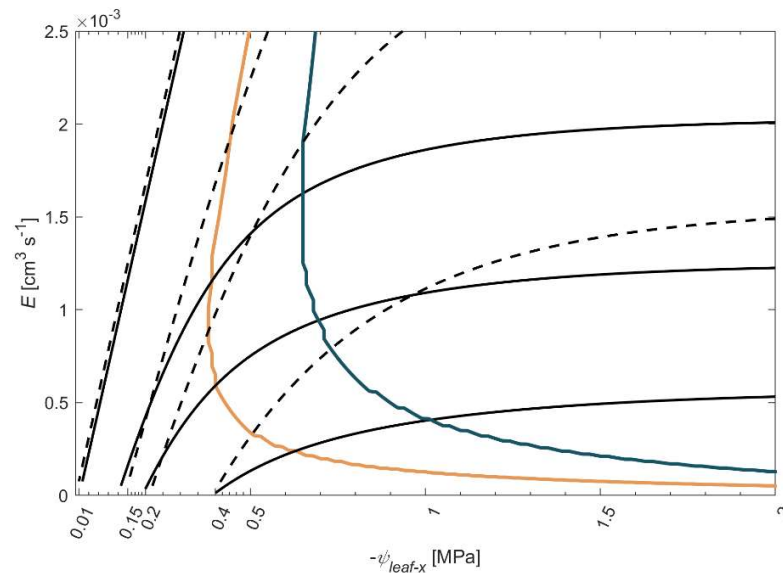
Figure 3.1 Hypothesis: *Reduction in root length causes an earlier drop in soil hydraulic conductance and an earlier stomatal closure. Relation between transpiration (E) and leaf xylem pressure ($\psi_{leaf\text{-}x}$) as simulated by a model of water flow across the soil, the root system and along the xylem, including the non-linearity of their hydraulic conductances (Carminati and Javaux 2020). The model hypothesizes that stomata close at the onset of hydraulic limitation (SOL), which is defined as the point at which the slope of $E(\psi_{leaf\text{-}x})$ reaches 50% of its maximum (see Methods and Table S2). $E(\psi_{leaf\text{-}x})$-relations were simulated at soil matric potentials of -0.01, -0.15 -0.2, and -0.4 MPa. Plants with short root system (solid black lines, and orange SOL) require larger gradients in soil matric potential around their roots, which results in a marked non-linearity in $E(\psi_{leaf\text{-}x})$, compared to plants with a long root system (dashed lines, and blue SOL). Consequently, stomatal closure occurs at less negative $\psi_{leaf\text{-}x}$ for plants with short root systems (orange line for the short and blue line for the long root system).*

3.3 MATERIALS AND METHODS

3.3.1 Plant preparation

Two tomato varieties with contrasting root lengths were used as rootstocks; *Lycopersicon hirsutum* and a hybrid of *L. hirsutum* and the wild tomato *L. pimpinellifolium* were used as long- and short-rooted plants, respectively. Scions from *Solanum lycopersicum* L. (M82 variety) were grafted onto these two rootstocks. Seeds were provided by Rootility (Israel). Seeds were sown in polyvinyl chloride (PVC) columns 30 cm in height and 10 cm in diameter. The columns had five holes with a diameter of 5 mm on the side to facilitate soil moisture content measurements. The PVC columns were topped (using a silicon rubber glue; Teroson, Henkeln, Germany) with a 0.8-cm-thick aluminum plate that had a centered-hole of 1.4 cm in diameter.

Plants were grafted ~1 week after germination when their stem diameters were matching (Notaguchi *et al.*, 2020). Immediately after grafting, plants were placed inside a chamber at ~95% relative humidity and 200 µmol m^{-2} s^{-1} Photosynthetic photon flux density (PPFD) for 4 d to avoid scion desiccation (Rosskopf *et al.*, 2017). Thereafter, plants were placed in a climate-controlled room with a day/night temperature of 28/18 °C, a day/night relative humidity of 57/65 %, 14 h photoperiod and PPFD of 600 µmol m^{-2} s^{-1} during the daytime (Luxmeter PCE-174, Meschede, Germany).

After 12 d, plants were moved to the laboratory and sealed at the collar using glue (UHU plus Endfest 300, Bühl, Germany). During the experiments, leaves were imaged to determine leaf area (LA; cm^2) using ImageJ 1.50e (http://imagej.nih.gov/ij). After the experiments, roots were washed and root length was measured using WinRihzo (Regent Instruments, Canada). Figure S1 shows root length and leaf area.

3.3.2 Soil preparation

A sandy loam soil was used in the experiments. Quartz sand and loamy soil were sieved through a 1-mm sieve. The sieved substrates were mixed in the ratio of 62.5 % loamy soil and 37.5 % quartz sand. The soil water content (θ [cm^3 cm^{-3}]) was measured using a time-domain refractometer (TDR) (E-Test, Lublin, Poland). The hydraulic properties of the soil mixture

were determined via a Hyprop system (UMS, Munich, Germany), which implemented the evaporation method. The water retention curve and the unsaturated hydraulic conductivity were fitted using the Peters–Durner–Iden (PDI) model (Peters *et al.*, 2015). The corresponding parameters were estimated by fitting the measured soil matric potential and solving the Richards equation.

3.3.3 Transpiration and leaf xylem water pressure measurements

We used a novel root pressure chamber system (RPCS) to simultaneously measure transpiration (E) and leaf xylem water pressure ($\psi_{\text{leaf-x}}$) within an intact plant (Cai *et al.* 2020a). The construction and calibration of RPCS was recently described in Cai *et al.*(2020b). Briefly, RPCS is composed of a pressure chamber topped with a cuvette and a control unit. Four groups of light-emitting diode (LED) lamps were vertically attached to the cuvette. The lamps provided PPFD that ranged adjustably from 0 to 1000 µmol m^{-2} s^{-1}. We altered E by changing PPFD, and the latter was measured via a fixed radiometric sensor (Gamma Scientific, San Diego, USA). A constant airflow passed through the cuvette (8.25 L min^{-1}) and a fan was used to stir the air inside. Combined temperature–humidity sensors (Galltec-Mela, Bondorf, Germany) continuously measured the temperature and the relative humidity of the inward and the outward air. We determined E by multiplying the airflow by the difference between the outward and the inward humidity. Canopy conductance was calculated as $g_c = (E/LA)/(VPD/P_{\text{atm}})$ according to Jarvis and McNaughton (1986), where VPD is vapour pressure deficit and P_{atm} is atmospheric pressure.

The basic principle of the method was to balance the negative water pressure inside the plant by applying a pneumatic pressure to the soil and root system, thereby bringing water inside the leaf xylem to atmospheric pressure (Passioura, 1980; Carminati *et al.,* 2017; Cai *et al.,* 2020a) (Supplementary Data Figure S2). The applied pressure (balancing pressure; P) is numerically equal to leaf xylem tension before pressurization (Passioura, 1980). A meniscus system was connected to a leaf cut to evaluate the stability of the droplet. We determined $\psi_{\text{leaf-x}}$ when the meniscus was stable for ~10 minutes (Cai *et al.* 2020a).

To measure $E(\psi_{\text{leaf-x}})$ relation, plants were positioned inside the RPCS, with the column inside the pressure chamber and the shoot inside the cuvette. We modified E by gradually increasing

PPFD from 0 to 200, 400, 600, 800, and 1000 μmol m^{-2} s^{-1}. Simultaneously, the corresponding $\psi_{\text{leaf-x}}$ was determined at each PPFD. Additionally, E was also measured without pressurization at 1000 μmol m^{-2} s^{-1}. Canopy conductance (g_c [mol m^2 s^{-1}]) was calculated from E without pressurization. Each plant was measured for several days during soil drying (Supplementary Data Figure S3 and Table S1).

In parallel, we measured $\psi_{\text{leaf-x}}$ at the highest E for unpressurized plants using a leaf pressure chamber (Soil Moisture Equipment Corp., Santa Barbara, CA, USA) as described in Scholander *et al.* (1965). These measurements were utilized to assess $\psi_{\text{leaf-x}}$ values obtained from pressurized plants at the same values of E and θ (Abdalla *et al.*, 2021).

3.3.4 Osmotic potential

Leaf osmotic potential was measured using a vapour pressure osmometer (VAPRO, Wescore). Xylem sap was collected from a leaf cut using a 10 μL pipette after applying 0.1 MPa more than the balancing pressure. Leaf osmotic potential was measured at different soil matric potentials during soil drying. Soil osmotic potential was measured when the soil was saturated.

3.3.5 Root hydraulic capacitance

Root hydraulic capacitance was obtained by measuring the root water content at decreasing soil matric potentials. Plants from both rootstock genotypes were grown in the sandy loam. When individuals reached targeted soil matric potential, plants were left overnight inside a humid chamber (relative humidity ≈100 %) to allow soil and roots to equilibrate to the same water pressure. Roots were carefully removed from the soil and were gently shaken to remove any attached soil, and initial fresh weight was measured. Root dry weight was obtained after drying the roots for 24 h at 105°C. The difference between fresh and dry weights of the roots was divided by their dry weight at different soil matric potentials to calculate root hydraulic capacitance (see eqn 15).

3.3.6 Soil–plant hydraulic model

We used a soil–plant hydraulic model to simulate the water flow in the soil–plant continuum and fit the measured $E(\psi_{\text{leaf-x}})$ relation. Water flow was modelled through a series of resistances

across the soil, across the soil–root interface, across the root to the root xylem, and along the xylem. We briefly describe the model here.

The Buckingham-Darcy law, ignoring gravity, was used to describe the radial water flow in soil towards the root surface:

$$q = -K_s(\psi_m)\frac{\partial \psi_m}{\partial r} \qquad (1)$$

Where q is the water flux (cm s^{-1}), K_s is the soil hydraulic conductivity, which is a function of the soil matric potential ψ_m (hPa), r is the radial distance (cm) and $\frac{\partial \psi_m}{\partial r}$ is the gradient in matric potential. Note that when the soil matric potential is expressed in unit heads (cm, 1 hPa $\approx$ 1 cm), K_s has units of cm s^{-1}. We use this unit throughout the text when describing soil water flow.

The boundary conditions were expressed as follows:

$$q(r_0) = \frac{E}{2\pi r_0 L} \qquad (2)$$

$$q(r_b) = 0 \qquad (3)$$

Where r_0 and r_b are the root radius and the exterior radius of soil around the root (cm), E is the transpiration rate (cm^3 s^{-1}) and L is the root length active in water uptake (cm); r_b is determined by L and the volume of the column V (cm^3), according to:

$$r_b = \sqrt{\frac{V}{\pi L}} \qquad (4)$$

We parameterized K_s according to the Brooks and Corey model:

$$K_s(\psi_m) = K_{sat}\left(\frac{\psi_m}{\psi_0}\right)^\tau \qquad (En\ 5)$$

Where K_{sat} is the saturated hydraulic conductivity of the soil (cm s^{-1}), ψ_0 is the soil air entry value (cm), and τ is a fitting parameter (–). We obtained the parameters for Eqn (5) by matching the PDI and Brooks and Corey models (Abdalla *et al.*, 2021). According to de Jong van Lier *et al.* (2008), and assuming a steady-rate behaviour for the water flow in the soil, the radial geometry of water flow could be reformulated using the matric flux potential (Φ, cm^2 s^{-1}):

$$\Phi(\psi) = \int_{-\infty}^{\psi_m} K(x)dx \qquad (6)$$

The solution of Eqn (6) describes the matric flux potential at the outer boundary $r=r_b$:

$$\Phi_{soil} = \frac{k_{sat} \cdot \psi_m{}^{1-\tau} \cdot \psi_0{}^{-\tau}}{1-\tau} \qquad (7)$$

Where Φ_{soil} is the matric flux potential in the bulk soil (cm^2 s^{-1}) corresponding to the measured bulk soil matric potential (ψ_m). Meanwhile, the radial flow could be described by combing Eqns (1, 5 and 6) as:

$$q = - \frac{\partial \emptyset (\psi_m)}{\partial r} \qquad (8)$$

We obtain the flux boundary condition at the soil–root interface, Φ_{root_soil} (cm^2 s^{-1}), by combining Eqns (5 and 6) and the radial Richards equation (Schröder *et al.*, 2009):

$$\Phi_{root\_soil} = - \frac{E}{2\pi} \left(\frac{1}{2} - r_b^2 \frac{\ln(r_b/r_0)}{r_b^2 - r_0^2} \right) + \frac{k_{sat} \cdot \psi_m{}^{1-\tau} \cdot \psi_0{}^{-\tau}}{1-\tau} \qquad (9)$$

The water flow in the root is given by

$$E = -K_{root}\left(\psi_{root\_xylem} - \psi_{root\_soil}\right) \qquad (10)$$

Where E is the water flow in the root equal to the transpiration rate (cm^3 s^{-1}), ψ_{root_soil} is the water potential at the root–soil interface (here converted to MPa, 1 MPa $\approx 10^4$ cm), ψ_{root_xylem} is the water potential at the xylem collar (MPa) and K_{root} (cm^3 s^{-1} MPa^{-1}) is the root hydraulic conductance. Note that differences in osmotic potential between soil and root xylem can occur and affect the driving force of water flow across the root–soil interface. Therefore, ψ_{root_soil} and ψ_{root_xylem} are the sum of their respective matric/hydrostatic potentials and osmotic potentials. Doing so, we assume that the reflection coefficient of the root is 1. The difference between leaf and soil osmotic potential is equal to the measured difference between soil matric potential and leaf xylem pressure when water flow is negligible (Cai *et al.* 2020a).

We assume no further change in osmotic potential along the xylem. The xylem conductance, K_x (cm^3 s^{-1} MPa^{-1}), which includes the effect of cavitation, is given by:

$$K_x = K_{root} \left(\frac{\psi_{leaf-x}}{\psi_{0x}}\right)^{-\tau_x} \qquad (11)$$

where, $\psi_{leaf\text{-}x}$ is the leaf xylem pressure (MPa), ψ_{0x} is the xylem pressure (MPa) at which K_x drops and τ_x is a fitting parameter (–) that determines the rate of this drop.

The plant conductance, K_{plant} (cm^3 s^{-1} MPa^{-1}), is given by the harmonic mean of K_{root} and K_x:

$$\frac{1}{K_{plant}} = \frac{1}{K_{root}} + \frac{1}{K_x} \tag{12}$$

The leaf matric flux potential is calculated as:

$$\Phi_{leaf} = -E + \Phi_{root\_xylem} \tag{13}$$

Leaf xylem pressure $\psi_{leaf\text{-}x}$ is calculated by inserting K_x into Eqn (6) and combining Eqns (11 and 13):

$$\psi_{leaf\_x} = (\psi_{root\_xylem}^{1-\tau_x} - \frac{E\,(\tau_x - 1)}{\psi_{0x}^{\tau_x}\,K_{root}})^{\frac{1}{1-\tau_x}} \tag{14}$$

Note that the unit of the matric flux potentials in Eqn (13) differs from those of Eqn (9) because soil and xylem hydraulic conductivities have different units.

Data were firstly fitted for each day of measurements (i.e. at each measured soil water content) individually to estimate K_{root}, L and the offset between soil matric potential and leaf xylem pressure. Inverse simulations revealed that L increased as soil dries (reported and discussed later). Therefore, we conducted direct simulations for each group of plants allowing the parameter L to vary during soil drying. We obtained K_{root} from individual simulations by fitting the linear part of the $E(\psi_{leaf\text{-}x})$-relation, which was constant during soil drying (Abdalla *et al.*, 2021).

The onset of hydraulic limitation is defined as the point at which the slope of $E(\psi_{leaf\text{-}x})$ reaches 50 % of its maximum (the soil matric potential being kept constant: soil isolines) (Carminati and Javaux, 2020). Note that the 50 % is rather arbitrary and indeed a value between 40 and 60 % would give the same shape of the stress onset line (SOL). The maximum slope of $E(\psi_{leaf\text{-}x})$ at any given soil matric potential is at null transpiration – i.e. the slope of $E(\psi_{leaf\text{-}x})$ decreases with increasing E (Carminati and Javaux, 2020).

The model was used (1) to predict the onset of hydraulic limitation and compare it with measurements of transpiration reduction, and (2) to test whether the decline of $E(\psi_{\text{leaf-x}})$ is explained by the loss of soil hydraulic conductivity for the two root systems.

3.3.7 Soil–plant hydraulic model including root capacitance

The model above assumed that all water transpired was taken up from the soil (no changes in root water content) and that the change in soil water content during one measurement cycle was negligible. The calculated $E(\psi_{\text{leaf-x}})$ lines were referred to as soil isolines. The consequence of these assumptions was tested by including measurements of root capacitance and soil drying in the model. We examined to what extent root capacitance attenuates the decline in soil and leaf water potential during one measurement cycle consisting of increasing transpiration rates over a period of ~6 h. The rationale is that root capacitance diminishes the water uptake from the soil. This leads to more water remaining in the soil and a less negative leaf water potential to sustain transpiration.

Root capacitance and soil drying were modelled during one exemplary measurement cycle. The relation between root water content and water potential was obtained by fitting the measured gravimetric root water content θ_g, defined as weight of water in the root divided by root dry weight. The volumetric root water content θ_{root} was calculated based on densities of water and roots ρ_{H2O} and ρ_{wet}:

$$\theta_{root} = \theta_g * \frac{\rho_{wet}}{\rho_{H_2O}} \qquad \text{(Eqn)}$$

where ρ_{wet} is the dry root weight divided by the volume of the wet root. The water flow resulting from root shrinkage is the time derivative of the root water volume. This flow was subtracted from the transpiration rate to obtain the root water uptake. To do so, soil matric potential and root water content were estimated for each time step. We simulated two scenarios: (1) soil drying but no root capacitance; and (2) soil drying and root capacitance. The two scenarios were compared with two isolines calculated using the steady-state soil–plant hydraulic model described in the paragraph above (no root capacitance and no changes in soil water content). We calculated one isoline corresponding to the soil matric potential at the beginning of the measurement cycle (fitted to the first two points) and one soil isoline corresponding to the soil matric potential at the end of the measurement cycle (fitted with the last measurement).

3.3.8 Statistical analysis

We used a mixed model to analyse the influence of root system, soil water content, PPFD and their interactions on E using analysis of variance. Replicates were taken as random factor and the remaining parameters were taken as fixed factors. Furthermore, we tested the values of stomatal closure in $E(\psi_{\text{leaf-x}})$ of the two rootstocks using analysis of covariance. MATLAB 2019a (9.6.0., Mathworks®) was used to perform the statistical analysis.

3.4 RESULTS AND DISCUSSION

Tomato plants were grafted on two contrasting root systems to evaluate the impact of root length on soil–plant hydraulic conductance and stomatal regulation during soil drying. The length of the two root systems differed by a factor of 3 ($P < 0.05$), whereas root diameter and leaf area were similar ($P > 0.05$; Supplementary Data Figure S1).

The relationship between transpiration rates (E) and leaf xylem water pressure ($\psi_{\text{leaf-x}}$) varied between the two root systems (Figure 3.2). $E(\psi_{\text{leaf-x}})$ was linear in wet soils ($\theta \geq 0.15$), with the slope being equal to the plant hydraulic conductance. The relation became non-linear as the soil dried (Figure 3.2). The long root system sustained higher E during soil drying, while a more marked non-linearity in $E(\psi_{\text{leaf-x}})$ appeared in the short root system at relatively high $\psi_{\text{leaf-x}}$ and soil water content (θ). Longer roots ensured the linearity of $E(\psi_{\text{leaf-x}})$ for a broader range of E and θ.

The $\psi_{\text{leaf-x}}$ of pressurized and unpressurized plants, for the same values of E and θ, matched well (Figure 3.3, $r^2 = 0.81$). This result demonstrates that the total hydraulic conductances of pressurized and unpressurized plants were similar, which is consistent with Abdalla *et al.* (2021). Note that pressurization maintained the water pressure in the xylem equal to the atmospheric pressure and hence cavitation did not occur during the measurements. Additionally, pressurized plants had a turgid shoot, whose conductivity is likely to have remained constant during the measurements. The latter is in line with the finding of Skelton *et al.* (2017), who showed a decline in leaf hydraulic conductance when leaf water potential dropped beyond -1.28 MPa in tomato. Further, we used roots of *L. hirsutum* and its hybrid with the wild tomato *L. pimpinellifolium*, which might potentially have more resistant xylem.

Therefore, the non-linearity of $E(\psi_{\text{leaf-x}})$ must have been caused by a decline in the below-ground hydraulic conductivity, either in the soil, in the root system or at their interface.
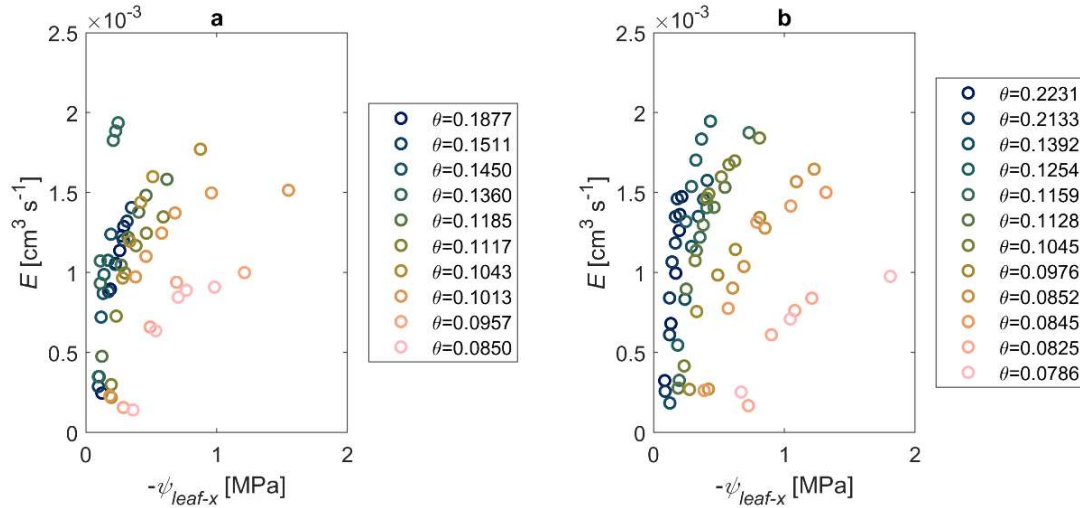
Figure 3.2 *Measured relation between transpiration (E) and leaf xylem pressure (ψ_{leaf-x}) in tomato plants grafted onto (**a**) short root system and (**b**) long root system during soil drying (θ: soil water content [$cm^3\ cm^{-3}$], N = 6).*

The $E(\psi_{\text{leaf-x}})$ and $E(\psi_{\text{soil}})$ relations were well reproduced by the soil–plant hydraulic model of Carminati and Javaux (2020) (black lines in Figure 3.4, a – d). The model calculates the water potential gradients across the soil–plant continuum based on the measured transpiration rates, soil water content and soil hydraulic properties (Materials and methods and Supplemental Data Table S2 for details of the model description and parameters). The fitting parameters were the root length active in root water uptake L, which was allowed to vary with soil drying, root conductance K_{root}, and xylem water pressure at which xylem conductivity drops. The latter was set to -1.5 MPa, which is the most negative value measured in the experiments, and thus does not affect the simulations. This choice was based on the observation that pressurized and non-pressurized plants had the same hydraulic conductance, which means that cavitation did not affect the plant hydraulic conductance. The model reproduced well the experimental observation that a more marked non-linearity in the $E(\psi_{\text{leaf-x}})$ relation occurred in the short root system (Figure 3.4e).
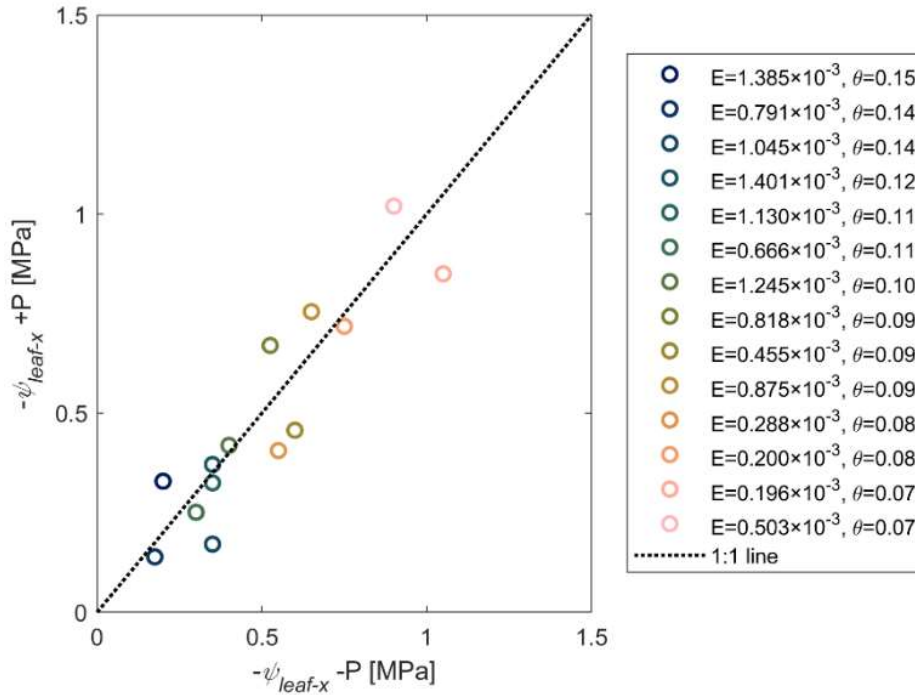
Figure 3.3 *Leaf xylem pressure (ψ_{leaf-x}) in pressurized (+P) and unpressurized (-P) tomato plants at the same soil water content (θ [cm^3 cm^{-3}]) and transpiration rate (E [cm^3 s^{-1}]). ψ_{leaf-x} of pressurized plants was measured by the Root Pressure Chamber System, while ψ_{leaf-x} of unpressurized plants was measured by Scholander leaf pressure chamber (N = 6). ψ_{leaf-x} of pressurized and unpressurized plants, for the same values of E and θ, matched well (r^2 = 0.81).*

The measurements of soil and leaf xylem osmotic potential are consistent with the offset between soil matric potential and predawn leaf xylem pressure. Soil osmotic potential was around -0.02 MPa at soil saturation. This supports the interpretation that the offset was caused by the difference in osmotic potentials. No visible differences were observed between the osmotic potentials of the two root systems, possibly also due to the variability in the measurements (Figure 3.5a).
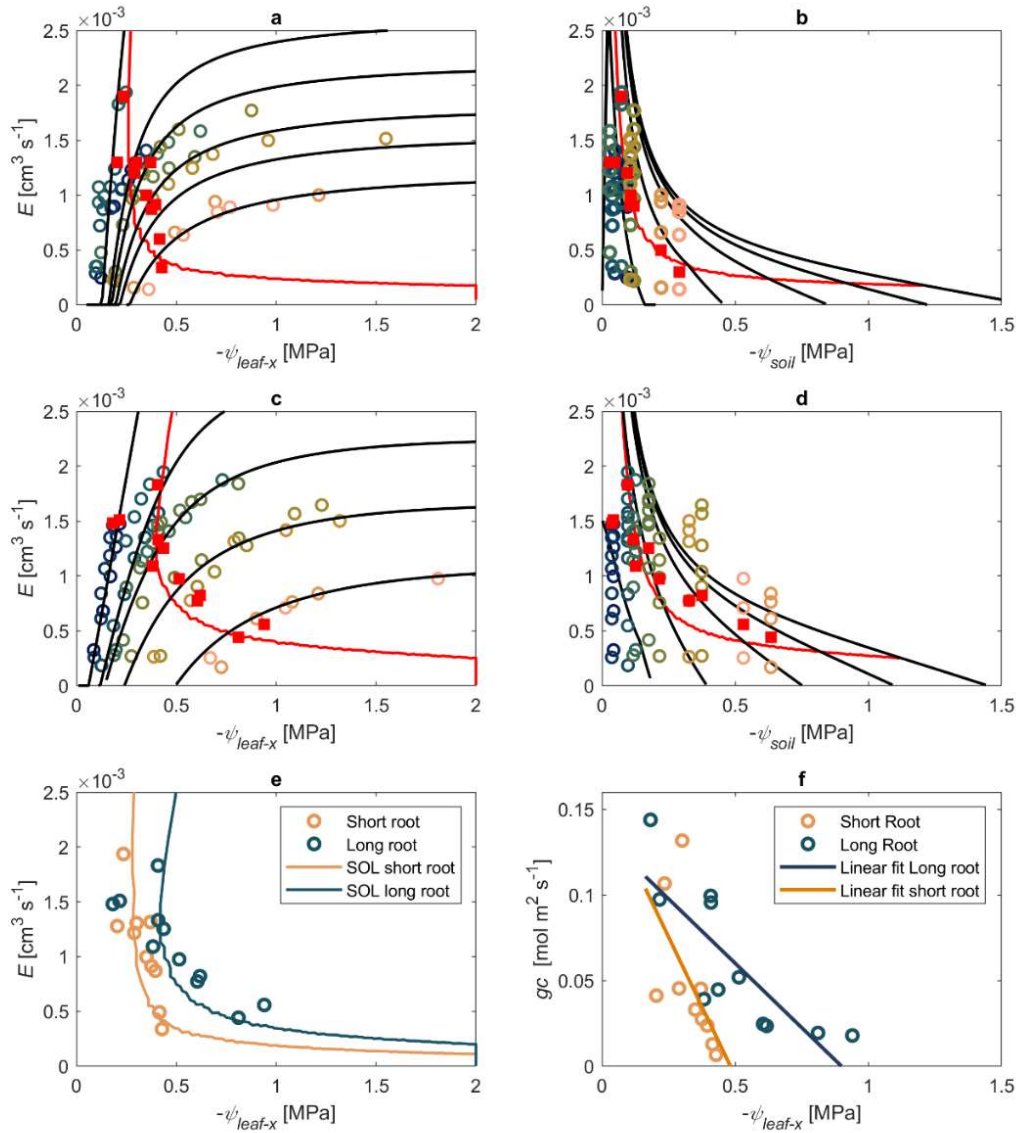
Figure 3.4 *Relation between transpiration rate (E) and leaf xylem pressure (ψ$_{leaf-x}$) (a and c) as well as soil matric potential (ψ$_{soil}$) (b and d), for the short (a and b) and long (c and d) root systems. The measurements (open symbols) were well reproduced by the model (black lines) at different soil water contents (different colors). The relation shifted from linear to non-linear during soil drying. The red line marks the onset of the non-linearity (SOL). The red squares are the measured transpiration rates during soil drying in unpressurized plants (short root system, r^2 = 0.74, 0.72; long root system, r^2 = 0.82, 0.78; from leaf and soil views, respectively (a - d). (e) The onset of hydraulic limitation (SOL) for long rooted (blue line) and short rooted plants (orange line) match well the reduction in transpiration (blue and orange open symbols, respectively). The reduction in transpiration of long and short rooted*

78

plants is significantly different (p-value < 0.001; Figure S4), with the shorter root system reducing transpiration at less negative ψ_{leaf-x}. (f) Canopy conductance (gc) as a function of ψ_{leaf-x} for the short-rooted (orange open symbol) and long-rooted plants (blue open symbol). The slope and the intercept of the linear fit were utilized for the analysis of covariance, which showed a significant difference of stomatal closure between the two root systems (p-value < 0.01).
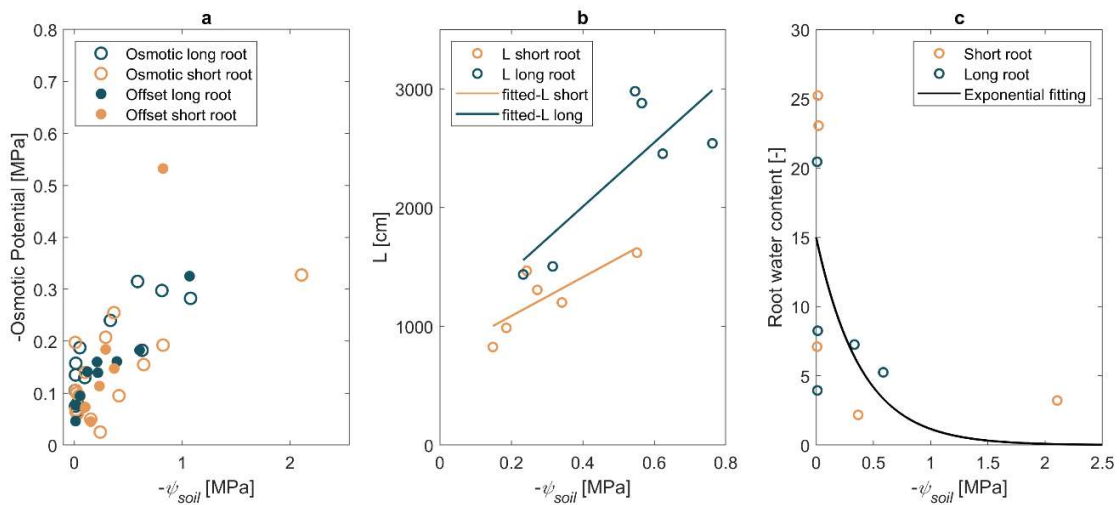
Figure 3.5 a) *Model predictions of the leaf xylem osmotic potential (closed symbols) matched the direct measurements of leaf osmotic potential (open symbols) in both root systems (blue and orange for long and short root systems, respectively) during soil drying.* ***b)*** *Active root length (L) as a function of soil matric potential (ψ_{soil}) for short-rooted (orange open symbol) and long-rooted plants (blue open symbol). Longer rooted plants (blue line) have more active roots, especially in the dry range of ψ_{soil}.* ***c)*** *The difference between root fresh and dry weight was divided by the dry weight to obtain root shrinkage. Root water content decreases exponentially as soil matric potential declines.*

The simulations predict the active root length L as a function of the ψ_{soil} (Figure 3.5b). The simulated active root length L was greater in the plants with the long root system. The explanation is that a longer root length requires a lower flow rate of water at the root–soil interface and smaller gradients in soil matric potential to sustain the same transpiration rate. The simulations support the hypothesis that the non-linearity in the $E(\psi_{leaf-x})$ relation is mainly caused by soil hydraulics. Interestingly, active root length increased as the soil dried, which might be a mechanism to compensate limited fluxes per root segment. The increase in L during

soil drying was also observed in maize (Cai *et al.*, 2021) and might reflect root hydraulic adjustment to soil drying. However, *L* has to be interpreted with caution. *L* is a fitting parameter and might reflect oversimplification of the plant–soil hydraulic model, such as the representation of the root system with a single root and the assumption that the rhizosphere has the same hydraulic conductivity as the bulk soil.

An alternative explanation of the better ability of the long root system to sustain transpiration during soil drying could be the effect of root capacitance. We investigated the effect of root capacitance by including in the simulations the measured decrease in root water content at decreasing soil matric potential (Figure 3.5c). The simulated trajectories of plants with and without root capacitance (green and pink) were very close, indicating that root capacitance had a minor contribution to $E(\psi_{\text{leaf-x}})$ (Figure 3.6). By contrast, the decrease in soil water content during a measurement cycle had significant effects. To understand the effect of decreasing soil water content during a measurement cycle, we plotted the soil isolines at the initial and final stage (orange and blue) of the measurement cycle using the steady-state model. The two isolines perfectly envelop the measurements using a root length of 4000 cm, which is 2.5 times longer than the value estimated using a single line to simulate all points of the measurement cycle ($L = 1496$ cm). The difference in *L* shows the problems in using the isolines to fit the data and interpret *L* as the active root length. The isoline would predict a shorter root length than the actual value, and this mismatch is caused by neglecting the decrease in soil water content. In contrast, the potential role of root capacitance in buffering the decline of soil and leaf water potentials was negligible. However, the choice against specific model simplifications (root shrinkage, rapid soil drying) must match with the research questions addressed. For example, to predict the onset of non-linearity, the classical model approach with soil isolines (solid black line in Figure 3.6) is acceptable. However, to reproduce the leaf water potential measurements and properly estimate the active root length, simulations should include the role of soil drying. In summary, the model simulations reinforce the explanation that the drop in soil conductivity is the main cause of non-linearity in the soil–plant system.
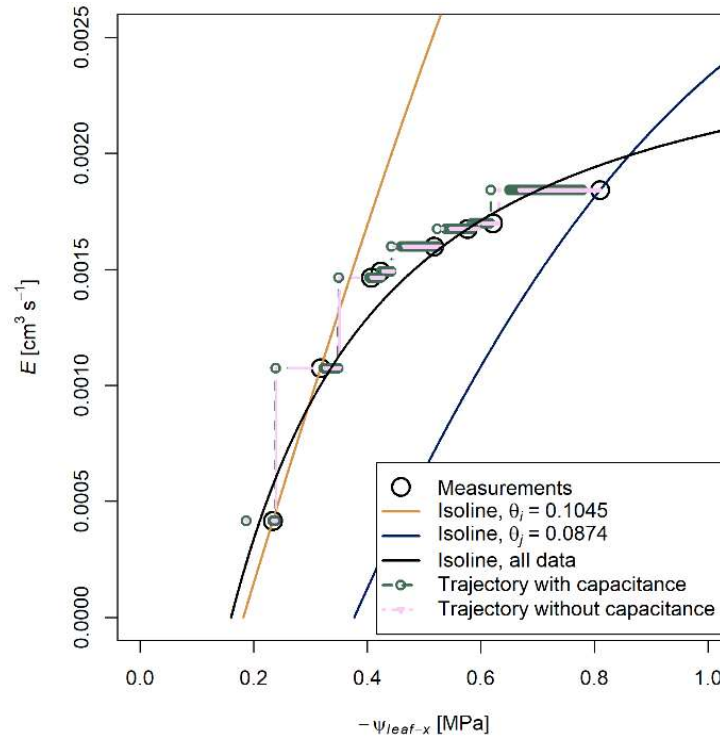
Figure 3.6 *Relation between transpiration rate (E) and leaf xylem pressure ($\psi_{leaf\text{-}x}$) for one exemplary measurement cycle (θ = 0.1045). Different model simulations were compared regarding their explanatory values. The measurements (open black circles) were well captured by a single soil isoline fitted to all data points (solid black line) using the steady-state soil–plant hydraulic model. To understand the effect of decreasing soil water content during the measurement cycle, we plotted the soil isolines at the initial (θ_i = 0.1045) and final (θ_j = 0.0874) soil water content of the measurement cycle (solid orange and blue lines) using the steady-state model but with different fitting parameters (L and K_{root}) compared to the single soil isoline. The simulated trajectories with and without root capacitance (green and pink) were very close, indicating that root capacitance had a minor contribution to the E($\psi_{leaf\text{-}x}$)-relation. Both trajectories reproduced the measurements very well.*

The onset of hydraulic non-linearity (SOL) was defined as the point when the slope of $E(\psi_{\text{leaf-x}})$ decreased down to 50 % of its maximum (Carminati and Javaux, 2020). The SOL matches well with the transpiration rate of unpressurized plants (Figure 3.4a-e). This supports the idea that stomata close when the relation between transpiration rate and leaf water potential becomes non-linear, as hypothesized by Sperry and Love (2015) and Carminati and Javaux (2020).

The measured $E(\psi_{\text{leaf-x}})$ relation as well as the SOL of the long and short root systems differed (Figure 3.4e), which supports our hypothesis (Figure 3.1). Analysis of covariance shows that stomatal closure was significantly different between the two root systems without pressurization ($P < 0.001$, Figure 3.4f, Supplementary Data S4 and Tables S3 and S4). Plants with the short root system reached 50 % transpiration at $\psi_{\text{leaf-x}}$ = -0.3 MPa compared to $\psi_{\text{leaf-x}}$ = -0.5 MPa with the long root system (Figure 3.4e).

Taken together, the measured relations between transpiration rate and leaf water pressure proved that stomata close at the onset of hydraulic non-linearity, as hypothesized in previous models (Sperry and Love, 2015; Carminati and Javaux, 2020). Additionally, the measurements show that a decrease in root length induces an earlier non-linearity in the soil–plant hydraulic conductance and triggers an earlier stomatal closure, which supports our hypothesis (Figure 3.1).

We conclude that the relation between stomatal conductance and leaf water potential is affected by root length and below-ground hydraulics, particularly soil hydraulic conductance. This finding has important implications for understanding and predicting the response of transpiration to drought. So far, the current trend puts the focus on the coordination between stomatal closure and xylem vulnerability (Wolf *et al.*, 2016; Anderegg *et al.*, 2017; Henry *et al.*, 2019; Eller *et al.*, 2020). However, to properly predict stomatal closure and understand its relation to soil–plant hydraulics, root length, root and soil hydraulic conductivities are essential. Our results show a tied link between soil hydraulic conductivity, active root length and stomatal conductance, and the coordination between these variables is central in predicting the ability of plants to cope with water shortage. Further research would be needed to explore variations between plant species growing in contrasting soil textures and climatic conditions.

Acknowledgments

Authors contributions

MA, MAA, GC and AC designed the experiments. MA performed the experiment and wrote the first draft. MA, FW and AC made the simulations. MAA, GC, MJ and AC contributed to the writing. All authors discussed the results and approved the final version.

3.5 REFERENCES

Abdalla M, Carminati A, Cai G, Javaux M, Ahmed MA. **2021**. Stomatal closure of tomato under drought is driven by an increase in soil–root hydraulic resistance. *Plant, Cell & Environment* **44**: 425–431.

Albuquerque C, Scoffoni C, Brodersen CR, Buckley TN, Sack L, McElrone AJ. **2020**. Coordinated decline of leaf hydraulic and stomatal conductances under drought is not linked to leaf xylem embolism for different grapevine cultivars. *Journal of Experimental Botany* **71**: 7286–7300.

Anderegg WRL, Wolf A, Arango-Velez A, *et al*. 2017. Plant water potential improves prediction of empirical stomatal models (R Aroca, Ed.). *PLOS ONE* **12**: e0185481.

Bartlett MK, Klein T, Jansen S, Choat B, Sack L. **2016**. The correlations and sequence of plant stomatal, hydraulic, and wilting responses to drought. *Proceedings of the National Academy of Sciences* **113**: 13098–13103.

Bourbia I, Pritzkow C, Brodribb TJ. **2021**. Herb and conifer roots show similar high sensitivity to water deficit. *Plant Physiology*.

Buckley TN. **2019**. How do stomata respond to water status? *New Phytologist* **224**: 21–36.

Cai G, Ahmed Mutez Ali, Dippold MA, Zarebanadkouki M, Carminati A. **2020a**. Linear relation between leaf xylem water potential and transpiration in pearl millet during soil drying. *Plant and Soil* **447**: 565–578.

Cai G, Ahmed M.A., Reth S, Reiche M, Kolb A, Carminati A. **2020b**. Measurement of leaf xylem water potential and transpiration during soil drying using a root pressure chamber system. *Acta Horticulturae*: 131–138.

Cai G, Carminati A, Abdalla M, Ahmed MA. **2021**. Soil textures rather than root hairs dominate water uptake and soil–plant hydraulics under drought. *Plant Physiology* **187**: 858–872.

Carminati A, Javaux M. **2020**. Soil Rather Than Xylem Vulnerability Controls Stomatal Response to Drought. *Trends in Plant Science* **25**: 868–880.

Carminati A, Passioura JB, Zarebanadkouki M, *et al.* 2017. Root hairs enable high transpiration rates in drying soils. *New Phytologist* **216**: 771–781.

Choat B, Brodribb TJ, Brodersen CR, Duursma RA, López R, Medlyn BE. 2018. Triggers of tree mortality under drought. *Nature* 558: 531–539.

Corso D, Delzon S, Lamarque LJ, *et al.* 2020. Neither xylem collapse, cavitation, or changing leaf conductance drive stomatal closure in wheat. *Plant, Cell & Environment* **43**: 854–865.

Deans RM, Brodribb TJ, Busch FA, Farquhar GD. 2020. Optimization can provide the fundamental link between leaf photosynthesis, gas exchange and water relations. *Nature Plants* **6**: 1116–1125.

Eller CB, Rowland L, Mencuccini M, *et al.* 2020. Stomatal optimization based on xylem hydraulics (SOX) improves land surface model simulation of vegetation responses to climate. *New Phytologist* **226**: 1622–1637.

Fisher RA, Williams M, Vale RLD, Costa ALD, Meir P. 2006. Evidence from Amazonian forests is consistent with isohydric control of leaf water potential. *Plant, Cell & Environment* **29**: 151–165.

Gollan T, Passioura JB, Munns R. 1986. Soil water status affects the stomatal conductance of fully turgid wheat and sunflower leaves. *Australian Journal of Plant Physiology* **13**: 459–464.

Gollan T, Turner NC, Schulze E-D. 1985. The responses of stomata and leaf gas exchange to vapour pressure deficits and soil water content. *Oecologia* **65**: 356–362.

Grossiord C, Buckley TN, Cernusak LA, *et al.* 2020. Plant responses to rising vapor pressure deficit. *New Phytologist* **226**: 1550–1566.

Henry C, John GP, Pan R, *et al.* 2019. A stomatal safety-efficiency trade-off constrains responses to leaf dehydration. *Nature Communications* **10**: 1–9.

Hetherington AM, Woodward FI. 2003. The role of stomata in sensing and driving environmental change. *Nature* **424**: 901–908.

Huber AE, Melcher PJ, Piñeros MA, Setter TL, Bauerle TL. **2019**. Signal coordination before, during and after stomatal closure in response to drought stress. *New Phytologist* **224**: 675–688.

Jarvis PG, McNaughton KG. **1986**. Stomatal Control of Transpiration: Scaling Up from Leaf to Region In: MacFadyen A, Ford ED, eds. *Advances in Ecological Research*. Academic Press, 1–49.

de Jong van Lier Q, van Dam JC, Metselaar K, de Jong R, Duijnisveld WHM. **2008**. Macroscopic Root Water Uptake Distribution Using a Matric Flux Potential Approach. *Vadose Zone Journal* **7**: 1065–1078.

Lier Q de J van, Dam JC van, Durigon A, Santos MA dos, Metselaar K. **2013**. Modeling Water Potentials and Flows in the Soil–Plant System Comparing Hydraulic Resistances and Transpiration Reduction Functions. *Vadose Zone Journal* **12**: vzj2013.02.0039.

Martin-StPaul N, Delzon S, Cochard H. **2017**. Plant resistance to drought depends on timely stomatal closure (H Maherali, Ed.). *Ecology Letters* **20**: 1437–1447.

Notaguchi M, Kurotani K, Sato Y, *et al.* 2020. Cell-cell adhesion in plant grafting is facilitated by β-1,4-glucanases. *Science* **369**: 698–702.

Passioura JB. **1980**. The Transport of Water from Soil to Shoot in Wheat Seedlings. *Journal of Experimental Botany* **31**: 333–345.

Peters A, Iden SC, Durner W. **2015**. Revisiting the simplified evaporation method: Identification of hydraulic functions considering vapor, film and corner flow. *Journal of Hydrology* **527**: 531–542.

Rodriguez-Dominguez CM, Brodribb TJ. **2020**. Declining root water transport drives stomatal closure in olive under moderate water stress. *New Phytologist* **225**: 126–134.

Rosskopf E, Pisani C, Di Gioia F. **2017**. Crop specific grafting methods, rootstocks and scheduling: Tomato

Scholander PF, Bradstreet ED, Hemmingsen EA, Hammel HT. **1965**. Sap Pressure in Vascular Plants: Negative hydrostatic pressure can be measured in plants. *Science* **148**: 339–346.

Schröder T, Javaux M, Vanderborght J, Körfgen B, Vereecken H. **2009**. Implementation of a Microscopic Soil–Root Hydraulic Conductivity Drop Function in a Three-Dimensional Soil–Root Architecture Water Transfer Model. *Vadose Zone Journal* **8**: 783–792.

Scoffoni C, Albuquerque C, Brodersen CR, *et al.* 2017. Outside-Xylem Vulnerability, Not Xylem Embolism, Controls Leaf Hydraulic Decline during Dehydration. *Plant Physiology* **173**: 1197–1210.

Scoffoni C, Vuong C, Diep S, Cochard H, Sack L. **2014**. Leaf Shrinkage with Dehydration: Coordination with Hydraulic Vulnerability and Drought Tolerance. *Plant Physiology* **164**: 1772–1788.

Skelton RP, Brodribb TJ, Choat B. **2017**. Casting light on xylem vulnerability in an herbaceous species reveals a lack of segmentation. *New Phytologist* **214**: 561–569.

Sperry JS, Love DM. **2015**. What plant hydraulics can tell us about responses to climate-change droughts. *New Phytologist* **207**: 14–27.

Wang Y, Sperry JS, Anderegg WRL, Venturas MD, Trugman AT. **2020**. A theoretical and empirical assessment of stomatal optimization modeling. *New Phytologist* **227**: 311–325.

Williams M, Bond BJ, Ryan MG. **2001**. Evaluating different soil and plant hydraulic constraints on tree function using a model and sap flow data from ponderosa pine. *Plant, Cell & Environment* **24**: 679–690.

Wolf A, Anderegg WRL, Pacala SW. **2016**. Optimal stomatal behavior with competition for water and risk of hydraulic impairment. *Proceedings of the National Academy of Sciences* **113**: E7222–E7230.

Wolz KJ, Wertin TM, Abordo M, Wang D, Leakey ADB. **2017**. Diversity in stomatal function is integral to modelling plant carbon and water fluxes. *Nature Ecology & Evolution* **1**: 1292–1298.

3.6 Supplementary Data
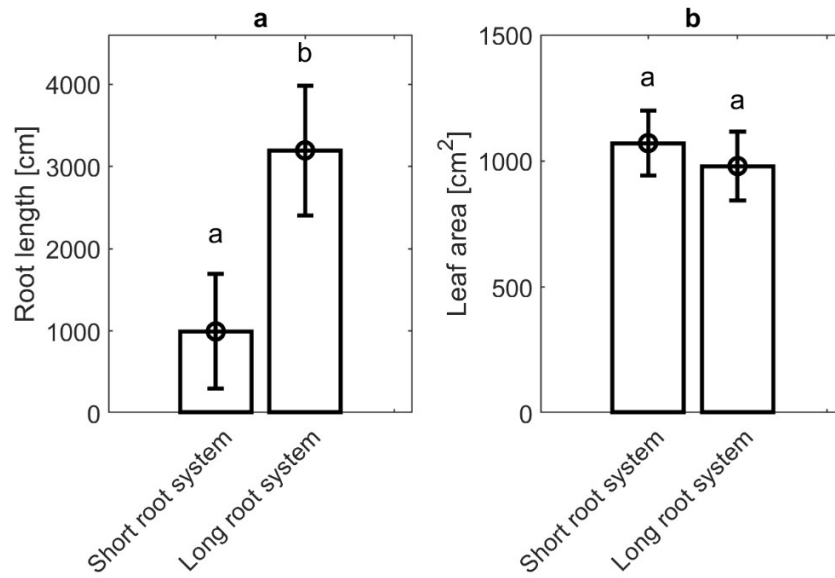
Supplementary figure S1: (**a**) Root length and (**b**) leaf area of tomato plants grafted onto two root systems. Root length was significantly different (*p-value* < 0.05), while the leaf area was similar (*p-value* > 0.05) (*n* = 3).
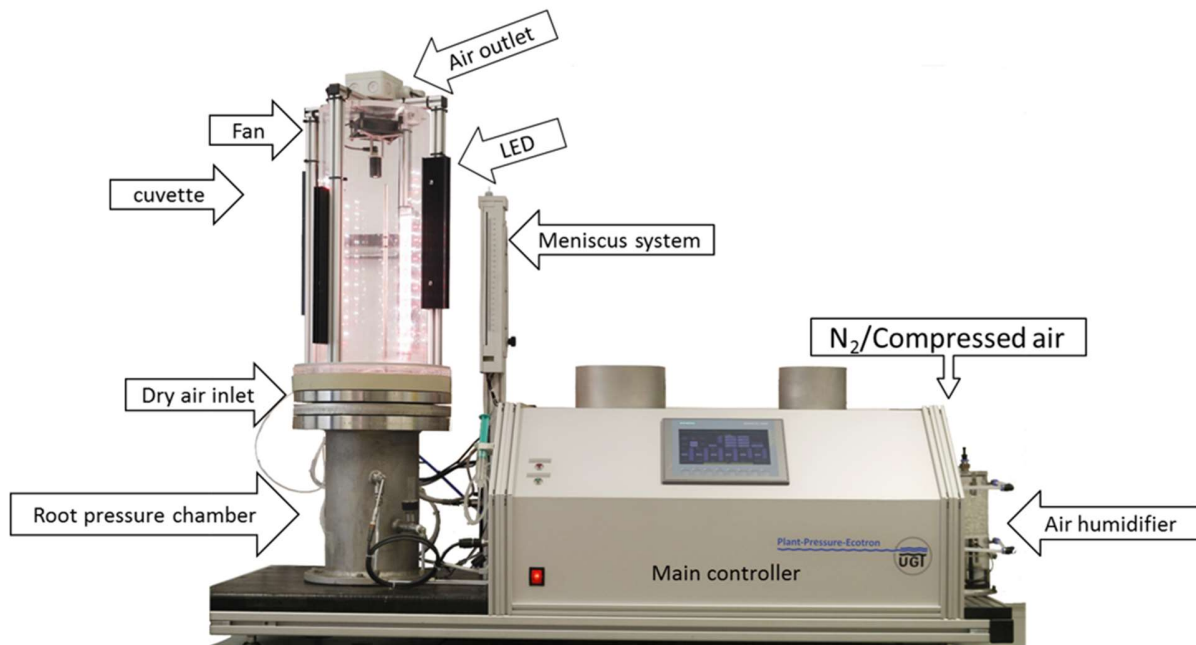
Supplementary figure S2: The root pressure chamber system (RPCS) used to measure the relation between transpiration (E) and leaf xylem water pressure ($\psi_{\text{leaf-x}}$). Plants were placed inside the RPCS, with the column in the root pressure chamber and the shoot in the cuvette. The E was altered by increasing the photosynthetic photon flux density (PPFD) stepwise. Pneumatic pressure was applied to balance the water pressure inside the leaf xylem at atmospheric pressure. The balancing pressure is numerically equal to the leaf xylem water pressure ($\psi_{\text{leaf-x}}$). Both E and $\psi_{\text{leaf-x}}$ were simultaneously determined at each PPFD.
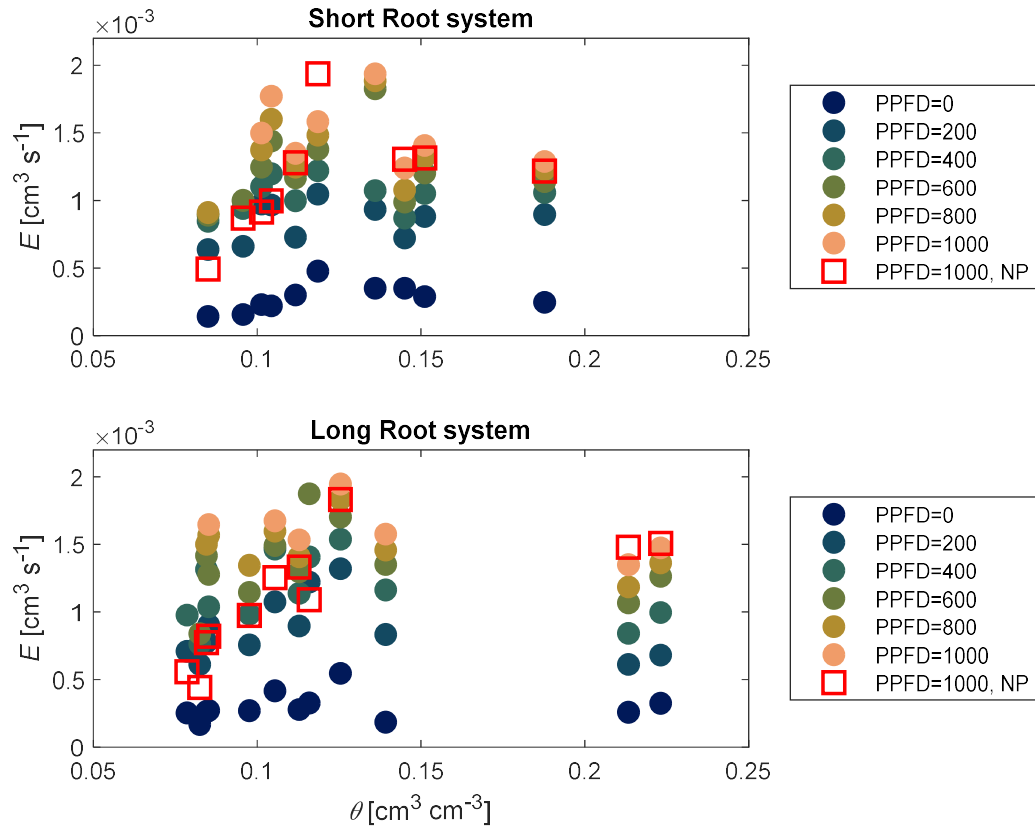
Supplementary figure S3: Transpiration rate (*E*) of plants with short and long root systems during soil drying. At a specific soil water content (*θ*), *E* was measured under different photosynthetic photon flux densities (PPFD [μmol m⁻² s⁻¹]), as shown in closed symbols. *E* was measured during plant pressurization to obtain the corresponding leaf water pressure (ψ_{leaf-x}) that was shown in figures 3.2 and 3.4. Additionally, *E* was measured without plant pressurization (NP) under the highest PPFD (=1000 μmol m⁻² s⁻¹) as shown as open red squares.
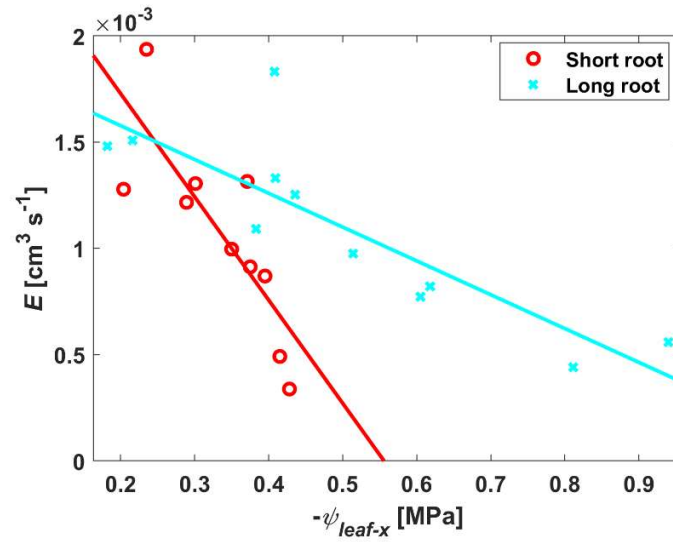
Supplementary figure S4: Linear fit of the $E(\psi_{\text{leaf-x}})$-relation measured in unpressurized plants with the two root systems (as shown in Figure 3.4e). Slope and intercept of the linear fit were utilized for analysis of covariance, which showed significant difference of stomatal closure between the two root systems. Measurements were obtained at different soil water contents during soil drying.

Supplementary Table S1. Analysis of variance for the influence of different factors on the transpiration rate (E) under plant pressurization, (*p-value* <0.001***, *p-value*<0.01**, *p-value*<0.05*)

Source of variation	Sum Sq. ¶	d.f.	Mean Sq.	F	Prob>F
Root system	3.40e-7	1	3.40e-7	8.86	0.0039**
Soil water content¶¶	1.02e-6	2	5.14e-7	13.31	<<0.001***
Replicate (root-system, soil water content, and Photosynthetic photon flux density (PPFD))	2.45e-6	65	3.77e-8	0.78	0.8009
PPFD	1.54e-5	5	3.08e-6	80.14	<<0.001***
Root-system * soil water content	6.01e-7	2	3.00e-7	7.81	0.0008***
Root-system * PPFD	2.91e-8	5	5.82e-9	0.15	0.979
Soil water content * PPFD	6.93e-8	10	6.93e-9	0.18	0.9972
Error	1.40e-6	29	4.85e-8		
Total	2.60e-5	119			

¶ Sum. Sq: Sum of squares, d.f: Degree of freedom, Mean Sq: Mean Sum of Squares, F: F-statistic value.

¶¶ Soil water content was clustered into three groups, namely, 1: ≥ 0.13, 2: 0.12 - 0.10, and 3: < 0.10.

Supplementary Table S2. Parameters used in the model

Parameter	Symbol	value	Unit
Soil conductivity	K_s	2.1×10^{-5}	cm s^{-1}
Fitting parameter for the unsaturated conductivity	τ	2	-
Root conductance	K_{root}	short 3.2×10^{-6} long 1.01×10^{-6}	cm^3 s^{-1} hPa^{-1}
Soil air entry value	ψ_0	-8.33×10^{-4}	MPa
Xylem air entry value	ψ_{0x}	-1.5	MPa
Fitting parameter for xylem conductivity	τ_x	5	-
Active root length in water uptake	L	short 760-1700 long 930-3700	cm
Root radius	r_0	0.02	cm
Soil radius around the root	r_b	1	cm

Supplementary Table S3. Coefficient estimates for stomatal closure $E(\psi_{\text{leaf-x}})$ in the two rootstocks in terms of the slope and the intercept.

Term	Estimate	Std. Err.	T	Prob > | T |
Intercept	0.0023	0.00022	10.53	0***
Short Root	0.0004	0.00022	1.84	0.0829
Long Root	-0.0004	0.0002	-1.84	0.0829
Slope	-0.0032	0.00059	-5.42	0***
Short Root	-0.0016	0.00059	-2.75	0.0138
Long Root	0.0016	0.00059	2.75	0.0138

Supplementary Table S4. Analysis of variance to identify the significant difference between the slope and the intercept of $E(\psi_{\text{leaf-x}})$ as shown in Supplementary table 2.

Source	d.f.	Sum Sq.	Mean Sq.	F	Prob>F
Root system	1	4.93e-7	4.93e-7	7.34	0.0149
Leaf xylem water pressure	1	2.07e-6	2.07e-6	30.77	<<0.001
Root system * Leaf xylem water pressure	1	5.07e-7	5.07e-7	7.54	0.0138
Error	17	1.14e-6	6.72e-8		

4 Chapter four: The role of ABA in stomatal response to hydraulic non-linearity

Mohanned Abdalla[1,2*], and Mutez Ali Ahmed[1]

[1]Chair of Soil Physics, Bayreuth Center of Ecology and Environmental Research (BayCEER), University of Bayreuth, Bayreuth, Germany.

[2]Department of Horticulture, Faculty of Agriculture, University of Khartoum, Khartoum North, Sudan.

ORCID: **MA** (0000-0002-4220-8761); **MAA** (0000-0002-7402-1571).

4.1 ABSTRACT

Although recent empirical and modelling studies have demonstrated that stomata close at the onset of hydraulic non-linearity between transpiration rate and leaf water potential, the mechanism that allows plants to respond to non-linearity remains unknown. It is well accepted that ABA is a key hormone regulating stomatal closure during water deficit. However, the role of ABA in stomatal response to non-linearity has not been explored. To fill this knowledge gap, we used a novel root pressure chamber to measure the relationship between transpiration rate and leaf water potential of two tomato genotypes: ABA-deficient mutant and the corresponding wild type (WT). We hypothesize that ABA would allow the WT to maintain a linear relationship between transpiration rate and leaf water potential, whereas the ABA-deficient mutant would quickly enter the non-linear zone, even under wet soil conditions. Hence, to test this hypothesis, the experiments were conducted under wet soil conditions. The results demonstrated that WT exhibited a linear relation between transpiration rate and leaf water potential. On the other hand, ABA-deficient mutant exhibited a non-linear relation already in wet soil conditions. These novel results provide the first experimental evidence that ABA could be a potential mechanism that allows plant to respond to non-linearity in relationship between transpiration rate and leaf water potential. Future studies would investigate the role of ABA in plant response to non-linearly among diverse plant species and soil types.

Keywords:

4.2 INTRODUCTION

Stomata regulate carbon and water exchange between the atmosphere and terrestrial vegetation, hence driving global productivity and water yield (Hetherington and Woodward, 2003; Wolz *et al.*, 2017; Buckley, 2019; Deans *et al.*, 2020). Despite the great importance of stomata for vegetation functioning (Hetherington and Woodward, 2003), fundamental question remains regarding the mechanisms by which stomata behave under environmental factors that influence water availability. Various hypotheses have been established to understand stomatal behavior. Carbon optimization theory, a pioneering concept predicting stomatal responses to water availability, posits that stomata maximize carbon gain for a penalty of water loss (Cowan and Farquhar, 1977; Wang *et al.*, 2020). Stomatal regulation has been proposed to 'passively' respond to declining leaf water potential or 'actively' controlled by abscisic acid (ABA) (Brodribb and McAdam, 2011; Merilo *et al.*, 2018; Buckley, 2019). Other studies suggested that a combination of chemical and hydraulic signal controls stomata closure (Tardieu and Davies, 1993). Thus, it is not fully revealed how stomata detect and react to their intrinsic and extrinsic environment, especially under drought conditions (Brodribb and McAdam, 2011; Buckley, 2019).

Although the underlying mechanisms governing stomatal regulation at the mechanistic and molecular levels are yet to be fully revealed (Buckley, 2005, 2019), recent studies have demonstrated that we still could anticipate stomatal response to soil and atmospheric drought from its emergent hydraulic properties (Sperry *et al.*, 2016). A hydraulic framework is proposed to predict stomatal closure following a supply-demand function (Sperry and Love, 2015). The premise is that stomata close by responding to the incidence of non-linearities in the relation between transpiration rate and leaf water potential, which allows plants to obviate excessive decline in leaf water potential (Sperry and Love, 2015). Furthermore, stomata optimization models were shown to exhibit improved predictions skills when based on hydraulics (Wolf *et al.*, 2016; Eller *et al.*, 2020; Wang *et al.*, 2020). The primary hydraulic limitation among soil–plant continuum is a matter of debate. For instance, Sperry *et al.* (2002) argued that either xylem or rhizosphere are primary hydraulic limitations to transpiration. Afterward, Sperry and Love (2015) suggested xylem as the main hydraulic constraint to

transpiration. Carminati and Javaux (2020) proposed that declining soil hydraulic conductance is the driver of stomatal closure. The authors, utilizing meta-analysis, validated their concept among different plant species and soil types (Carminati and Javaux, 2020). Although there is no consensus regarding the primary hydraulic limitation, either above- or below-ground, both models argue that stomata respond to the hydraulic non-linearity (Sperry and Love, 2015; Carminati and Javaux, 2020).

Indeed, recent studies experimentally demonstrated that stomata close at the onset of hydraulic non-linearity (Abdalla *et al.*, In Press) (Figure 4.1). Further, the onset of non-linearity was proved to respond to changes in below-ground traits. For instance, Carminati *et al.* (2017) demonstrated that, in barley, root-hairless mutant exhibited non-linear relation between transpiration rate and leaf water potential, while the wild type counterpart showed linear relation. Cai *et al.* (2021) illustrated diverse onset of hydraulic non-linearity based soil texture for identical maize genotypes. Abdalla *et al.* (In Press) showed that changing root length altered the onset of hydraulic non-linearity, and that below-ground hydraulics control stomatal closure of tomato during soil drying. Furthermore, recent studies demonstrated that stomata closure was driven by declining root hydraulic conductance (Rodriguez-Dominguez and Brodribb, 2020; Bourbia *et al.*, 2021). These conclusions together support that a decline in below-ground hydraulics, i.e. root, soil and/or interface, constitutes non-linearity between transpiration rate and leaf water potential. Nonetheless, the mechanism that allows stomata to respond to such non-linearity remains obscure (Javaux and Carminati, 2021).

Abscisic acid is a potential candidate allowing stomata to function optimally in response to diverse environmental stressors. A potential mechanism might be through a chemical signal that mediates stomatal closure. Mounting evidence established the inverse relation between ABA and stomatal conductance (Davies and Zhang, 1991; Schurr *et al.*, 1992; Dodd, 2005; Brodribb and McAdam, 2011; McAdam and Brodribb, 2018). Earlier studies suggested a cross-talk between root and shoot under stress conditions. Roots were suggested to produce ABA that is transferred to the shoot and induces stomatal closure (Davies and Zhang, 1991; Dodd, 2005). However, root-sourced ABA has been shown to play no role in stomatal closure of tomato (Holbrook *et al.*, 2002). Furthermore, recent studies demonstrated that ABA was *de novo* synthesized in leaf mesophyll and drove stomatal closure (McAdam and Brodribb, 2018).

Together these studies suggest that there is little consensus regarding the location of ABA production, but emphasizing its essentiality to guard cells movement. The fact that ABA initiates stomatal closure suggests a potential correlation between ABA abundance/synthesis and the onset of hydraulic non-linearity (Wankmüller and Carminati, 2021). Here we ask: what is the role of ABA in stomatal response to the hydraulic non-linearity.

We hypothesize that ABA would allow plants to avoid non-linearity by the earlier stomatal closure sustain higher leaf water potential. The rationale is that, in the non-linear zone, a tiny increment in transpiration would require a large drop in leaf water potential, which is inconvenient for plant. On the other hand, the ABA-deficient mutant might not respond to non-linearity and show limited stomatal regulation, which would require higher water fluxes at the root surface, causing a steep drop in matric potential in the vicinity around the root. This in turn would entail a more negative water potential in leaves of ABA-deficient plants, and consequently, incidence of the non-linearity, which might possibly occur in a combination of wet soil conditions and high transpiration rates.

This study investigated the interplay between ABA and the onset of hydraulic non-linearity, using an ABA-deficient mutant and the corresponding wild type (Holbrook *et al.*, 2002; Brodribb *et al.*, 2021). We tested this hypothesis by concomitantly measuring transpiration rate and leaf water potential of the ABA-deficient mutant and its near-isogenic parent line. We used a root pressure chamber that facilitates measurements with high temporal resolution in intact plants and allows exploring the zone beyond stomatal closure by keeping shoots turgid.

4.3 MATERIALS AND METHODS

4.3.1 Plant and soil

Two tomato varieties were used in this study, ABA-deficient mutant, *sitiens*, and its near-isogenic parent line, *Rheinlands Rhum* (Holbrook *et al.*, 2002). Seeds of both genotypes were surface-sterilized using 30 % H_2O_2 for 30 seconds, then germinated on saturated filter paper in a petri dish for five days. Germinated seeds were transplanted in polyvinyl chloride columns (22 cm height and 7 cm diameter). The columns were filled with sandy soil that was sieved through 1-mm sieve, as described by Vetterlein et al. (2021). Aluminum disk was used to top up the column with a center hole for seedlings. Three holes (diameter of 0.5 cm) were made

every 6 cm on columns sides to allow measurements of soil water content, for which we used a time-domain refractometer (TDR, E-Test, Lublin, Poland). The soil water retention curve and soil unsaturated hydraulic conductivity curve were reported in Vetterlein *et al.* (2021).

Seedlings were grown under the ambient conditions (temperature: 25 °C; relative humidity: 55 %; photosynthetic photon flux density: 185 μmol m^{-2} s^{-1}) for five weeks. The soil was kept wet by irrigating every other day. Before starting the measurements, plants were glued at the collar to the surrounding aluminum plate to facilitate the anticipated pressurization.

4.3.2 Transpiration and leaf water potential

Root pressure chamber system (RPCS) was used to conduct simultaneous measurements of transpiration and leaf water potential in intact plants. A detailed description of the RPCS was presented in both chapter two and three. Briefly, RPCS incorporates a root pressure chamber, a cuvette and a central control unit. Light-emitting diodes were attached to the cuvette and provided adjustable levels of photosynthetic photon flux density (PPFD). Temperature and relative humidity were measured in the ingoing and outgoing air. A controlled airflow passed continuously through the cuvette in a rate of 8.2 L min^{-1}. Transpiration rate was calculated by multiplying the airflow rate by the difference between the ingoing and outgoing humidity, while leaf water potential was obtained by pressurization. The premise of the RPCS is balancing the suction inside leaf xylem to the atmospheric pressure by applying pneumatic pressure to the soil and intact root system. The balancing pressure is numerically equal to the suction inside leaf xylem before pressurization (Passioura, 1980; Abdalla *et al.*, 2021). During the measurements, a meniscus system was connected to a leaf cut evaluating droplet stability.

Photosynthetic photon flux density (PPFD) was increased from 0 to 1000 μmol m^{-2} s^{-1}, stepwise, to increase transpiration rate. Simultaneously, corresponding leaf water potential was measured at each PPFD. Plants of both genotypes were measured under wet soil conditions.

As demonstrated in chapter two, the slope of the relation between transpiration rate and leaf water potential in wet soil depicts root hydraulic conductance. Root hydraulic conductance of both genotypes was measured by applying Darcy's low (considering plant as a porous medium)

and knowing the transpiration fluxes as well as the pressure gradients and assuming steady-state conditions.

Figure 4.1 Relation between transpiration rate and leaf water potential for a) Lycopersicon hirsutum, b) a hybrid of Lycopersicon hirsutum and Solanum pimpinellifolium and c) Solanum lycopersicon. The relation was linear in wet soils (blue-green) and non-linear in dry soils (brown-pink). Stomata close at the onset of the non-linearity (red squares). See chapter two and three for more details.

4.4 RESULTS AND DISCUSSION

In chapter two and three, we demonstrated that tomato exhibited linear relation between transpiration rate and leaf water potential in wet soils and non-linear only under dry soils. Figure 4.1 shows that stomata close at the onset of the hydraulic non-linearity. In other words, stomata closed to avoid excessive and non-linear decline in leaf water potential. The drier the soil, the lower the transpiration rate at which non-linearity occurred and stomata closed (Figure 4.1; see also chapter two and three). For a specific shoot, the onset of the non-linearity was shifted by changing the root length, and hence, stomatal closure was shifted (see the red squares in Figure 4.1, a – b). These findings demonstrated that stomata responded to the incidence of hydraulic non-linearity, and maintained plant within the linear zone by regulating proportionality between transpiration rate and leaf water potential.
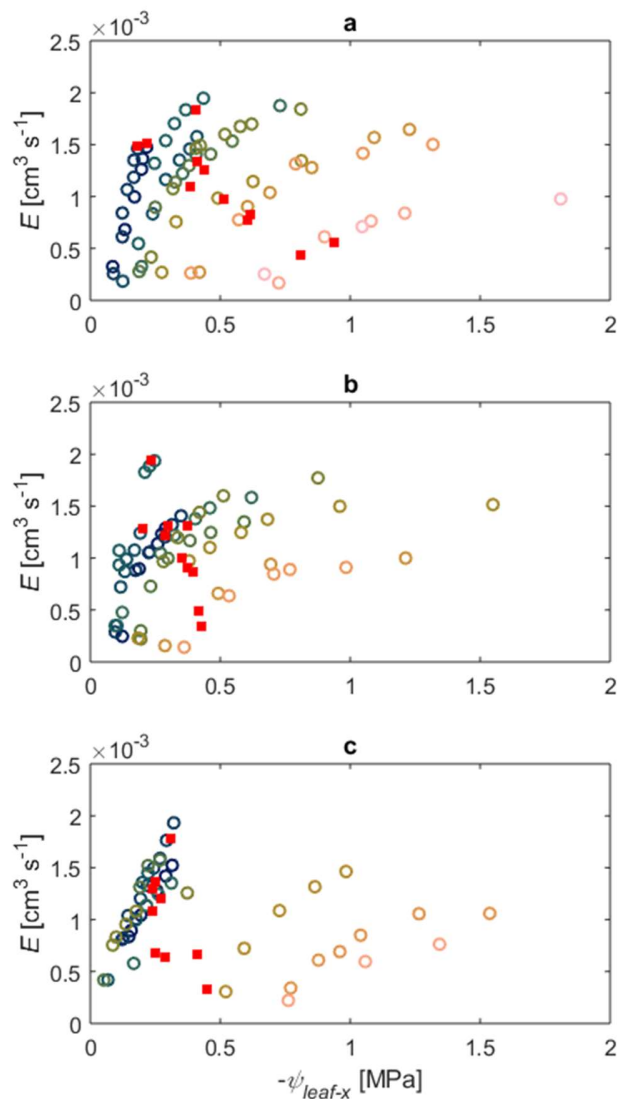
The relation between transpiration rate and leaf water potential in the wild type was linear (Figure 4.2). However, ABA-deficient mutant exhibited non-linearity in wet soil, where leaf water potential abruptly declined in response to a tiny increment in transpiration rate (Figure 4.2). This result supports our hypothesis that ABA facilitated earlier stomatal closure that reduced transpiration rates allowing a proportional decline in leaf water potential, as observed in wild type in Figure 4.2. Furthermore, ABA-deficient mutant showed higher transpiration rates, which required higher water fluxes at the root surface, causing a steep drop of matric potential in the vicinity around the root and, consequently, more negative leaf water potential.
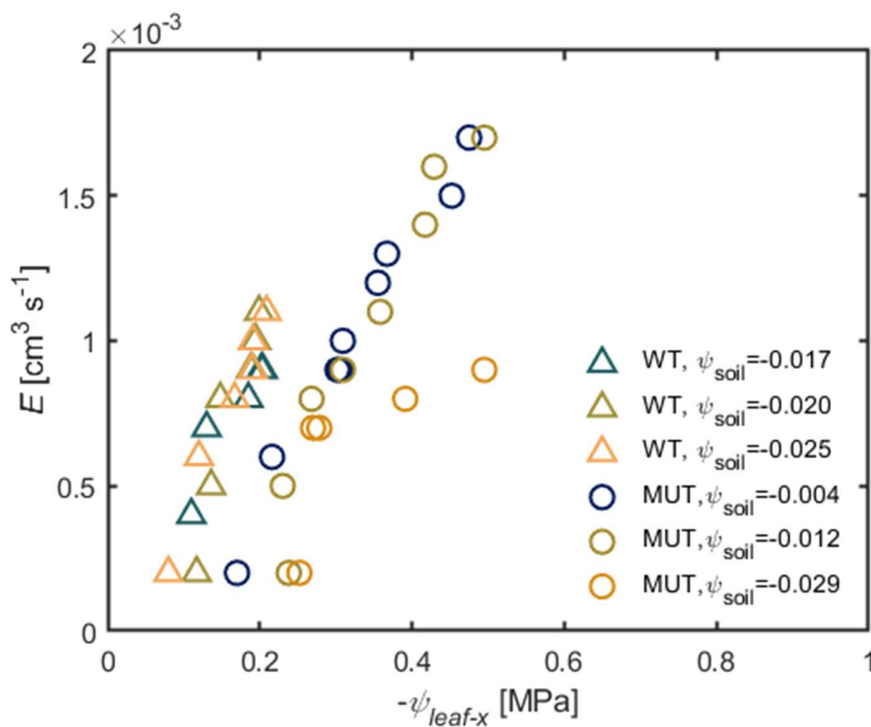
Figure 4.2 *Relation between transpiration rate (E) and leaf xylem water potential (ψ_{leaf-x}) in wet soil conditions (soil water potential: ψ_{soil} [MPa]). Wild type (WT; triangles) exhibited linear relation between E and ψ_{leaf-x}, while ABA-deficient mutant (MUT; open symbols) shows non-linear relation, even in wet soils.*

Maximum transpiration rate of both genotypes revealed limited stomatal regulation in ABA-deficient mutant, unlike the wild type. The transpiration rate in WT reached a maximum of 1.1×10^{-3} cm^3 s^{-1} after the plant exposure to a PPFD of 1000 μmol m^2 s^{-1}. Meanwhile, ABA-deficient mutant increased transpiration rate more than 1.7×10^{-3} cm^3 s^{-1} as PPFD reached 1000

μmol m^2 s^{-1} (Figure 4.3). These results support that ABA facilitates earlier stomatal closure and diminishes maximum water loss. Greater stomatal conductance was observed in ABA-deficient tomato in previous studies (Holbrook *et al.*, 2002). Moreover, over-accumulation of ABA was shown to cause a reduction of stomatal conductance in tomato plants (Lamarque *et al.*, 2020) and attenuate the increment in transpiration in pearl millet despite increased vapor pressure deficit (VPD) (Kholová *et al.*, 2010). Minimizing water loss under higher transpiration demand was suggested as a mechanism to overcome water stress in crops (Kholová *et al.*, 2010; López *et al.*, 2021; Sadok *et al.*, 2021).
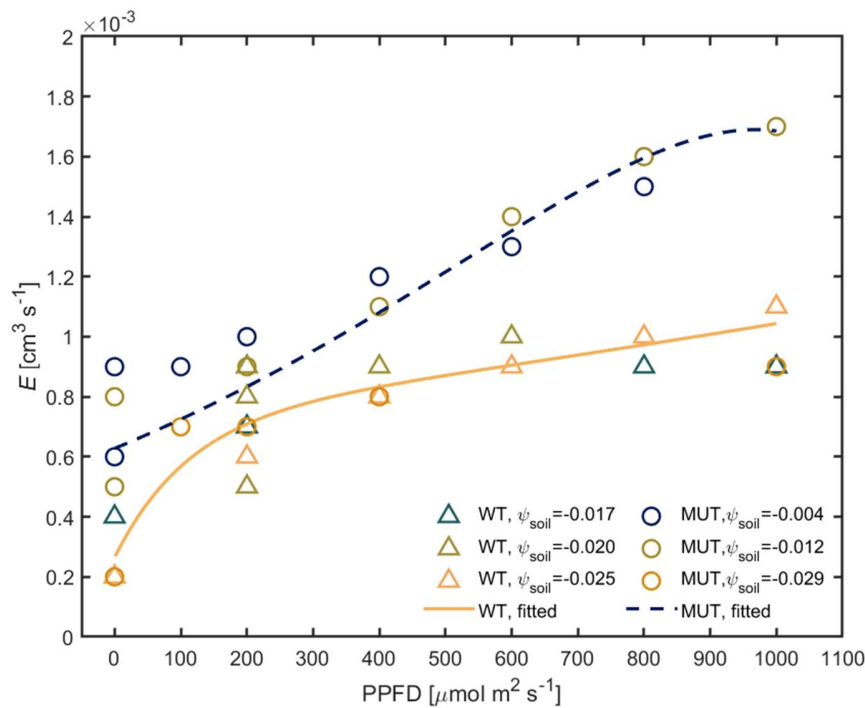
Figure 4.3 *Light response curve of wild type (WT) and ABA-deficient mutant (Mut). ABA facilitates lower transpiration rates (E) despite increasing photosynthetic photon flux density (PPFD).*

The slope of the relation between transpiration rate and leaf water potential depicts soil-root hydraulic conductance (Abdalla *et al.*, 2021). Interestingly, the WT displayed higher soil-root hydraulic conductance, which was equal to 9.6×10^{-3} cm^3 s^{-1} MPa^{-1}. Meanwhile, the Mut showed *ca.* 70 % less soil–plant hydraulic conductance, equal to 5.5×10^{-3} cm^3 s^{-1} MPa^{-1}. This

result is in line with the findings of Thompson *et al.* (2007), who demonstrated an improved root hydraulic conductance that associated with ABA over-accumulation in tomato.

Predawn leaf water potential, being the intercept of $E(\psi_{\text{leaf-x}})$-relation, was more negative in Mut compared to WT (Figure 4.2), which is in line with the findings of Lamarque *et al.* (2020), who showed less negative predawn leaf water potential of tomato that over-accumulated ABA (Lamarque *et al.*, 2020). Shifts in predawn water potential were related to the differences in osmotic potential between soil and plant (Abdalla *et al.*, In Press; Donovan *et al.*, 2001; Cai *et al.*, 2020b; Zhang *et al.*, 2021). Naturally, plants exclude numerous ions during water uptake (Munns and Gilliham, 2015). ABA was documented to facilitate ion exclusion during root water uptake (Chen *et al.*, 2001). Hence, ABA-deficient mutant might not exclude ions as efficiently as WT and consequently had more negative osmotic potential that must have contributed to the deviation in predawn leaf water potential. Additionally, transpiration rate was higher in Mut (as shown in Figure 4.3), which means more solutes must have been accumulated inside Mut than WT. Anticipated differences in osmotic potential, due to ABA-assisted ion exclusion, might explain the offset in predawn leaf water potential between Mut and WT.

In conclusion, we have demonstrated that ABA could be a mechanism that allows plants to close stomata to avoid the incidence of hydraulic non-linearity in the relation between transpiration and leaf water potential. Further investigations are needed to reveal the interplay between ABA, leaf water potential, stomatal conductance, and carbon assimilation rate during soil drying in different species and soil types.

4.5 REFERENCES

Abdalla M, Ahmed MA, Cai G, Wankmueller F, Schwartz N, Lititg O, Javaux M, Carminati A. **In Press**. Stomatal closure during water deficit is controlled by below-ground hydraulics.

Abdalla M, Carminati A, Cai G, Javaux M, Ahmed MA. **2021**. Stomatal closure of tomato under drought is driven by an increase in soil–root hydraulic resistance. *Plant, Cell & Environment* **44**: 425–431.

Bourbia I, Pritzkow C, Brodribb TJ. **2021**. Herb and conifer roots show similar high sensitivity to water deficit. *Plant Physiology* **186**: 1908–1918.

Brodribb TJ, McAdam SAM. **2011**. Passive Origins of Stomatal Control in Vascular Plants. *Science* **331**: 582–585.

Buckley TN. **2019**. How do stomata respond to water status? *New Phytologist* **224**: 21–36.

Cai G, Ahmed MA, Dippold MA, Zarebanadkouki M, Carminati A. **2020**. Linear relation between leaf xylem water potential and transpiration in pearl millet during soil drying. *Plant and Soil* **447**: 565–578.

Cai G, Carminati A, Abdalla M, Ahmed MA. **2021**. Soil textures rather than root hairs dominate water uptake and soil–plant hydraulics under drought. *Plant Physiology* **187**: 858–872.

Carminati A, Javaux M. **2020**. Soil Rather Than Xylem Vulnerability Controls Stomatal Response to Drought. *Trends in Plant Science* **25**: 868–880.

Carminati A, Passioura JB, Zarebanadkouki M, Ahmed MA, Ryan PR, Watt M, Delhaize E. **2017**. Root hairs enable high transpiration rates in drying soils. *New Phytologist* **216**: 771–781.

Chen S, Li J, Wang S, Hüttermann A, Altman A. **2001**. Salt, nutrient uptake and transport, and ABA of Populus euphratica; a hybrid in response to increasing soil NaCl. *Trees* **15**: 186–194.

Cowan I, Farquhar G. **1977**. Stomatal function in relation to leaf metabolism and environment: Stomatal function in the regulation of gas exchange. *Symposia of the Society for Experimental Biology* **31**: 471–505.

Davies WJ, Zhang J. **1991**. Root Signals and the Regulation of Growth and Development of Plants in Drying Soil. *Annual Review of Plant Physiology and Plant Molecular Biology* **42**: 55–76.

Deans RM, Brodribb TJ, Busch FA, Farquhar GD. **2020**. Optimization can provide the fundamental link between leaf photosynthesis, gas exchange and water relations. *Nature Plants* **6**: 1116–1125.

Dodd IC. **2005**. Root-To-Shoot Signalling: Assessing The Roles of 'Up' In the Up and Down World of Long-Distance Signalling In Planta. *Plant and Soil* **274**: 251–270.

Donovan L, Linton M, Richards J. **2001**. Predawn plant water potential does not necessarily equilibrate with soil water potential under well-watered conditions. *Oecologia* **129**: 328–335.

Eller CB, Rowland L, Mencuccini M, Rosas T, Williams K, Harper A, Medlyn BE, Wagner Y, Klein T, Teodoro GS, *et al.* **2020**. Stomatal optimization based on xylem hydraulics (SOX) improves land surface model simulation of vegetation responses to climate. *New Phytologist* **226**: 1622–1637.

Hetherington AM, Woodward FI. **2003**. The role of stomata in sensing and driving environmental change. *Nature* **424**: 901–908.

Holbrook NM, Shashidhar VR, James RA, Munns R. **2002**. Stomatal control in tomato with ABA-deficient roots: response of grafted plants to soil drying. *Journal of Experimental Botany* **53**: 1503–1514.

Javaux M, Carminati A. **2021**. Soil hydraulics affect the degree of isohydricity. *Plant Physiology* **186**: 1378–1381.

Kholová J, Hash CT, Kumar PL, Yadav RS, Kočová M, Vadez V. **2010**. Terminal drought-tolerant pearl millet [Pennisetum glaucum (L.) R. Br.] have high leaf ABA and limit transpiration at high vapour pressure deficit. *Journal of Experimental Botany* **61**: 1431–1440.

Lamarque LJ, Delzon S, Toups H, Gravel A-I, Corso D, Badel E, Burlett R, Charrier G, Cochard H, Jansen S, *et al.* **2020**. Over-accumulation of abscisic acid in transgenic tomato plants increases the risk of hydraulic failure. *Plant, Cell & Environment* **43**: 548–562.

López J, Way DA, Sadok W. 2021. Systemic effects of rising atmospheric vapor pressure deficit on plant physiology and productivity. *Global Change Biology* **27**: 1704–1720.

McAdam SAM, Brodribb TJ. 2018. Mesophyll Cells Are the Main Site of Abscisic Acid Biosynthesis in Water-Stressed Leaves. *Plant Physiology* **177**: 911–917.

Merilo E, Yarmolinsky D, Jalakas P, Parik H, Tulva I, Rasulov B, Kilk K, Kollist H. 2018. Stomatal VPD Response: There Is More to the Story Than ABA. *Plant Physiology* **176**: 851–864.

Munns R, Gilliham M. 2015. Salinity tolerance of crops – what is the cost? *New Phytologist* **208**: 668–673.

Passioura JB. 1980. The Transport of Water from Soil to Shoot in Wheat Seedlings. *Journal of Experimental Botany* **31**: 333–345.

Rodriguez-Dominguez CM, Brodribb TJ. 2020. Declining root water transport drives stomatal closure in olive under moderate water stress. *New Phytologist* **225**: 126–134.

Sadok W, Lopez JR, Smith KP. 2021. Transpiration increases under high-temperature stress: Potential mechanisms, trade-offs and prospects for crop resilience in a warming world. *Plant, Cell & Environment* **44**: 2102–2116.

Schurr U, Gollan T, Schulze E-D. 1992. Stomatal response to drying soil in relation to changes in the xylem sap composition of Helianthus annuus. II. Stomatal sensitivity to abscisic acid imported from the xylem sap. *Plant, Cell & Environment* **15**: 561–567.

Sperry JS, Hacke UG, Oren R, Comstock JP. 2002. Water deficits and hydraulic limits to leaf water supply. *Plant, Cell and Environment* **25**: 251–263.

Sperry JS, Love DM. 2015. What plant hydraulics can tell us about responses to climate-change droughts. *New Phytologist* **207**: 14–27.

Tardieu F, Davies WJ. **1993**. Integration of hydraulic and chemical signalling in the control of stomatal conductance and water status of droughted plants. *Plant, Cell & Environment* **16**: 341–349.

Thompson AJ, Andrews J, Mulholland BJ, McKee JMT, Hilton HW, Horridge JS, Farquhar GD, Smeeton RC, Smillie IRA, Black CR, *et al.* **2007**. Overproduction of Abscisic Acid in Tomato Increases Transpiration Efficiency and Root Hydraulic Conductivity and Influences Leaf Expansion. *Plant Physiology* 143: 1905–1917.

Vetterlein D, Lippold E, Schreiter S, Phalempin M, Fahrenkampf T, Hochholdinger F, Marcon C, Tarkka M, Oburger E, Ahmed M, *et al.* **2021.** Experimental platforms for the investigation of spatiotemporal patterns in the rhizosphere—Laboratory and field scale. *Journal of Plant Nutrition and Soil Science* 184: 35–50.

Wang Y, Sperry JS, Anderegg WRL, Venturas MD, Trugman AT. **2020**. A theoretical and empirical assessment of stomatal optimization modeling. *New Phytologist* **227**: 311–325.

Wankmüller FJP, Carminati A. Stomatal regulation prevents plants from critical water potentials during drought: Result of a model linking soil–plant hydraulics to abscisic acid dynamics. *Ecohydrology* **n/a**: e2386.

Wolf A, Anderegg WRL, Pacala SW. **2016**. Optimal stomatal behavior with competition for water and risk of hydraulic impairment. *Proceedings of the National Academy of Sciences* **113**: E7222–E7230.

Wolz KJ, Wertin TM, Abordo M, Wang D, Leakey ADB. **2017**. Diversity in stomatal function is integral to modelling plant carbon and water fluxes. *Nature Ecology & Evolution* **1**: 1292–1298.

Zhang H, Li X, Wang W, Pivovaroff AL, Li W, Zhang P, Ward ND, Myers-Pigg A, Adams HD, Leff R, *et al.* **2021.** Seawater exposure causes hydraulic damage in dying Sitka-spruce trees. *Plant Physiology* 187: 873–885.

5 Chapter five: Coupled effects of soil drying and salinity on soil–plant hydraulics

Mohanned Abdalla[1,2*], Mutez Ali Ahmed[1], Gaochao Cai[1], Mohsen Zarebanadkauki[1]**,** and Andrea Carminati[3]

[1]Chair of Soil Physics, Bayreuth Center of Ecology and Environmental Research (BayCEER), University of Bayreuth, Bayreuth, Germany.

[2]Department of Horticulture, Faculty of Agriculture, University of Khartoum, Khartoum North, Sudan.

[3]Physics of Soils and Terrestrial Ecosystems, Institute of Terrestrial Ecosystems, Department of Environmental Systems Science, ETH Zürich, Zurich, Switzerland.

[*]Correspondence to: Mohanned.Abdalla@uni-bayreuth.de

ORCID: **MA** (0000-0002-4220-8761); **MAA** (0000-0002-7402-1571); **GC** (0000-0003-4484-1146); **MZ** (0000-0001-6342-5792); **AC** (0000-0001-7415-0480).

Short title: Soil–plant hydraulics shift under abiotic stress

One-sentence summary: A physical model interprets transpiration reduction under drought and salinity as a consequence of osmotic gradients at the root surface that cause a severe drop in leaf water potential.

5.1 ABSTRACT

Salinity and soil drying are expected to induce salt accumulation at the root-soil interface of transpiring plants. However, the consequences of this on the relationship between transpiration rate (E) and leaf xylem water potential (ψ_{leaf-x}) are yet to be quantified. Here we used a non-invasive root pressure chamber to measure the $E(\psi_{leaf-x})$ relationship of tomato (*Solanum lycopersicum* L.) treated with (saline) or without 100 mM NaCl (non-saline conditions). The results were reproduced and interpreted with a soil-plant hydraulic model. Under non-saline conditions, the $E(\psi_{leaf-x})$ relationship became progressively more non-linear as the soil dried ($\theta \leq 0.13$ cm^3 cm^{-3}, $\psi_{soil} \leq -0.08$ MPa). Under saline conditions, plants exhibited an earlier non-linearity in the $E(\psi_{leaf-x})$ relationship ($\theta \leq 0.15$ cm^3 cm^{-3}, $\psi_{soil} \leq -0.05$ MPa). During soil drying, salinity induced a more negative ψ_{leaf-x} at predawn, reduced transpiration rate, and caused a reduction in root hydraulic conductance (from 1.48×10^{-6} to 1.30×10^{-6} cm^3 s^{-1} hPa^{-1}). The model suggested that the marked non-linearity was caused by salt accumulation at the root surface and the consequential osmotic gradients. In dry soils, most of water potential dissipation occurred in the bulk soil and rhizosphere rather than inside the plant. Under saline-dry conditions, the loss in osmotic potential at the root surface was the preeminent component of the total dissipation. The physical model of water flow and solute transport supports the hypothesis that a build-up of osmotic potential at the root-soil interface causes a large drop in ψ_{leaf-x} and limits transpiration rate under drought and salinity.

Keywords:

5.2 INTRODUCTION

Plants are increasingly subjected to episodes of edaphic and atmospheric water deficit during their life spans (Choat et al., 2018; Brodribb et al., 2020). Simultaneously, plants suffer from salinity in many areas worldwide (Kumar and Sharma, 2020; Harper et al., 2021; Hopmans et al., 2021). Hence, understanding how plants react to co-occurring stressors can play a substantial role not only in stabilizing crop performance under combined stress, but also in the conservation of natural vegetation (Chaves et al., 2009).

Using soil-plant hydraulic frameworks, recent studies have endeavored to understand plant responses to water deficit in both soil and atmosphere (Sperry and Love, 2015; Carminati and Javaux, 2020; Liu et al., 2020). Soil water deficit generates hydraulic limitations to water uptake and transpiration (Draye et al., 2010; Rodriguez-Dominguez and Brodribb, 2020; Abdalla et al., 2021; Bourbia et al., 2021). In dry soils, below-ground hydraulic limitations shape the relationship between transpiration rate and leaf water potential and subsequently the onset of stress (Carminati and Javaux, 2020; Abdalla et al., 2021; Bourbia et al., 2021; Cai et al., 2021; Javaux and Carminati, 2021; Abdalla et al., 2022). Revealing the mechanism involved in shaping the relationship between transpiration rate and leaf water potential, as well as triggering stomatal closure under drought, is a prerequisite to understanding transpiration reduction under other coexisting biotic and/or abiotic stresses.

Soil salinity can limit crop growth and productivity, with great impacts in arid and semi-arid regions (Munns, 2002; Fricke et al., 2004; Munns and Tester, 2008; Chaves et al., 2009). High salt concentration in soil limits the ability of roots to take up water (Munns and Tester, 2008), similar to the impact of soil drying (Munns, 2002). Salinity triggers stomatal closure, subsequently impacting photosynthesis and plant growth and development (Munns, 2002; Fricke et al., 2004; Munns and Tester, 2008; Chaves et al., 2009). Besides reducing water availability, salt accumulation in soil induces toxic effects of sodium and chlorine ions in crops and trees (Munns and Tester, 2008; van Zelm et al., 2020; Zhang et al., 2021).

Recently, Munns et al. (2020b) postulated that plant must exclude 98% of Na^+ and Cl^- from saline soil while taking up water to avoid ion accumulation inside plant tissues (Munns and Gilliham, 2015; Munns et al., 2020b). Consequently, salts might build up around roots and

possibly induce osmotic stress (Stirzaker and Passioura, 1996). Nonetheless, determining salt concentrations at the root-soil interface of intact plants during soil drying is difficult and our understanding of salt accumulation is incomplete.

Various experimental approaches have been utilized to explore salt accumulation around the root. Hamza and Aylmore (1992a; 1992b) integrated invasive and non-invasive methods to determine water extraction, Na^+ concentration near roots, transpiration rate, and the corresponding leaf water potential (Hamza and Aylmore, 1992b). The authors showed salt accumulated at the root-soil interface in wet soils (Hamza and Aylmore, 1992a; Hamza and Aylmore, 1992b). However, their method was prone to experimental artifacts in dry soil conditions (Hamza et al., 2001). Magnetic resonance imaging (MRI) has also been utilized for non-invasive imaging of solute transport to roots (Haber-Pohlmeier et al., 2017). However, its application to quantify NaCl concentrations at the root-soil interface has been limited to specific soil types and relatively small sample sizes (Perelman et al., 2020b). Furthermore, the leaf water potential was not measured in the latter study. Stirzaker and Passioura (1996) investigated the resistances in water pathways from soil to leaf and the consequences of the osmotic stress. The authors used non-saline nutrient solution, which mimicked the range of osmotic potential in field conditions, i.e., $\geq$ -0.07 MPa (Stirzaker and Passioura, 1996). The authors concluded that osmotic stress had occurred due to salt build-up at the root-soil interface (Stirzaker and Passioura, 1996). However, the combined effects of salinity and water stress were not investigated.

Salts are transported towards the root surface due to convective and diffusive processes during root water uptake. Convection processes are driven by transpiration and the water fluxes toward the root surface and tend to increase salt content at the root-soil interface. Diffusive transport of solutes tends to equalize the concentration of salts (within the liquid phase). Solute accumulation at the root surface depends on the relative importance of convection and diffusion. As soil moisture affects both the water fluxes and the diffusion coefficient (Moldrup et al., 2001), it is a prerequisite to knowing the gradients in soil moisture around the roots, which depend on both soil hydraulic properties and transpiration rates. Therefore, to fully predict salt accumulation at the root-soil interface, one needs to couple models of water flow to the root with a model of solute transport in soils (de Jong van Lier et al., 2009; Schröder et

al., 2014; Jorda et al., 2018). However, experimental validations and measured parameters for these simulations remain lacking.

We hypothesize that salt accumulation at the root surface will hinder transpiration by increasing the osmotic gradients at the root surface. Hence, a further decline in leaf water potential will be required to sustain transpiration under salinity conditions. Additionally, salt might reduce root hydraulic conductance possibly as a consequence of salt accumulation inside the root or due to sodium toxicity affecting internal root tissues (Azaizeh and Steudle, 1991; Azaizeh et al., 1992; Fricke et al., 2004; Boursiac et al., 2005). Furthermore, NaCl has been documented to impact the swelling and dispersion of clay particles within soil aggregates (Gupta and Verma, 1985), which potentially changes soil structure and pore geometry and hence impacts soil hydraulic properties (Tuller et al., 1999; Klopp and Daigh, 2020).

In this study, we combined a root pressure chamber (Cai et al., 2020b) and a model of soil water flow and salt transport to investigate the coupled effects of soil drying and salinity on soil-plant hydraulics. We measured the relationship between transpiration rate and leaf xylem water potential of tomato (*Solanum lycopersicum* L.) with and without NaCl treatment. This method accurately measures the drop in water potential at the root surface in intact plants with high temporal resolution (Carminati et al., 2017; Cai et al., 2020b; Cai et al., 2021), which can be potentially induced by salt accumulation. In parallel, we also evaluated the effect of salinity (100 mM NaCl) on the hydraulic properties of the soil. We used a soil-plant hydraulic model of Carminati and Javaux (2020) to reproduce and interpret the measurements. The model accounts for the series of resistances across the soil-plant continuum to predict transpiration rate and leaf water potential at a given soil water potential. The model was implemented to include the effect of salt accumulation at the root surface.

5.3 RESULTS

Plants were grown in similar conditions and NaCl treatment was applied just before the drying cycle. We found no significant differences in total root length (31.9 m $\pm$ 7.9 and 37.5 m $\pm$ 3.1 standard deviation; *p-value* = 0.323) and root radius (0.0215 cm $\pm$ 0.0002 and 0.0219 cm $\pm$ 0.0008; *p-value* = 0.44) between the non-saline and saline conditions, respectively (Supplemental Figure S1; n = 3).

The NaCl treatment influenced the relationship between transpiration rate and leaf xylem water potential during soil drying (Figure 5.1). In wet conditions, leaf xylem water potential in non-saline plants decreased linearly with increasing transpiration rate, whereas NaCl-treated ones showed non-linearity under relatively wet soil conditions ($\theta \leq 0.15$ cm^3 cm^{-3}; Figure 5.1; Table 1). In dry soils, non-linearity emerged in both treatments, and it was more marked under saline conditions (Figure 5.1). Non-linear relationship (significant quadratic term of regression, p-value < 0.05) occurred at $\theta \leq 0.15$ cm^3 cm^{-3} under saline conditions, whereas, in non-saline conditions, the non-linearity (significant quadratic term of regression, p-value < 0.05) was observed at $\theta \leq 0.13$ cm^3 cm^{-3}. We have additionally fitted two linear lines to the measurements as shown in Supplemental Figure S2 and Supplemental Figure S3.

Salinity significantly reduced the maximum transpiration rate during soil drying, with and without plant pressurization (Figure 5.2; *p-value* < 0.01; Supplemental Tables S1 and S2; $n = 3$). Pressurization sustained higher transpiration rates in dry soils as well as in wet soils under salinity conditions (Figure 5.2). The increment in photosynthetic photon flux density significantly increased transpiration rate during soil drying (Figure 5.2; Supplemental Tables S2; *p-value* < 0.001; $n = 6$).

Predawn leaf xylem water potential deviated from soil matric potential as soil started to dry in both treatments. Non-saline plants showed higher (less negative) predawn leaf water potential in comparison to the soil matric potential in dry soil (Figure 5.3). By contrast, plants with 100 mM NaCl treatment showed lower (more negative) predawn leaf water potential in wet conditions with a progressive decline as the soil dried (e.g., from -0.05 to -0.3 MPa in wet soil and from -0.2 to -0.9 MPa in dry soil; Figure 5.3). The analysis of covariance showed a significant shift to lower (more negative) predawn leaf water after 100 mM NaCl treatment (*p-value* < 0.01; $n = 3$; Supplemental Figure S4, Supplemental Tables S3 and S4). In wet soils, osmotic potential in soil was -0.02 MPa and declined to -0.29 MPa with salinity treatment. NaCl treatment showed no significant influence (confidence intervals at 95%) on either water retention curve or unsaturated hydraulic conductivity curve of the sandy loam used in this study, especially within the range of measurements (Figure 5.4).
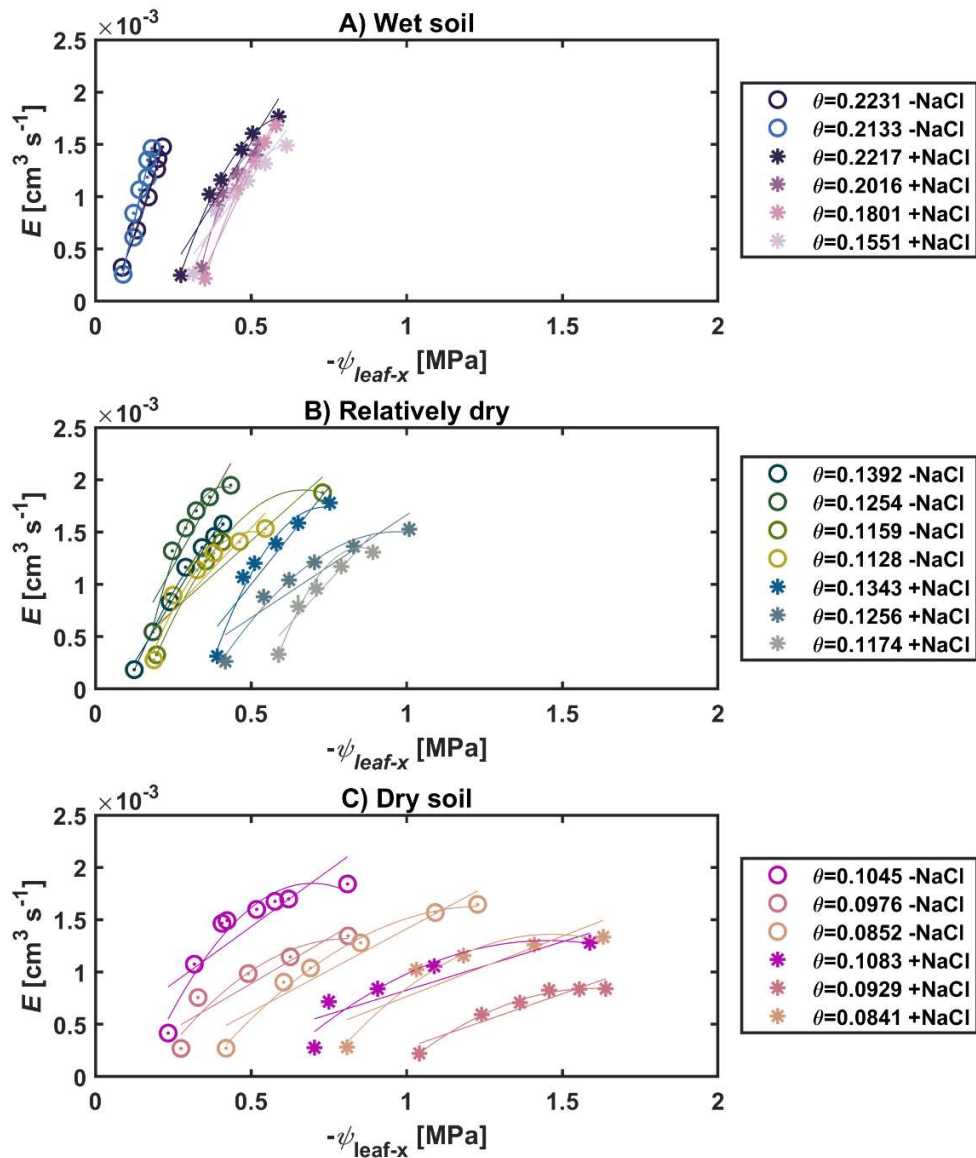
Figure 5.1 *Relationship between transpiration (E) and leaf xylem potential (ψ_{leaf-x}) in non-saline (-NaCl; open symbols) and saline-treated plants (+NaCl; asterisks) during soil drying. Without NaCl treatment, the relationship is linear in wet conditions (**A**), starts to bend as the soil dries (**B**), eventually shows clear non-linearity in dry soils (**C**). Under saline conditions (i.e., 100 mM NaCl), E(ψ_{leaf-x})-relation shows a more marked non-linearity, especially with high E during soil drying. The relationship was fitted, at each soil water content, with linear and quadratic functions (see values of R^2 in Table 5.1). In sum, soil drying accentuates the impacts of NaCl. Similar colors within each subplot stand for similar soil water contents (θ; cm^3 cm^{-3}).*

Table 5.1. Estimations of R^2 for linear and non-linear (quadratic) models fitting the relationship between transpiration rate and leaf water potential under saline and non-saline conditions in Figure 5.1.

Saline										
SWC*	**0.2217**	**0.2016**	**0.1801**	**0.1551**	**0.1343**	**0.1256**	**0.1174**	**0.1083**	**0.0929**	**0.0841**
R^2 Linear	0.92	0.90	0.97	0.91	0.87	0.86	0.81	0.77	0.88	0.75
R^2 quadratic	0.99	0.98	0.99	0.98	0.97	0.98	0.95	0.89	0.99	0.96
Non-Saline										
SWC*	**0.2231**	**0.2133**	**0.1392**	**0.1254**	**0.1159**	**0.1128**	**0.1054**	**0.0976**	**0.0852**	
R^2 linear	0.99	0.95	0.98	0.85	0.84	0.84	0.73	0.85	0.91	
R^2 quadratic	0.99	0.95	0.99	0.98	0.99	0.96	0.94	0.92	0.99	

*SWC: soil water content (cm^3 cm^{-3}).
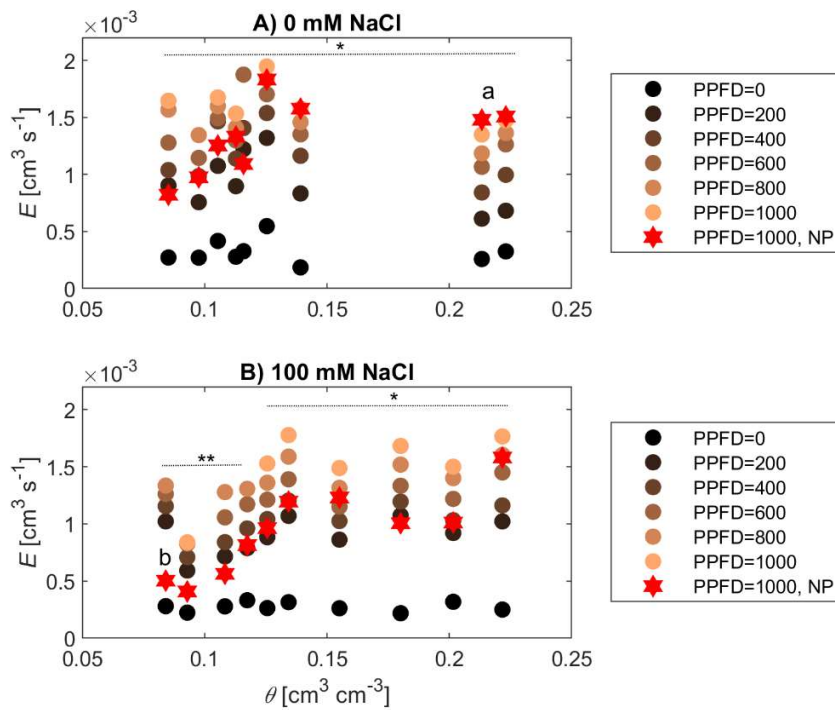
Figure 5.2 *Transpiration (E) at different soil water contents (θ) and photosynthetic photon flux densities (PPFD; μmol m⁻² s⁻¹). (**A**) under non-saline conditions and (**B**) under saline conditions. E was obtained with (closed symbol) and without plant pressurization (red stars; NP). Salinity significantly reduced maximum E during soil drying as denoted by lowercase letters for unpressurized (p-value < 0.01, n = 3, Tukey-Kramer test) and asterisks for pressurized measurements (p-value < 0.001, n = 3, Tukey-Kramer test).*
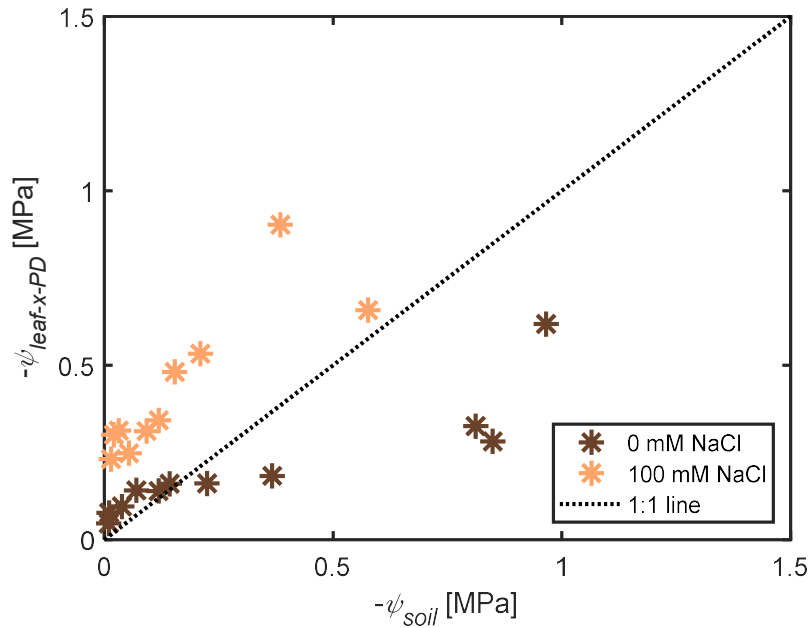
Figure 5.3 *Impacts of salinity on predawn leaf water potential ($\psi_{leaf\text{-}x\text{-}PD}$) at different soil matric potentials (ψ_{soil}). Values of $\psi_{leaf\text{-}x\text{-}PD}$ are corresponding to the intercept of $E(\psi_{leaf\text{-}x})$-relations in Figure 5.1. Salinity shifted $\psi_{leaf\text{-}x\text{-}PD}$ to be more negative compared to the non-saline treatment at similar soil matric potential (p-value < 0.01; n = 3; analysis of covariance followed by Tukey-Kramer test; see Supplemental Figure S4 and Supplemental Tables S3 and S4).*

The soil-plant hydraulic model reproduced the relationship between transpiration rate and leaf xylem water potential during soil drying with and without NaCl treatments (Figure 5.5, A and B). The modeling results showed that salt treatment induced a rapid decline in leaf xylem water potential compared to non-saline treatment (Figure 5.6, A and B). The decline in leaf xylem water potential during soil drying was accelerated by salinity (Figure 5.6, A and B). In the model, we inversely varied root length (as a fitting parameter) to reproduce the measured relationship between leaf xylem water potential and transpiration rate. Root length active in water uptake was estimated to be 1536 and 5244 cm for non-saline and saline treatment, respectively. The estimated root length must be interpreted with caution (see Discussion). With NaCl treatment, root hydraulic conductance (1.30×10^{-6} cm^3 s^{-1} hPa^{-1}) was slightly lower than the non-saline treatment in wet soil conditions (1.48×10^{-6} cm^3 s^{-1} hPa^{-1}; *p-value* = 0.692, *n* = 3).
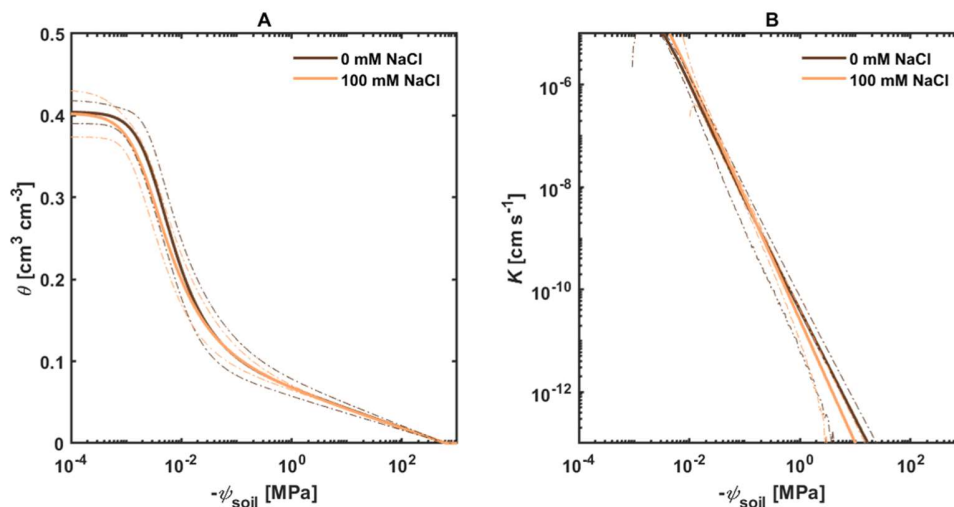
Figure 5.4 *Soil hydraulic properties of the non-saline (0 mM NaCl) and saline (100 mM NaCl) sandy loam soil. (**A**) Soil water retention curves, i.e. the relationship between soil water potential (ψ_{soil}) and soil water content (θ). (**B**) Soil hydraulic conductivity (K) curves. The curves were parameterized with Peters-Durner-Iden model (Peters et al., 2015). NaCl treatment did not show significant influence on soil hydraulic properties (dotted lines depict confidence intervals at 95%, n = 3), especially within the range of measurements (θ: 0.22 - 0.07 $cm^3 cm^{-3}$; K: 10^{-5} - 10^{-11} $cm\ s^{-1}$).*

The modeling results suggested that, in dry and saline conditions, the salt concentration at the root surface increased by a factor of three within one day of measurements (Figure 5.6, C and D), which was less evident in non-saline conditions (Figure 5.6 C). These results revealed that salts have accumulated at the root surface under dry and saline soil conditions. Note that also in non-saline soil a minimal build-up of solutes occurred under high transpiration rate and dry soil conditions. The decline in leaf xylem water potential temporally followed the accumulation of NaCl at the root surface, particularly with salt treatment (Figure 5.6). We simulated the depletion in soil water content within the vicinity around the root (0.05 – 0.2 cm) during the measurements (Figure 5.7). In wet conditions, during measurements time (five and three hours for non-saline and saline-treated measurements, respectively), soil water content decreased from 0.23 to 0.22 $cm^3\ cm^{-3}$ and from 0.22 to 0.19 $cm^3\ cm^{-3}$ with and without NaCl treatment, respectively (Figure 5.7, A and B). The maximum transpiration rate under wet non-saline conditions was 1.5×10^{-3} $cm^3\ s^{-1}$ (Figure 5.2 A). The limited decrease of soil water content in wet saline conditions was a reflection of the limited transpiration rate under these conditions (see transpiration without pressurization in Figure 5.2 B). In dry conditions, the

depletion rate was lower (~ 0.01 cm^3 cm^{-3}; Figure 5.7, C – F). The corresponding maximum transpiration rate obtained without plant pressurization (~ 0.5×10^{-3} cm^3 s^{-1}) was only one third of that in wet conditions (Figure 5.2 A). Note that small changes in soil water content generate large gradients in soil water potential in dry conditions compared to wet conditions (see Figure 5.4).
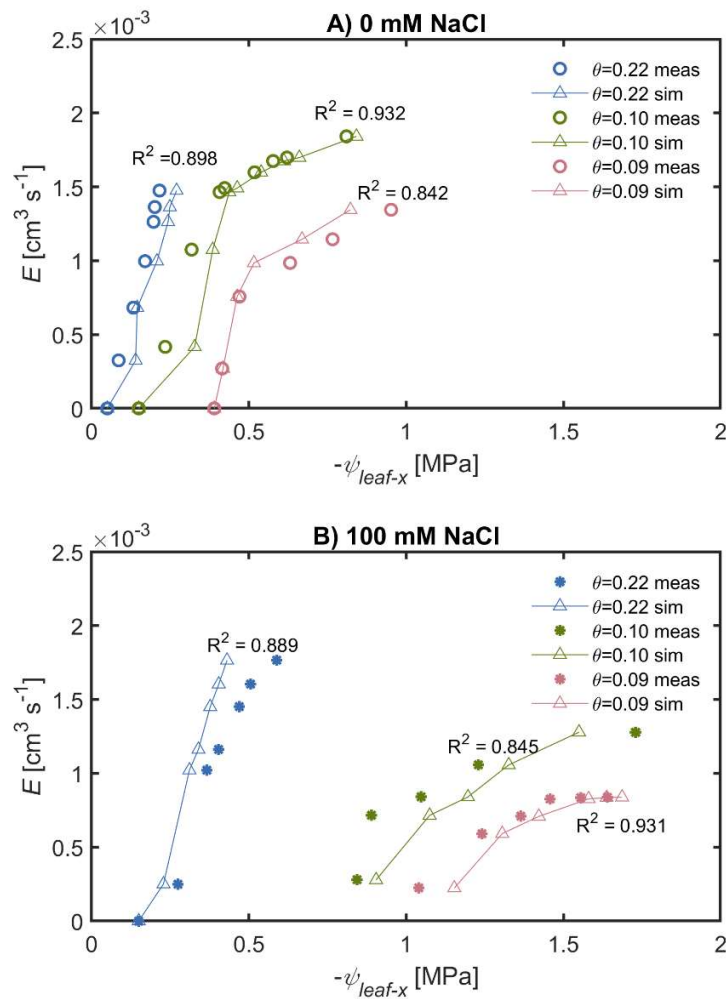
Figure 5.5 *Comparison of transpiration rate (E) and leaf xylem water potential (ψ$_{leaf-x}$) between non-saline and saline conditions. The relationship between E and ψleaf-x was reproduced by the soil-plant hydraulic model for A) non-saline and B) saline-treated plants during soil drying. Water stress level was represented at three soil water contents (θ = 0.22, 0.10 and 0.09 cm^3 cm^{-3}) for both non-saline and saline-treated plants (meas: measured; sim: simulated).*
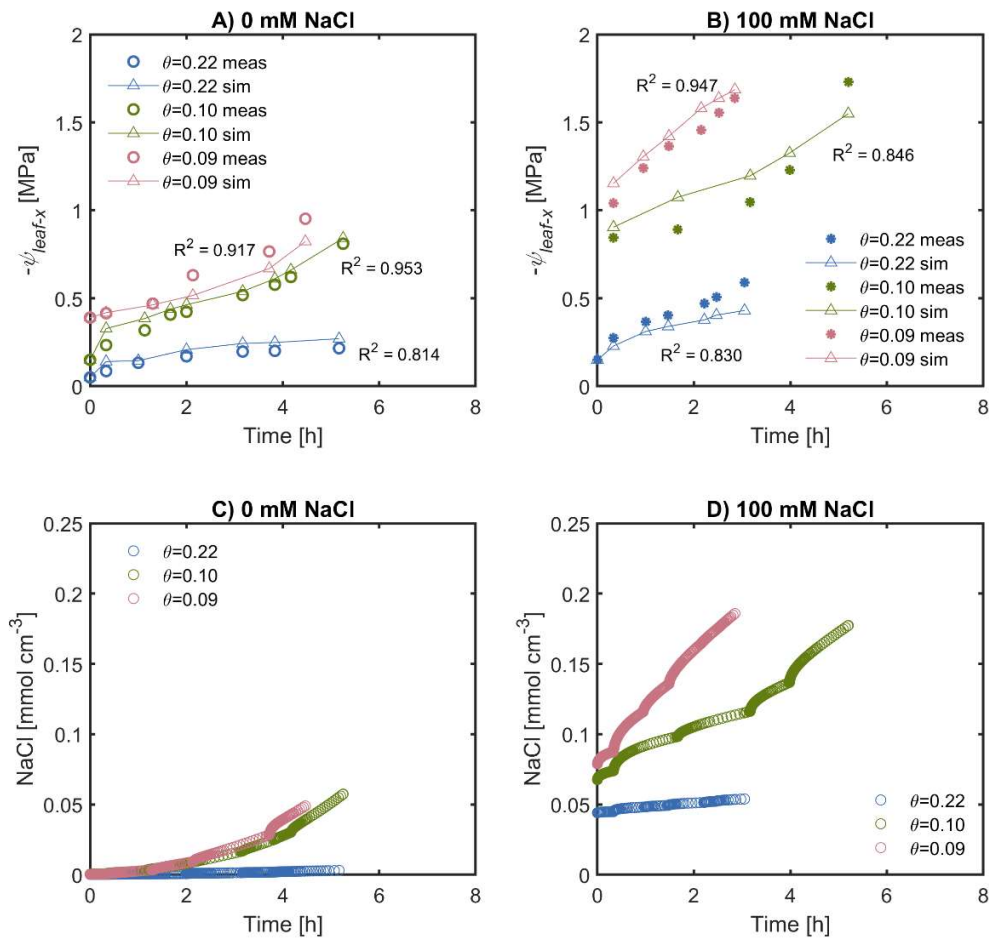
Figure 5.6 *Changes in leaf xylem water potential ($\psi_{leaf\text{-}x}$) and NaCl over time. The dynamics of $\psi_{leaf\text{-}x}$ over time (**A** and **B**) follow salt accumulation at root surface for the corresponding time periods (**C** and **D**). Open symbols and asterisks denote measurements of non-saline and 100 mM NaCl treatment, respectively (**A** – **B**). Connected triangles stand for the simulated values (**A** – **B**; meas: measured; sim: simulated). Salt accumulation was simulated by the soil-plant model in non-saline (**C**), and saline conditions (**D**).*

Osmotic potentials (ψ_π) around roots were lower after NaCl treatment (Figure 5.8). The decline in ψ_π was more pronounced near the root surface after several hours of transpiration (Figure 5.8, A – D). In wet soils, the decrease of ψ_π was negligible in non-saline plants; however, it declined to -0.24 MPa in saline conditions (Figure 5.8, A and B). In dry soils, ψ_π at the root surface was -0.2 MPa in non-saline plants and dropped to -0.8 MPa after salt treatment (Figure 5.8, E – F).
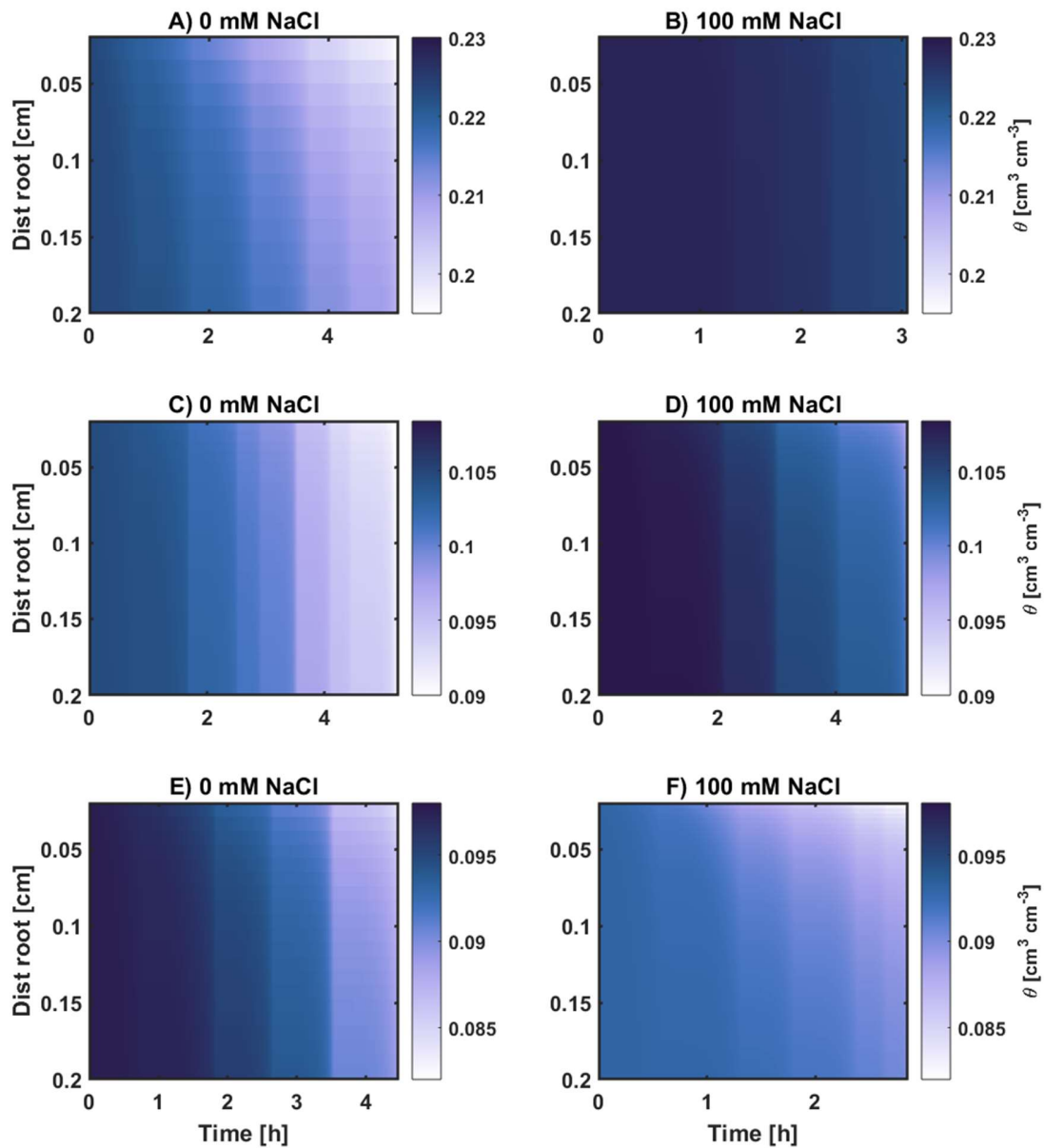
Figure 5.7 *Spatiotemporal distribution of soil water content (θ; cm³ cm⁻³) toward the root surface. The panels show three levels of water stress, namely, $\theta \approx 0.22$ cm³ cm⁻³ for **A** – **B**, 0.10 cm³ cm⁻³ for **C** – **D**, and 0.09 cm³ cm⁻³ for **E** – **F**. The gradients in θ are more pronounced in wet soil (when the transpiration was greater) without NaCl treatment (which had a smaller root length active in water uptake). In dry soils and salt-treated ones, the gradients are less marked, reflecting (1) an impeded water uptake (2) the shape of the water retention curve. In these figures, color bars depict θ.*
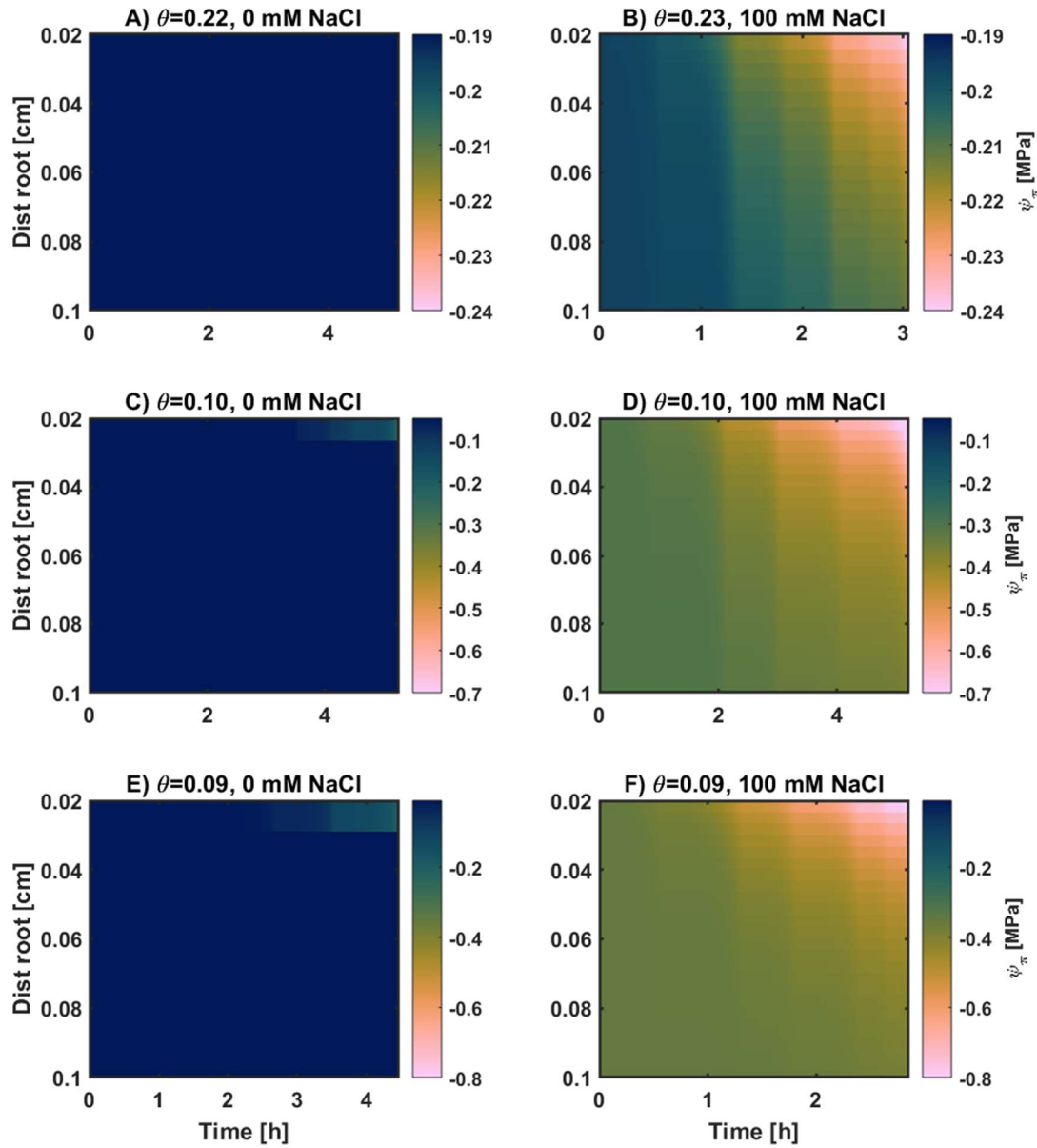
Figure 5.8 *Spatiotemporal distribution of soil osmotic potential (ψπ; MPa) toward the root surface. Initial soil water content for **A** and **B** θ = 0.22, **C** and **D** θ = 0.10, **E** and **F** θ = 0.09 cm³ cm⁻³. The gradients of ψ_π were originated from salt accumulation at the root surface (Figure 5.6, C and D), and the corresponding profile of soil water content in Figure 5.7. Salt treatments induced additional osmotic gradients at the root surface. Here, color bars stand for ψ_π gradients and have three scales based on soil water content. Please note the different time scales on the x-axes.*

The decreases in water potentials across the soil-plant continuum were estimated from modeling the experimental results and are shown at the maximum transpiration rates for three exemplary soil water contents. In wet conditions (soil water content = 0.22), the decrease of the potential in non-saline treatment occurred mainly in the plant due to the resistance to water flow (-0.17 MPa). Under saline conditions, the decrease in the osmotic potential was important (-0.24 MPa; Figure 5.9). In dry soil conditions (soil water content = 0.10, 0.09), water potential dissipation in the bulk soil and the rhizosphere were greater than the loss inside the plant (Figure 5.9). The loss in osmotic potential at the root surface was the preeminent component of the total loss under saline-dry conditions (-0.83 MPa; Figure 5.9). The total loss represented leaf water potential at maximum transpiration rate. Note that these values are based on the model results. Although the model well fitted the data, the underlying assumptions did impact the results. For instance, processes such as root shrinkage and the consequent loss of conductivity in the rhizosphere are not explicitly simulated. Shrinkage is likely to have occurred in wetter soils under saline conditions due to the buildup of solutes. The model would compensate for neglecting such a process but underestimating the model parameters, such as the active root length L.

5.4 DISCUSSION

We demonstrated that the combined effects of salinity and soil drying altered the relationship between transpiration and leaf xylem water potential in tomato. Without salt treatment, the relationship between transpiration rate and leaf xylem water potential was mostly linear in wet soil conditions; thereafter, as soil progressively dried, the relationship became non-linear (Figure 5.1). These results are in line with previous findings in tomato (Abdalla et al., 2021), as well as other crops (Passioura, 1980; Deery et al., 2013; Carminati et al., 2017; Hayat et al., 2019; Cai et al., 2020a; Hayat et al., 2020; Cai et al., 2021). On the other hand, saline and dry soil entailed a more severe decline in leaf xylem water potential for increasing transpiration (Figure 5.1 and Figure 5.5). The reduction in the slope of the $E(\psi_{\text{leaf-x}})$ relationship can be explained by the accumulation of salts at the root-soil interface and the decrease in osmotic potential at low soil water contents or at high transpiration rates. Indeed, the model of solute-diffusion coupled with water flow confirmed this explanation. However, we cannot exclude the possibility that NaCl also impacts root hydraulic conductance, which might be due to salt

accumulation inside the root or at the root surface (Stirzaker and Passioura, 1996). The premise is that NaCl accumulates inside the root and reduces its hydraulic conductance at the cellular level (Tyerman et al., 1989; Azaizeh and Steudle, 1991; Azaizeh et al., 1992; Wan, 2010), as well as the entire root system (Boursiac et al., 2005; Fricke et al., 2014). Under saline conditions, the decline in root conductance might potentially explain transpiration reduction even in wet soils, owing to the fact that root resistance is a considerable hydraulic limitation to transpiration (Vadez, 2014; Ahmed et al., 2018; Carminati et al., 2020; Rodriguez-Dominguez and Brodribb, 2020; Abdalla et al., 2021; Cai et al., 2022).
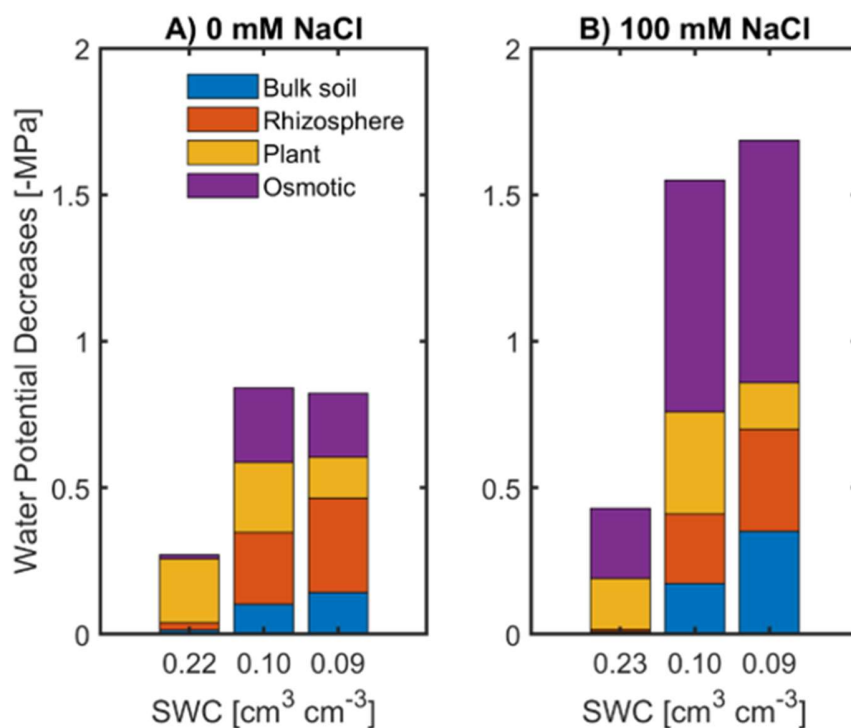
Figure 5.9 Dissipation of water potentials across the soil-plant continuum, divided in its components. (A) non-saline and (B) saline conditions. Under low soil water content (SWC = 0.10, 0.09), greater decreases in matric potentials occurred in the bulk soil and the rhizosphere compared to wet soil conditions (SWC = 0.22). Under saline conditions (100 mM NaCl), the decreases in soil osmotic potential were the greater contributor to the total decease, especially in dry soils.

Predawn leaf water potential deviated from soil matric potential in both treatments. In non-saline treatment, predawn leaf water potential was higher than that of the soil. However, the soil matric potential, as obtained from time-domain refractometer (TDR) and soil retention

126

curve, is an approximation of what the plant senses. Furthermore, the water retention curve was measured in unplanted soil, and plants might change this relationship (Helliwell et al. 2017). Additionally, the leaf xylem might have had a greater solute concentration than the soil in the non-saline treatment, which would explain the difference. Salinity induced a more negative predawn water potential in saline compared to non-saline conditions (Figure 5.3), which is well explained by the low osmotic potential of the soil (Donovan et al., 2001; Cai et al., 2020a; Zhang et al., 2021).

Na^+ and Cl^- exclusion during water uptake is proposed as a successful mechanism of salt tolerance in crops (Munns, 1985; Munns and Tester, 2008; van Zelm et al., 2020). Subsequently, salt concentration near roots will increase compared to bulk soils (Munns et al., 2020a; Munns et al., 2020b; Perelman et al., 2020a). This accumulation induces additional osmotic gradients at the root surface in dry soils, as predicted by the model (Figure 5.6, C and D; Figure 5.8). Generally, ions that are not excluded from the transpiration stream might accumulate inside plant tissues causing irreversible damage (Passioura, 2020), especially under prolonged exposure to saline conditions. Plant responses to salinity occur over a wide time range, starting from the first minutes of exposure up to several months in perennial species (Munns, 2002). Short-term exposure (1–3 days) was criticized as a non-sufficient time course allowing plant adaptation to salinity (Passioura, 2020). In the current study, the plants experienced salinity for 2–3 days before starting the measurements, which lasted circa 7–9 days, implying that either Na^+ and Cl^- exclusion was efficient and ions' concentrations remained below toxic levels or plants started to adapt and compartmentalized the ions within vacuoles. Prolonged exposure (> 8 days) to high concentrations of NaCl was reported to induce lethal consequences on leaves of barley (*Hordeum vulgare* cv. Clipper; Munns and Passioura, 1984). In our study, out of the previously mentioned ~7 days, each plant was pressurized for 3 or 4 days and only during daytime hours. Thus, salt-related responses (i.e. accumulation and root adaptation, especially within the context of soil-plant hydraulics) found sufficient time to occur, similarly to anticipated processes in field conditions in a comparable time frame (cf. Munns et al., 2000; Munns, 2002).

Applying pressurized gas to root and soil had kept the shoot turgid, which allowed plants to sustain higher transpiration rates, especially in dry soil conditions (Figure 5.2). Interestingly,

in wet and saline conditions, maximum transpiration was lower without plant pressurization, suggesting that an increase in salinity-initiated stress reduced maximum transpiration by decreasing root hydraulic conductance (from 1.48×10^{-6} to 1.30×10^{-6} cm^3 s^{-1} hPa^{-1}), which supports our hypothesis. These results are in line with previous findings of Boursiac et al. (2005) and Fricke et al. (2014). Another possible explanation is that sodium ion toxicity might have occurred in leaves (due to increased transpiration/root water uptake) and induced osmotic damage on leaf tissues (Li et al., 2021; Zhang et al., 2021). Limited water depletion under saline wet conditions was also captured by the model (Figure 5.7 B), which additionally supports the finding regarding reduced transpiration.

The model estimated an increase in the root length active in water uptake (L) under saline conditions compared to non-saline. It should be noted that L is a fitting parameter that controls the decreases in soil water potential around the root. Thus, this apparent increase in L under salt should be considered with caution (Abdalla et al., 2021; Cai et al., 2021). It is noteworthy that we used a simplified single root model, and the use of an architecture model has shown a decrease in effective root length in dry soils (Landsberg and Fowkes, 1978). In a previous study, Hayat et al. (2019) used both simplified and root architecture models to reproduce the relationship between transpiration rate and leaf water potential under heterogeneous soil moisture conditions. The authors found that the simplified model of root water uptake was capable of reproducing the relationship in wet and dry soils (Hayat et al., 2019). The drawback of using root architecture models is that they require additional parameters that are challenging to measure, especially in intact plants.

Sodium ions were found to impact the swelling and dispersion processes of clay particles within soil aggregates (Gupta and Verma, 1985; Klopp and Daigh, 2020), resulting in a different pore geometry. However, our data suggest that this was not the case for the sandy loam used in this study and hence salinity in soil solution did not impact the hydraulic properties of bulk soil (Figure 5.4). It is worth noting that substrates used in this study were not aggregated soil due to sieving through a 1-mm sieve. The absence of soil aggregates might explain the neutral effect of salinity on hydraulic properties. However, our data cannot exclude the possibility that NaCl can impact the hydraulic properties of soils with diverse textures and structures.

In conclusion, salinity impacted the relationship between transpiration and leaf water potential in a predictable way. According to our modelling exercise, limited transpiration rates are explained by the accumulation of salts at the root-soil interface. Complementary measurements of salt concentration at the root-soil interface would be needed to support this interpretation.

5.5 MATERIALS AND METHODS

5.5.1 Soil and Plant preparation

Grafted tomato (*Solanum lycopersicum* L.) plants were used in this study. Grafting facilitates the coupling of independent genotypes based on desirable traits of roots and shoots (Abdelhafeez et al., 1975; Albacete et al., 2015; Rouphael et al., 2018). Scions from the M82 variety were grafted onto wild tomato (*Lycopersicon hirsutum*) that provided rootstock, which was suggested to potentially tolerate salinity stress (Bolarín et al., 1991). Seeds of scion and rootstock were sown simultaneously in different pots. Rootstock seeds were grown in polyvinyl chloride (PVC) cylinders 30 cm in height and 10 cm in diameter. Five holes with a diameter of 5 mm were made on the cylinders' side every 5 cm for soil water content measurement. The cylinders were filled with sandy-loam soil with a bulk density of 1.4 g cm^{-3}. The soil was a mixture of 62.5% loamy soil and 37.5% quartz sand passing through a 1-mm sieve to facilitate homogeneity among replicates. After soil filling, the cylinders were capped with an aluminum plate with a central hole 1.4 cm in diameter using silicon rubber glue (Teroson, Henkeln, Germany).

Seeds were grown at a depth of 1.5 cm in the central hole of the aluminum plate. Seedlings of scions and rootstocks were grafted when the diameters of their stems matched, which occurred approximately one week after germination. Immediately after grafting, plants were placed inside a chamber at *ca.* 95% relative humidity and 200 μmol m^{-2} s^{-1} photosynthetic photon flux density (PPFD) for *ca.* five days. Thereafter, the established plants were placed in a climate-controlled room with a photoperiod of 14 hours, a day/night temperature of 28/18 °C, and a day/night relative humidity of 57/65%. The PPFD was *ca.* 600 μmol m^{-2} s^{-1} (Luxmeter PCE-174, Meschede, Germany). Soil water content was maintained above 0.15 cm^3 cm^{-3} during the growth.

Two weeks after grafting, plants were transferred to the laboratory (PPFD: 200 μmol m^{-2} s^{-1}; temperature 25/18°C) and sealed at the collar with a glue (Supplemental Figure S5; UHU plus Endfest 300, Bühl, Germany). To introduce saline conditions, three plants (out of six) were treated with 100 mM NaCl solution. Each plant received 200 ml within two to three days before the start of measurements. During plant growth, soil water content (θ) was measured using time-domain refractometer (TDR; E-Test, Lublin, Poland). Soil osmotic potential was measured in wet unplanted soil using an osmometer (VAPRO Pressure Osmometer 5600, ELITechGroup, USA).

At the end of the experiments, plant biomass was evaluated in terms of leaf area and root length measurements. Leaf area was determined using ImageJ software (1.50e http://imagej.nih.gov/ij). After the experiments, roots were collected and the total root length and diameter were obtained using WinRihzo software (Regent Instruments Inc., Canada).

5.5.2 Transpiration and leaf xylem water potential measurements

A root pressure chamber system (RPCS) was used to simultaneously measure transpiration (E) and leaf xylem water potential ($\psi_{\text{leaf-x}}$) in intact plants during soil drying (Passioura, 1980). The RPCS was recently described in Cai et al. (2020a) and Abdalla et al. (2021). Briefly, the pot was placed inside a root pressure chamber, with the shoots enclosed in a cuvette to obtain E. Light-emitting diodes (LEDs) were attached to the cuvette vertically to provide a PPFD for E regulation. A continuous airflow with a velocity of 8.25 L min^{-1} passed through the cuvette. Combined temperature-humidity sensors (Galltec-Mela, Bondorf, Germany) measured the temperature and the relative humidity of the inward and the outward air continuously. E was determined by multiplying the airflow rate by the difference between the outward and the inward humidity.

The basic concept of root pressure chambers was to balance the suction inside the plant by applying pneumatic pressure to the soil and roots. The applied pressure (balancing pressure; P) is numerically equal to leaf xylem tension before pressurization (Passioura, 1980; Abdalla et al., 2021). A meniscus system was connected to a leaflet cut (at the petiolule) to evaluate the stability of the droplet. The $\psi_{\text{leaf-x}}$ was determined when the meniscus was kept stable for *ca.* 10 minutes (Cai et al., 2020a).

E was changed by increasing the PPFD stepwise from 0 µmol m^{-2} s^{-1} to 200, 400, 600, 800, and 1000 µmol m^{-2} s^{-1}. Concomitantly, the corresponding $\psi_{\text{leaf-x}}$ was determined at each PPFD. Furthermore, E was measured at the highest PPFD (1000 µmol m^{-2} s^{-1}) without plant pressurization. Each plant was measured at different soil water contents from wet (first day) to dry (third/fourth day). Soil drying happened naturally during the days of measurements. In total, plants experienced salinity conditions for *ca.* 7 – 9 days.

5.5.3 Modeling water and solute flow in the soil–plant continuum

We used a model coupling water flow and solute transport to reproduce the measured relationship between transpiration rate and leaf xylem water potential. The mass conservation principle combined with the Richards equation for one-dimensional axisymmetric flow toward a single root, according to de Jong van Lier et al. (2006), can be written as:

$$\frac{\partial \theta}{\partial t} = \frac{C(\psi_m)\partial \psi_m}{\partial t} = -\frac{\partial(rq)}{\partial r} \qquad (1)$$

$$q = -K_s(\psi_m)\frac{\partial \psi_m}{\partial r} \qquad (2)$$

where θ is the volumetric soil water content (cm^3 cm^{-3}), C is the specific soil water capacity ($\partial\theta/\partial\psi_m, cm^{-1}$), q is the water flux (cm s^{-1}), K_s is the soil hydraulic conductivity (cm s^{-1}), ψ_m is the function of the soil matric potential (hPa, 1 hPa $\approx$ 1 cm), r is the radial distance (cm), $\frac{\partial\psi_m}{\partial r}$ is the gradient in matric potential and t is time (s). This equation (Eq. 2) was solved numerically using a fully implicit finite difference method in MATLAB software (Math Works, Inc., Natick, MA, USA). Hereafter, this equation was subjected to the following initial and boundary conditions:

$$\psi_m(t) = \psi_{m,0} \qquad t = 0 \qquad (3)$$

$$q(r) = \frac{E}{2\pi r_0 L} \qquad r = r_0 \qquad (4)$$

$$q(r) = 0 \qquad r = r_b \qquad (5)$$

where $\psi_{m,0}$ is the soil matric potential at time zero and corresponding to the average soil water content in the sample (cm), r_0 and r_b are the root radius and the exterior radius of soil around the root (cm), E is the transpiration rate (cm^3 s^{-1}), L is the root length active in water uptake

(cm), which was used as fitting parameters. In this model, L is a single root that represents the root system. The r_b is determined by L and the volume of the pot V (cm^3), according to:

$$r_b = \sqrt{\frac{V}{\pi L}} \qquad (6)$$

The solution of equation (1) gives the profile of soil matric potential as a function of radius from the root surface. We simulated NaCl transport and its concentration in the soil solution to include the effect of osmotic potential on the leaf xylem water potential. According to de Jong van Lier et al. (2009), the combined mass conservation principle and solute transport processes under one-dimensional axisymmetric flow conditions give:

$$\frac{\partial(\theta+b)C_w}{\partial t} = \frac{\partial}{r\partial r}\left(\theta r D(\theta)\frac{\partial C_w}{\partial r}\right) - \frac{\partial}{r\partial r}(rqC_w) \qquad (7)$$

where C_w is the concentration of NaCl in the soil solution (mol ml^{-1}), b is the coefficient describing the adsorption of Na by the solid phase (-), and $D(\theta)$ is the diffusion coefficient of Na in the soil solution (cm^2 s^{-1}) described as:

$$D(\theta) = D_0\frac{\theta^{10/3}}{\phi^2} \qquad (8)$$

where D_0 is self-diffusion coefficient of Na in free water (cm^2 s^{-1}), and ϕ is soil porosity (-). Equation (7) was solved numerically using a fully implicit finite difference method in MATLAB. Therefore, this equation was subjected to the following initial and boundary conditions:

$$C_w(t) = C_{w,0} \qquad\qquad t = 0 \qquad (9)$$

$$\theta r D\frac{\partial C_w}{\partial r} - rqC_w = 0 \qquad r = r_0 \qquad (10)$$

$$\theta r D\frac{\partial C_w}{\partial r} - rq_{w} = 0 \qquad r = r_b \qquad (11)$$

where $C_{w,0}$ is the concentration of Na in the soil solution (mol ml^{-1}) at time zero. Eq (10) and (11) impose a zero solute flux boundary condition at both ends of the soil domain (r_0 and r_b).

The solution of equation (7) gives the profile of solute concentration in the soil solution as a function of both distance from root surface and time. We used the following relationship to

estimate the osmotic potential (ψ_π [bar]) in the soil solution based on the profile of concentrations:

$$\psi_\pi = -\omega n R C_w T \qquad (12)$$

where ω is a unit-less osmotic coefficient depending on the type of solute ($\omega = 0.9$ for the case of NaCl), C_w is the molar concentration of Na in the soil solution (mol ml^{-1}), n is the number of ions produced when the solute undergoes dissociation ($n = 2$ for NaCl), R is the universal gas constant (0.0831 L bar mol^{-1} K^{-1}), and T is the temperature (Kelvin). The units were converted consistently in the model.

Combination of equations (1) to (12) gives the profile of water potential in the soil as a function of distance from the root surface. In the pressure chamber experiment, we measured leaf xylem water potential at varying transpiration rates for varying soil water contents. The slope of the linear part of $E(\psi_{\text{leaf-x}})$ depicts plant hydraulic conductance (K_{plant}), which is the harmonic mean of the stem xylem hydraulic conductance (K_x) and root hydraulic conductance (K_{root}). According to Abdalla et al. (2021), K_{plant} is approximately equal to K_{root}. Knowing transpiration rate and K_{root}, we estimated the dissipation of water potential between the soil-root interface and the plant leaf xylem. Based on this principle, the water potential in the leaf xylem is given by:

$$\psi_{leaf-x} = -\frac{E}{K_{root}} + \psi_m(r_0) + \psi_\pi(r_0) \qquad (13)$$

where K_{root} is the hydraulic conductance of root (cm^3 s^{-1} hPa^{-1}) and $\psi_m(r_0)$ and $\psi_\pi(r_0)$ are the matric potential and osmotic potential in the soil at the root surface.

The difference between soil and plant osmotic potential leads to a deviation between predawn leaf and soil water potential (Donovan et al., 2001; Cai et al., 2020a; Abdalla et al., 2022), which was added to the simulations as an offset.

5.5.4 Model parameterization

The hydraulic properties of the soil mixture used in this study were measured via the evaporative method implemented in the Hyprop (Meter Group, Munich, Germany). This device encompasses two tensiometers and a balance, it measures gravimetric soil water content

and the corresponding matric potential in soil samples as described hereafter. Soil samples were packed into a Hyprop sample holder (area of 50 cm^2 and height of 5 cm) at the same bulk density as the one achieved in the cylinders used for plant growth. Three samples were saturated with water, and the other three samples were with 100 mM NaCl solution from the bottom. The samples were let dry from the top via evaporation, and the changes in soil water content, matric potential at two depths (-1.25 and -3.75 cm) were recorded over time. Water retention curves and unsaturated hydraulic conductivity curves were parameterized according to the PDI (Peter-Durner-Iden) model (Peters et al., 2015). The parameters were estimated by fitting the obtained measurements and solving the Richards equation.

The K_{root} was obtained as the slope of the linear part of $E(\psi_{\text{leaf-x}})$ at each soil water content. Thus, dynamic K_{root} was used during the simulation. The root length active in water uptake (L) was a fitting parameter in the model. L value was obtained from inverse modeling of measured $E(\psi_{\text{leaf-x}})$-relation in different soil water contents, for both treatments. The inverse modeling approach minimized the difference between measured and simulated $\psi_{\text{leaf-x}}$ at each E value systematically. The following objective function (ObjFunc) was used:

$$ObjFunc = \sum_{i=1}^{i=n} \frac{\left(\psi_{leaf-} (i) - \psi_{leaf-},sim(i)\right)^2}{\psi_{leaf-x}(i)^2} \qquad (14)$$

5.5.5 Statistical analysis

The influences of salinity and drought on transpiration, with and without plant pressurization, were statistically evaluated using N-way analysis of variance followed by multiple comparison (Tukey-Kramer test). MATLAB (Math Works Inc., USA) was used to perform the analyses (N-way analysis of variance: *anovan*; multiple comparison: *multcompare*). The differences in measured root length and diameter between treatments were evaluated using *t*-test. Statistical significance was considered when *p-value* was < 0.05. Furthermore, we tested the values of predawn leaf water potential as a function of soil water potential for both treatments using analysis of covariance (ANCOVA). We estimated the confidence intervals at 95% to identify the influences of NaCl solution on soil retention curves and soil unsaturated hydraulic conductivity curves. The relationship between transpiration rate and leaf xylem water potential at a given soil moisture was fitted with both linear and quadratic functions to test the onset of hydraulic non-linearity statistically.

Supplemental Data

Supplemental Figure S1. Root parameters were similar in controlled and salt treated plants.

Supplemental Figure S2 Relationship between transpiration rate and leaf xylem water potential in different soil water contents under **non-saline** conditions.

Supplemental Figure S3 Relationship between transpiration rate and leaf xylem water potential in different soil water contents under **saline** conditions.

Supplemental Figure S4 Linear fit of the relationship between predawn leaf water potential and soil water potential.

Supplemental Figure S5: Tomato plant (*Solanum lycopersicum* L.) glued at the collar.

Supplemental Table S1 Analysis of variance (ANOVA) considering the influences of salinity, soil drying and their interactions on transpiration rate measured **without** plant pressurization.

Supplemental Table S2 Analysis of variance (ANOVA) considering the influences of soil drying, salinity, photosynthetic photon flux density and their interactions on transpiration rate measured **with** plant pressurization.

Supplemental Table S3 Coefficient estimates for the relationship between predawn leaf water potential and soil water potential in control and salt treatments in terms of slope and the intercept. **Supplemental Table S4**. Analysis of variance to identify the significant difference between the slope and the intercept of the relationship between predawn leaf water potential and soil water potential in control and salt treatments as shown in Supplemental Table **S3**.

Authors contributions

All authors conceptualized the study. MA performed the experiment and analyzed the data. AC, MZ and MA made the simulations. MA wrote the manuscript with contributions of MAA, GC, MZ and AC.

Funding

Acknowledgments

5.6 REFERENCES

Abdalla M, Ahmed MA, Cai G, Wankmüller F, Schwartz N, Litig O, Javaux M, Carminati A (2022) Stomatal closure during water deficit is controlled by below-ground hydraulics. Annals of Botany **129**: 161–170

Abdalla M, Carminati A, Cai G, Javaux M, Ahmed MA (2021) Stomatal closure of tomato under drought is driven by an increase in soil–root hydraulic resistance. Plant, Cell & Environment **44**: 425–431

Abdelhafeez AT, Harssema H, Verkerk K (1975) Effects of air temperature, soil temperature and soil moisture on growth and development of tomato itself and grafted on its own and eggplant rootstock. Scientia Horticulturae **3**: 65–73

Ahmed MA, Passioura J, Carminati A (2018) Hydraulic processes in roots and the rhizosphere pertinent to increasing yield of water-limited grain crops: a critical review. J Exp Bot **69**: 3255–3265

Albacete A, Martínez-Andújar C, Martínez-Pérez A, Thompson AJ, Dodd IC, Pérez-Alfocea F (2015) Unravelling rootstock×scion interactions to improve food security. Journal of Experimental Botany **66**: 2211–2226

Azaizeh H, Gunse B, Steudle E (1992) Effects of NaCl and CaCl2 on Water Transport across Root Cells of Maize (Zea mays L.) Seedlings. Plant Physiology **99**: 886–894

Azaizeh H, Steudle E (1991) Effects of Salinity on Water Transport of Excised Maize (Zea mays L.) Roots. Plant Physiology **97**: 1136–1145

Bolarín MC, Fernández FG, Cruz V, Cuartero J (1991) Salinity Tolerance in Four Wild Tomato Species using Vegetative Yield-Salinity Response Curves. Journal of the American Society for Horticultural Science **116**: 286–290

Bourbia I, Pritzkow C, Brodribb TJ (2021) Herb and conifer roots show similar high sensitivity to water deficit. Plant Physiology **186**: 1908–1918

Boursiac Y, Chen S, Luu D-T, Sorieul M, Dries N van den, Maurel C (2005) Early Effects of Salinity on Water Transport in Arabidopsis Roots. Molecular and Cellular Features of Aquaporin Expression. Plant Physiology **139**: 790–805

Brodribb TJ, Powers J, Cochard H, Choat B (2020) Hanging by a thread? Forests and drought. Science **368**: 261–266

Cai G, Ahmed MA, Abdalla M, Carminati A (2022) Root hydraulic phenotypes impacting water uptake in drying soils. Plant, Cell & Environment **45**: 650–663

Cai G, Ahmed MA, Dippold MA, Zarebanadkouki M, Carminati A (2020a) Linear relation between leaf xylem water potential and transpiration in pearl millet during soil drying. Plant Soil **447**: 565–578

Cai G, Ahmed MA, Reth S, Reiche M, Kolb A, Carminati A (2020b) Measurement of leaf xylem water potential and transpiration during soil drying using a root pressure chamber system. Acta Hortic 131–138

Cai G, Carminati A, Abdalla M, Ahmed MA (2021) Soil textures rather than root hairs dominate water uptake and soil–plant hydraulics under drought. Plant Physiology **187**: 858–872

Carminati A, Ahmed MA, Zarebanadkouki M, Cai G, Lovric G, Javaux M (2020) Stomatal closure prevents the drop in soil water potential around roots. New Phytologist **226**: 1541–1543

Carminati A, Javaux M (2020) Soil Rather Than Xylem Vulnerability Controls Stomatal Response to Drought. Trends in Plant Science **25**: 868–880

Carminati A, Passioura JB, Zarebanadkouki M, Ahmed MA, Ryan PR, Watt M, Delhaize E (2017) Root hairs enable high transpiration rates in drying soils. New Phytologist **216**: 771–781

Chaves MM, Flexas J, Pinheiro C (2009) Photosynthesis under drought and salt stress: regulation mechanisms from whole plant to cell. Annals of Botany **103**: 551–560

Choat B, Brodribb TJ, Brodersen CR, Duursma RA, López R, Medlyn BE (2018) Triggers of tree mortality under drought. Nature **558**: 531–539

Deery DM, Passioura JB, Condon JR, Katupitiya A (2013) Uptake of water from a Kandosol subsoil. II. Control of water uptake by roots. Plant Soil **368**: 649–667

Donovan L, Linton M, Richards J (2001) Predawn plant water potential does not necessarily equilibrate with soil water potential under well-watered conditions. Oecologia **129**: 328–335

Draye X, Kim Y, Lobet G, Javaux M (2010) Model-assisted integration of physiological and environmental constraints affecting the dynamic and spatial patterns of root water uptake from soils. Journal of Experimental Botany **61**: 2145–2155

Fricke W, Akhiyarova G, Veselov D, Kudoyarova G (2004) Rapid and tissue-specific changes in ABA and in growth rate in response to salinity in barley leaves. Journal of Experimental Botany **55**: 1115–1123

Fricke W, Bijanzadeh E, Emam Y, Knipfer T (2014) Root hydraulics in salt-stressed wheat. Functional Plant Biol **41**: 366–378

Gupta RK, Verma SK (1985) Hydraulic conductivity of a swelling clay in relation to irrigation water quality. CATENA **12**: 121–127

Haber-Pohlmeier S, Vanderborght J, Pohlmeier A (2017) Quantitative mapping of solute accumulation in a soil-root system by magnetic resonance imaging. Water Resources Research **53**: 7469–7480

Hamza M, Anderson S, Aylmore G (2001) Studies of soil water drawdown by single radish roots at decreasing soil water content using computer-assisted tomography. Soil Research **39**: 1387–1396

Hamza M, Aylmore G (1992a) Soil solute concentration and water uptake by single lupin and radish plant roots - I. Water extraction and solute accumulation. Plant and Soil **145**: 187–196

Hamza MA, Aylmore LAG (1992b) Soil solute concentration and water uptake by single lupin and radish plant roots. Plant Soil **145**: 197–205

Harper RJ, Dell B, Ruprecht JK, Sochacki SJ, Smettem KRJ (2021) Chapter 7 - Salinity and the reclamation of salinized lands. *In* JA Stanturf, MA Callaham, eds, Soils and Landscape Restoration. Academic Press, pp 193–208

Hayat F, Ahmed MA, Zarebanadkouki M, Cai G, Carminati A (2019) Measurements and simulation of leaf xylem water potential and root water uptake in heterogeneous soil water contents. Advances in Water Resources **124**: 96–105

Hayat F, Ahmed MA, Zarebanadkouki M, Javaux M, Cai G, Carminati A (2020) Transpiration Reduction in Maize (Zea mays L) in Response to Soil Drying. Front Plant Sci. doi: 10.3389/fpls.2019.01695

Helliwell JR, Sturrock CJ, Mairhofer S, Craigon J, Ashton RW, Miller AJ, Whalley WR, Mooney SJ (2017) The emergent rhizosphere: imaging the development of the porous architecture at the root-soil interface. Sci Rep 7: 1–10

Hopmans JW, Qureshi AS, Kisekka I, Munns R, Grattan SR, Rengasamy P, Ben-Gal A, Assouline S, Javaux M, Minhas PS, et al (2021) Chapter One - Critical knowledge gaps and research priorities in global soil salinity. *In* DL Sparks, ed, Advances in Agronomy. Academic Press, pp 1–191

Javaux M, Carminati A (2021) Soil hydraulics affect the degree of isohydricity. Plant Physiology **186**: 1378–1381

Jorda H, Perelman A, Lazarovitch N, Vanderborght J (2018) Exploring Osmotic Stress and Differences between Soil–Root Interface and Bulk Salinities. Vadose Zone Journal **17**: 170029

Klopp HW, Daigh ALM (2020) Soil hydraulic model parameters and methodology as affected by sodium salt solutions. Soil Science Society of America Journal **84**: 354–370

Kumar P, Sharma PK (2020) Soil Salinity and Food Security in India. Frontiers in Sustainable Food Systems **4**: 174

LANDSBERG JJ, FOWKES ND (1978) Water Movement Through Plant Roots. Annals of Botany **42**: 493–508

Li W, Zhang H, Wang W, Zhang P, Ward ND, Norwood M, Myers-Pigg A, Zhao C, Leff R, Yabusaki S, et al (2021) Changes in carbon and nitrogen metabolism during seawater-induced mortality of Picea sitchensis trees. Tree Physiology. doi: 10.1093/treephys/tpab073

Lier Q de J van, Dam JC van, Metselaar K (2009) Root Water Extraction under Combined Water and Osmotic Stress. Soil Science Society of America Journal 73: 862–875

Lier Q de J van, Metselaar K, Dam JC van (2006) Root Water Extraction and Limiting Soil Hydraulic Conditions Estimated by Numerical Simulation. Vadose Zone Journal 5: 1264–1277

Liu Y, Kumar M, Katul GG, Feng X, Konings AG (2020) Plant hydraulics accentuates the effect of atmospheric moisture stress on transpiration. Nat Clim Chang 10: 691–695

Moldrup P, Olesen T, Komatsu T, Schjønning P, Rolston D e. (2001) Tortuosity, Diffusivity, and Permeability in the Soil Liquid and Gaseous Phases. Soil Science Society of America Journal 65: 613–623

Munns R (2002) Comparative physiology of salt and water stress. Plant, Cell & Environment 25: 239–250

Munns R (1985) Na+, K+ and Cl− in Xylem Sap Flowing to Shoots of NaCl-Treated Barley. Journal of Experimental Botany 36: 1032–1042

Munns R, Day DA, Fricke W, Watt M, Arsova B, Barkla BJ, Bose J, Byrt CS, Chen Z-H, Foster KJ, et al (2020a) Energy costs of salt tolerance in crop plants. New Phytologist 225: 1072–1090

Munns R, Gilliham M (2015) Salinity tolerance of crops – what is the cost? New Phytologist 208: 668–673

Munns R, Guo J, Passioura JB, Cramer GR (2000) Leaf water status controls day-time but not daily rates of leaf expansion in salt-treated barley. Functional Plant Biol 27: 949–957

Munns R, Passioura J (1984) Effect of Prolonged Exposure to Nacl on the Osmotic Pressure of Leaf Xylem Sap From Intact, Transpiring Barley Plants. Functional Plant Biol 11: 497

Munns R, Passioura JB, Colmer TD, Byrt CS (2020b) Osmotic adjustment and energy limitations to plant growth in saline soil. New Phytologist 225: 1091–1096

Munns R, Tester M (2008) Mechanisms of Salinity Tolerance. Annual Review of Plant Biology **59**: 651–681

Passioura JB (1980) The Transport of Water from Soil to Shoot in Wheat Seedlings. J Exp Bot **31**: 333–345

Passioura JB (2020) Translational research in agriculture. Can we do it better? Crop Pasture Sci **71**: 517–528

Perelman A, Jorda H, Vanderborght J, Lazarovitch N (2020a) Tracing root-felt sodium concentrations under different transpiration rates and salinity levels. Plant Soil **447**: 55–71

Perelman A, Lazarovitch N, Vanderborght J, Pohlmeier A (2020b) Quantitative imaging of sodium concentrations in soil-root systems using magnetic resonance imaging (MRI). Plant Soil **454**: 171–185

Peters A, Iden SC, Durner W (2015) Revisiting the simplified evaporation method: Identification of hydraulic functions considering vapor, film and corner flow. Journal of Hydrology **527**: 531–542

Rodriguez-Dominguez CM, Brodribb TJ (2020) Declining root water transport drives stomatal closure in olive under moderate water stress. New Phytologist **225**: 126–134

Rouphael Y, Kyriacou MC, Colla G (2018) Vegetable Grafting: A Toolbox for Securing Yield Stability under Multiple Stress Conditions. Front Plant Sci. doi: 10.3389/fpls.2017.02255

Schröder N, Lazarovitch N, Vanderborght J, Vereecken H, Javaux M (2014) Linking transpiration reduction to rhizosphere salinity using a 3D coupled soil-plant model. Plant Soil **377**: 277–293

Sperry JS, Love DM (2015) What plant hydraulics can tell us about responses to climate-change droughts. New Phytologist **207**: 14–27

Stirzaker RJ, Passioura JB (1996) The water relations of the root–soil interface. Plant, Cell & Environment **19**: 201–208

Tuller M, Or D, Dudley LM (1999) Adsorption and capillary condensation in porous media: Liquid retention and interfacial configurations in angular pores. Water Resources Research **35**: 1949–1964

Tyerman SD, Oats P, Gibbs J, Dracup M, Greenway H (1989) Turgor-Volume Regulation and Cellular Water Relations of Nicotiana tabacum Roots Grown in High Salinities. Functional Plant Biol **16**: 517–531

Vadez V (2014) Root hydraulics: The forgotten side of roots in drought adaptation. Field Crops Research **165**: 15–24

Wan X (2010) Osmotic effects of NaCl on cell hydraulic conductivity of corn roots. Acta Biochimica et Biophysica Sinica **42**: 351–357

van Zelm E, Zhang Y, Testerink C (2020) Salt Tolerance Mechanisms of Plants. Annual Review of Plant Biology **71**: 403–433

Zhang H, Li X, Wang W, Pivovaroff AL, Li W, Zhang P, Ward ND, Myers-Pigg A, Adams HD, Leff R, et al (2021) Seawater exposure causes hydraulic damage in dying Sitka-spruce trees. Plant Physiology **187**: 873–885

5.7 Supplemental data
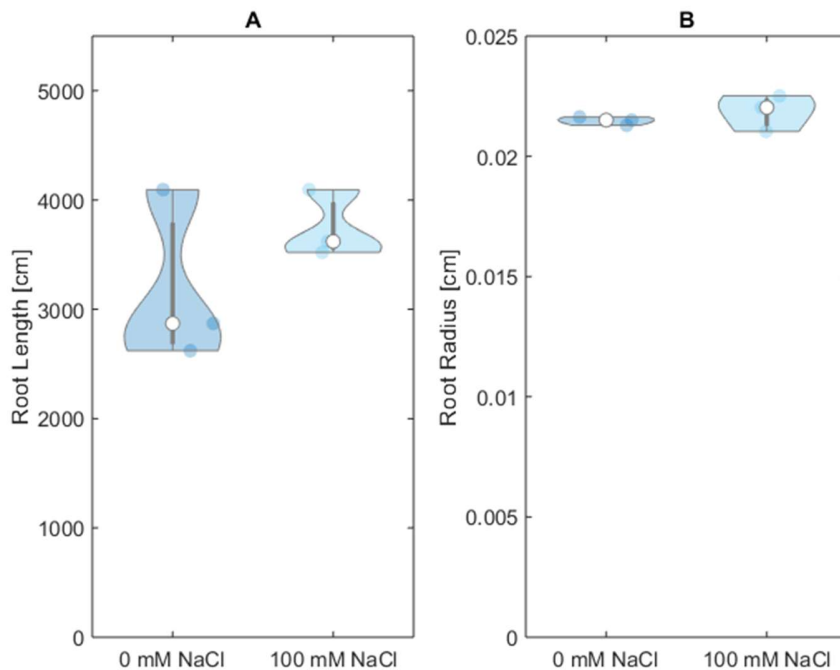
Supplemental Figure S1 Root parameters were similar in controlled and salt treated plants. **A**, Root length (*p-value* = 0.323) and **B**, root diameter (*p-value* = 0.44). The *t*-test was used for testing the statistical significance, $n = 3$. White symbol represents median. The thick vertical black line depicts the interquartile range by connecting first (below) and third (above) quartiles, while the thin vertical lines are the whiskers. The horizontal lines depict the upper and the lower adjacent values.
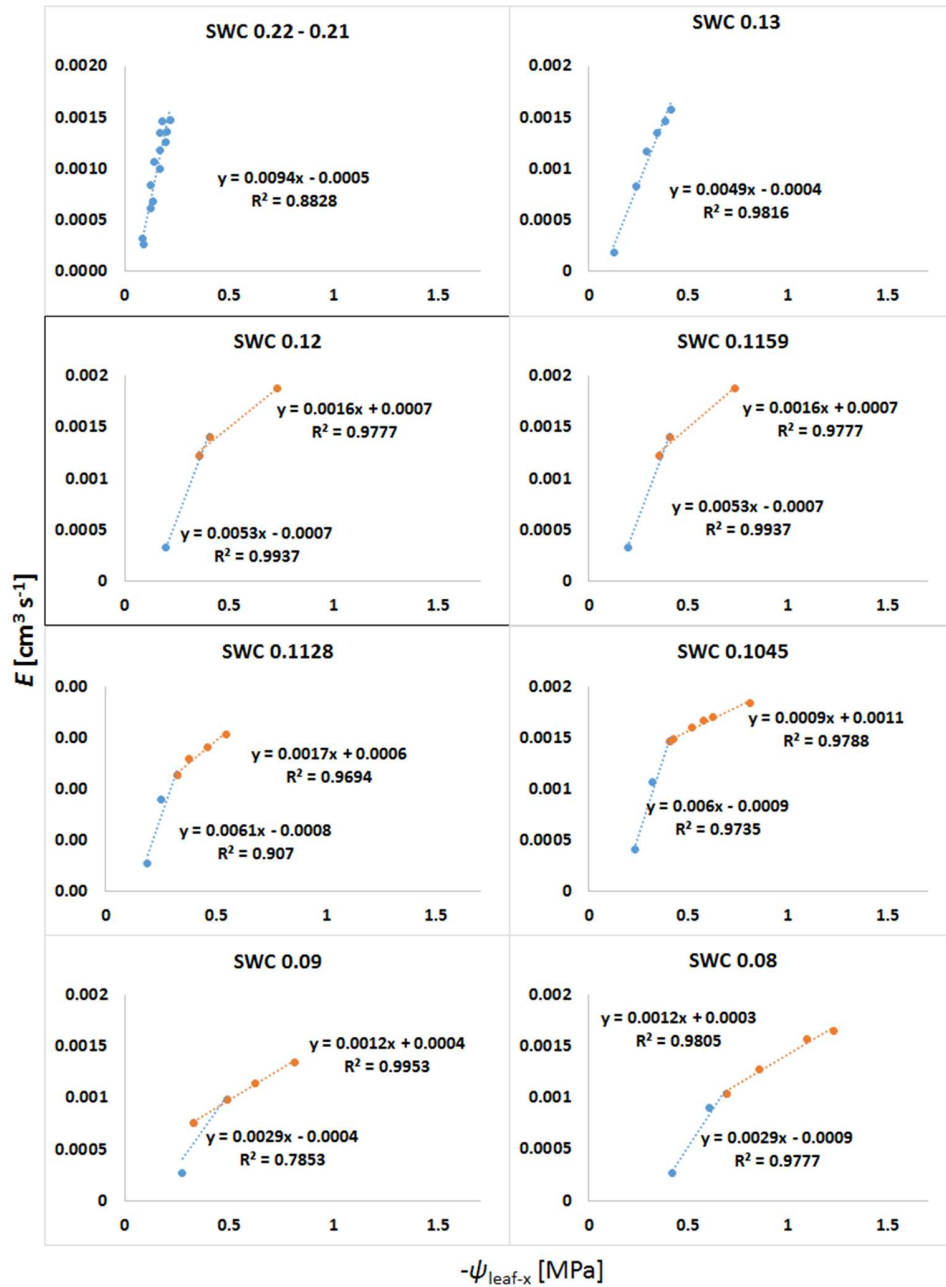
Supplemental Figure S2 Relationship between transpiration rate and leaf xylem water potential in different soil water contents under **non-saline** conditions. The relation was fitted with one linear line in wet conditions. However, in dry conditions (starting from SWC = 0.12 cm^3 cm^{-3}), two linear lines, with two different slopes, were needed to fit the relation, meaning that the relation verged from linear to non-linear.
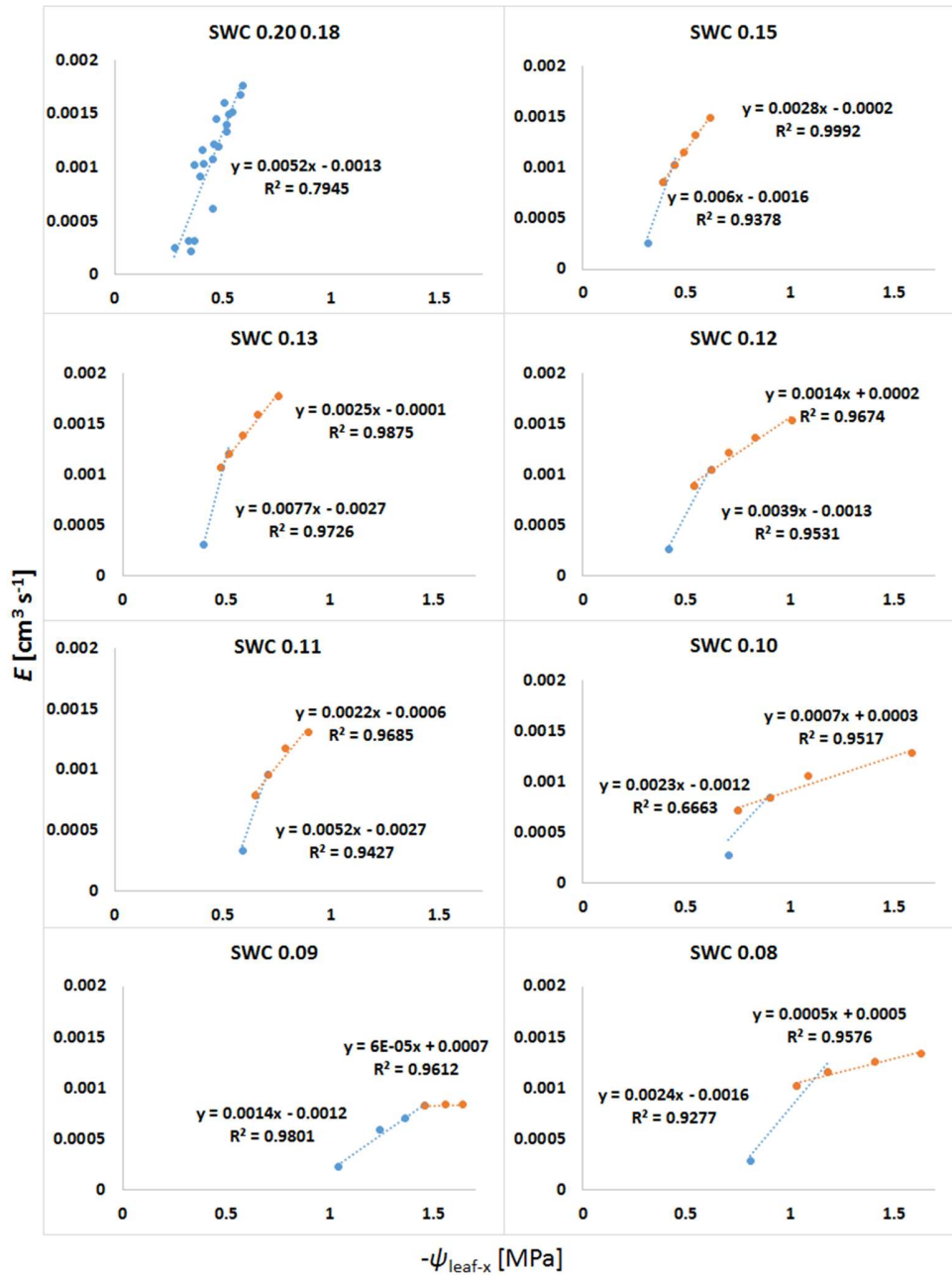
Supplemental Figure S3 Relationship between transpiration rate and leaf xylem water potential in different soil water contents under **saline** conditions. As in Supplementary Figure S2, the relation was fitted with one linear line in wet conditions. However, two lines with two different slopes were needed to fit the relation in wetter soils (SWC = 0.15 cm^3 cm^{-3}). This means the non-linearity occurred in wetter conditions under saline compared to non-saline conditions.
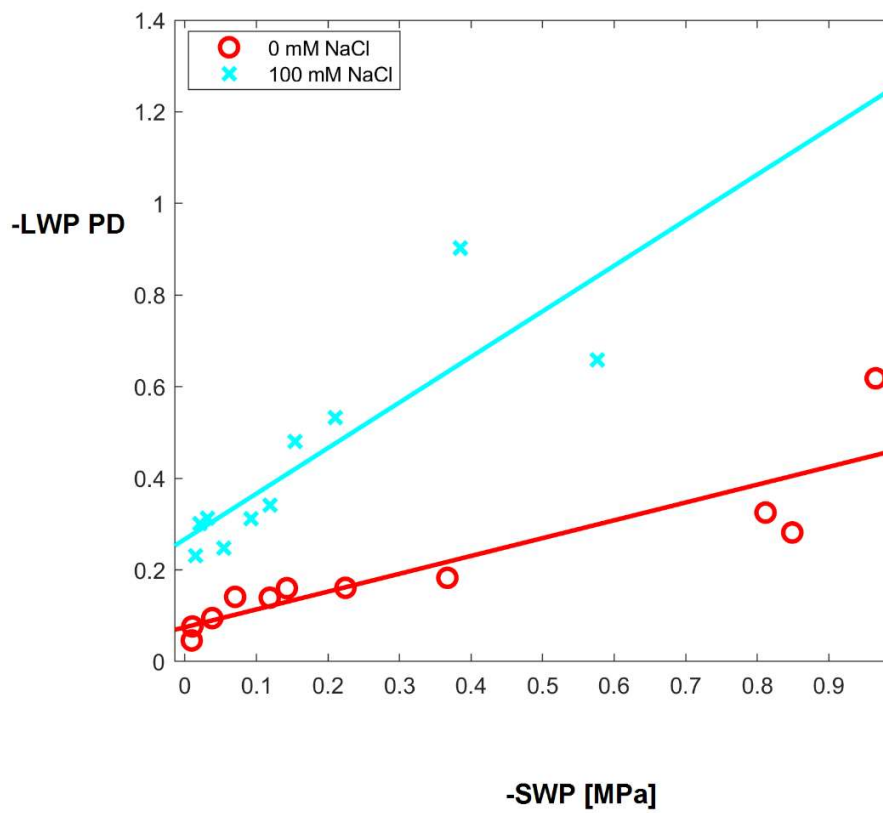
Supplemental Figure S4 Linear fit of the relationship between predawn leaf water potential (LWP PD [MPa]) and soil water potential (SWP [MPa]) as shown in Figure 3. Slope and intercept were utilized for the analysis of covariance (ANCOVA followed by Tukey-Kramer test; see Supplementary Tables S2 and S3), which showed significant shift of predawn leaf water potential to a more negative range after 100 mM NaCl treatment (*p-value* < 0.01, *n* = 3).
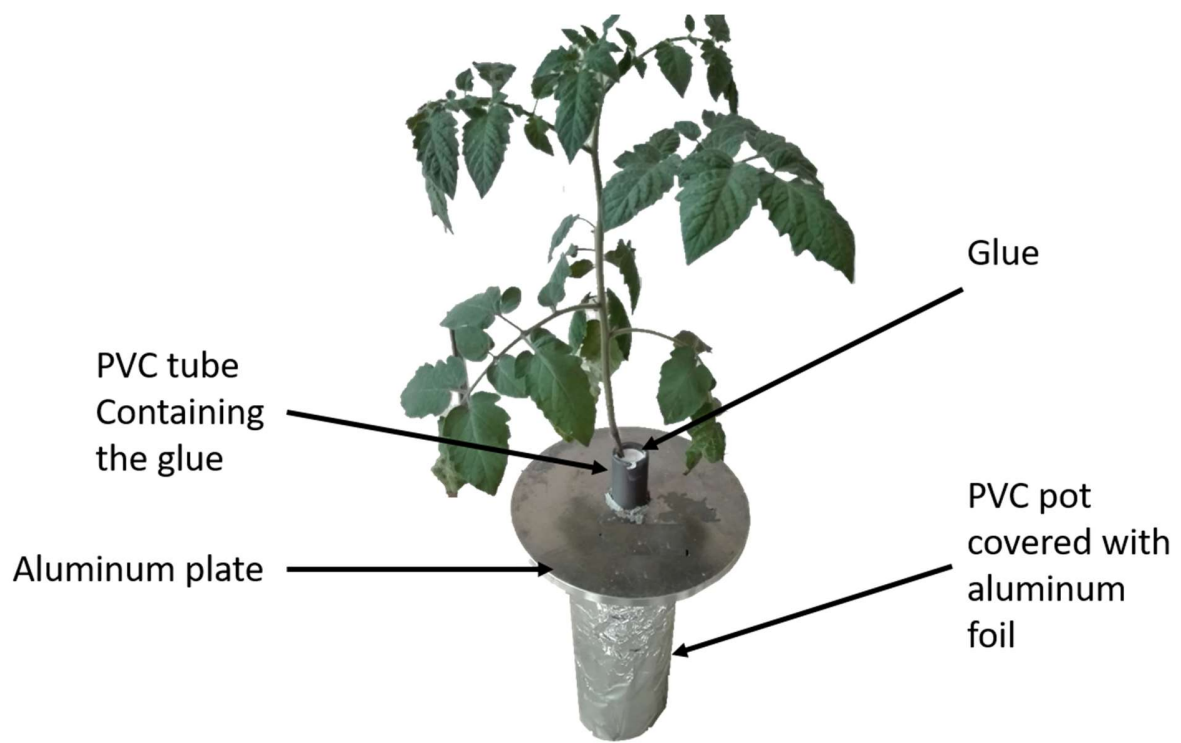
Glue

PVC tube
Containing
the glue

PVC pot
covered with
aluminum
foil

Aluminum plate

Supplemental Figure S5: Tomato plant (*Solanum lycopersicum* L.) glued at the collar.

Supplemental Table S1 ANOVA considering the influences of salinity, soil drying and their interactions on transpiration rate measured **without** plant pressurization.

Source		Sum Sq.¶	d. f.	Mean Sq.	F	Prob. > F
NaCl¶¶		8.22×10^{-7}	1	8.22×10^{-7}	14.75	**0.0027****
SWC¶¶¶		1.23×10^{-7}	3	4.09×10^{-7}	7.35	**0.0056****
NaCl SWC	×	6.33×10^{-7}	3	2.11×10^{-8}	0.38	0.7701
Error		6.13×10^{-7}	11	5.57×10^{-8}		
Total		2.73×10^{-6}	18			

$\P$ **Sum Sq**.: sum of squares, **d. f**.: degree of freedom, **Mean Sq.:** Mean sum of squares, **F**: F-statistic value. $p < 0.001$***, $p < 0.01$**, $p < 0.05$*.

$\P\P$NaCl treatment.

$\P\P\P$ SWC: soil water content, was clustered into four groups (>0.15; 0.13 – 0.11; 0.10; 0.09 – 0.07).

Supplemental Table S2 ANOVA considering the influences of soil drying, salinity, photosynthetic photon flux density and their interactions on transpiration rate measured **with** plant pressurization.

Source	Sum Sq.¶	d. f.	Mean Sq.	F	Prob. > F
NaCl¶¶	3.95×10^{-7}	1	3.95×10^{-7}	13.68	0.0004***
SWC¶¶¶	7.81×10^{-7}	3	2.61×10^{-7}	9.01	0***
PPFD¶¶¶¶	1.29×10^{-5}	5	2.58×10^{-6}	89.44	0***
NaCl × SWC	8.24×10^{-7}	3	2.74×10^{-7}	9.52	0***
NaCl × PPFD	7.93×10^{-8}	5	1.58×10^{-8}	0.55	0.7382
SWC × PPFD	1.84×10^{-7}	15	1.22×10^{-8}	0.43	0.9669
Error	2.16×10^{-6}	75	2.88×10^{-8}		
Total	2.23×10^{-5}	107			

¶ **Sum Sq**.: sum of squares, **d. f.:** degree of freedom, **Mean Sq**.: Mean sum of squares, **F**: F-statistic value. $p < 0.001$***, $p < 0.01$**, $p < 0.05$*.

¶¶NaCl treatment.

¶¶¶ SWC: soil water content, was clustered into four groups (>0.15; 0.13 – 0.11; 0.10; 0.09 – 0.07).

¶¶¶¶ PPFD: Photosynthetic photon flux density.

Supplemental Table S3 Coefficient estimates for the relation between predawn leaf water potential and soil water potential in control and salt treatments in terms of slope and the intercept.

Term	Estimate	Std. Err.	T	Prob > | T |
Intercept	0.171	0.03002	5.7	**0*****
- **Non-saline**	-0.0961	0. 03002	-3.2	0.0052
- **Saline**	0.0961	0. 03002	3.2	0.0052
Slope	0.6919	0.10069	6.87	**0*****
- **Non-saline**	-0.3029	0. 10069	-3.01	0.0079
- **Saline**	0.3029	0. 10069	3.01	0.0079

¶   p < 0.001***, p < 0.01**, p < 0.05*.

Supplemental Table S4. Analysis of variance to identify the significant difference between the slope and the intercept of the relation between predawn leaf water potential and soil water potential in control and salt treatments as shown in Supplemental table **S3**.

Source	d.f. ¶	Sum Sq.	Mean Sq.	F	Prob>F
Salinity treatment	1	0.46603	0.46603	46.74	**0*****
Soil water potential	1	0.41207	0.41207	41.33	**0*****
Salinity treatment × Soil water potential	1	0.09025	0.09025	9.05	**0.0079****
Error	17	0.16951	0.00997		

¶   **Sum Sq.:** sum of squares, **d. f.**: degree of freedom, **Mean Sq.**: Mean sum of squares, **F:** F-statistic value. p < 0.001***, p < 0.01**, p < 0.05*.

6   Chapter six: Arbuscular mycorrhiza symbiosis enhances water status and soil–plant hydraulic conductance under drought

Mohanned Abdalla[1,2*], and Mutez Ali Ahmed[1]

[1]Chair of Soil Physics, Bayreuth Center of Ecology and Environmental Research (BayCEER), University of Bayreuth, Bayreuth, Germany.

 [2]Department of Horticulture, Faculty of Agriculture, University of Khartoum, Khartoum North, Sudan.

*Corresponding author:

Mohanned Abdalla

Email: Mohanned.Abdalla@uni-bayreuth.de

6.1   ABSTRACT

Recent studies have identified soil drying as a dominant driver of transpiration reduction at the global scale. Although Arbuscular Mycorrhiza Fungi (AMF) are assumed to play a pivotal role in plant response to soil drying, studies investigating the impact of AMF on plant water status and soil–plant hydraulic conductance are lacking. Thus, the main objective of this study was to investigate the influence of AMF on soil–plant conductance and plant water status of tomato under drought. We hypothesized that AMF limit the drop in matric potential across the rhizosphere, especially in drying soil. The underlying mechanism is that AMF extend the effective root radius and hence reduce the water fluxes at the root-soil interface. The follow-up hypothesis is that AMF enhance soil–plant hydraulic conductance and plant water status during soil drying. To test these hypotheses, we measured the relation between transpiration, soil and leaf water potential of tomato with reduced mycorrhiza colonization (RMC) and the corresponding wild-type (WT). We inoculated the soil of the WT with *Rhizophagus irregularis* spores to potentially upsurge symbiosis initiation. During soil drying, leaf water potential of the WT did not drop below -0.8 MPa during the first six days after withholding irrigation, while leaf water potential of RMC dropped below -1 MPa already after four days. Furthermore, AMF enhanced the soil–plant hydraulic conductance of the WT during soil drying. In contrast, soil–plant hydraulic conductance of the RMC declined more abruptly as soil dried. We conclude that AMF maintained the hydraulic continuity between root and soil in drying soils, hereby reducing the drop in matric potential at the root-soil interface and enhancing soil–plant hydraulic conductance of tomato under edaphic stress. Future studies will investigate the role of AMF on soil–plant hydraulic conductance and plant water status among diverse plant species growing in contrasting soil textures.

Keywords: Soil drying, AMF, Abiotic stress, rhizosphere, root water uptake, biostimulants, microbiome.

6.2 INTRODUCTION

Water scarcity in soil and atmosphere escalates stress on vegetation and threatens future agricultural production and forest survival, especially in the face of climate change (Madadgar *et al.*, 2017; Brodribb *et al.*, 2020). Recent studies have identified soil drying as a primary cause of transpiration reduction globally, which is a greater stress factor than vapor pressure deficit (VPD) (Liu *et al.*, 2020). Thus, detailed knowledge of water flow processes, particularly below-ground, is required to fully understand and predict plant behavior under drought episodes and future climate conditions.

Water flow across the soil–plant-atmosphere continuum is driven by gradients in water potential between the atmosphere and soil. Water evaporation at the leaf surface (i.e. due to the increase in the vapor pressure deficit) creates a tension that propagates down to the roots and the soil. The leaf water potential (ψ_{leaf}) depends on both water potential in the soil (ψ_{soil}) and the hydraulic conductivities of the different elements (soil, root-soil interface, root, xylem and leaf) composing the soil–plant continuum. Sperry and Love (2015) used a hydraulic model of water flow to propose that stomata regulation allows plants not to exceed the water supply function determined by soil–plant hydraulics. In other words, downregulation of stomata in dry conditions avoids an excessive decline in leaf water potential before approaching a critical transpiration rate. This hypothesis implies that the leaf water potentials at which stomata close depend also on below-ground hydraulic properties (root, soil and their interface). Despite their importance, studies investigating the impact of below-ground traits on plant water status and soil–plant hydraulic conductance remain limited.

In wet soils, the hydraulic conductivity of soil is much higher than that of roots and hence water flow is mainly controlled by root hydraulic conductivity (Draye *et al.*, 2010). However, as soil dries, its conductivity drops by a few orders of magnitude, limiting the water flow towards the root surface (Passioura, 1980; Draye *et al.*, 2010). Indeed, Carminati and Javaux (2020) combined a soil–plant hydraulic model with meta-analysis to elucidate that the loss in soil conductivity, especially at the root-soil interface, controls stomatal response during water deficit. Similarly, we have recently showed that, in tomato, the decline in soil-root hydraulic conductance was the main driver of stomatal closure (Abdalla *et al.*, 2021). Rodriguez-Dominguez and Brodribb (2020) used a novel rehydration technique to demonstrate that the

154

loss in hydraulic conductivity at the root-soil interface occurred in parallel with stomatal closure. In a follow-up study, Bourbia et al. (2021) showed that a decline in root hydraulic conductivity was concomitant with a stomatal closure in both herbaceous and woody species. Plants developed various strategies to deal with the drop of conductivity at the root-soil interface (Carminati *et al.*, 2016; Ahmed *et al.*, 2018a). For instance, in barley, root hairs were not only documented to soften the gradients in matric potential at the root-soil interface (Carminati *et al.*, 2017), but also enhance plant water status and yield during water deficit (Marin *et al.*, 2020). Another example is mucilage, a gel exuded at the root tip, which was shown to facilitate water uptake in drying soils (Ahmed *et al.*, 2014). Furthermore, root-microbiome interactions (e.g. Arbuscular mycorrhiza fungi) provide fitness advantages to the host plant to mitigate water stress conditions (reviewed in Trivedi et al. (2020)).

Arbuscular mycorrhiza fungi (AMF) symbiosis, which occurs naturally between fungal and most plant species, is documented to play a positive role in plant water relations, especially under water deficit (Augé, 2001; Augé *et al.*, 2015; Ouledali *et al.*, 2018). For instance, Bitterlich et al. (2018b) showed that, in tomato, AMF facilitated higher transpiration rates in dry soils. Similarly, Chitarra et al. (2016) demonstrated that AMF enhanced tomato performance under water stress. The authors showed that AMF improved plant biomass and water use efficiency (Chitarra *et al.*, 2016). In maize, Quiroga et al. (2019) reported that AMF symbiosis enabled higher stomatal conductance under soil water deficit. Furthermore, it was also suggested that AMF increase root hydraulic conductivity (Aroca *et al.*, 2007; Quiroga *et al.*, 2019) and alter soil hydraulic properties (Bitterlich *et al.*, 2018a; Pauwels *et al.*, 2020). However, the impact of AMF on soil–plant hydraulic conductance, especially in drying soil, remain unknown. Note that this would be crucial to improve our current understanding of plant response to drought (Carminati *et al.*, 2020; Hayat *et al.*, 2020; Rodriguez-Dominguez and Brodribb, 2020; Abdalla *et al.*, 2021). Thus, there is an urgent need to investigate the influence of AMF on soil–plant hydraulic conductance during soil drying.

We hypothesize that AMF increase the root-soil contact and hence the effective root radius, especially in dry soil. This would reduce the flow velocity at the root surface and soften the drop in matric potential at the root-soil interface (Figure 6.1). This, in turn, would facilitate

higher (less negative) leaf water potential and enhance soil–plant hydraulic conductance during soil drying.

We tested this hypothesis in tomato plants inoculated with *Rhizophagus irregularis* spores. We utilized mutant variety with highly reduced AMF symbiosis and the corresponding wild-type. We measured transpiration rate, soil water content, water potentials in soil and leaf during soil drying. We used the relation between transpiration rate and leaf water potential to infer the hydraulic conductance of the soil–plant system for both genotypes during soil drying.
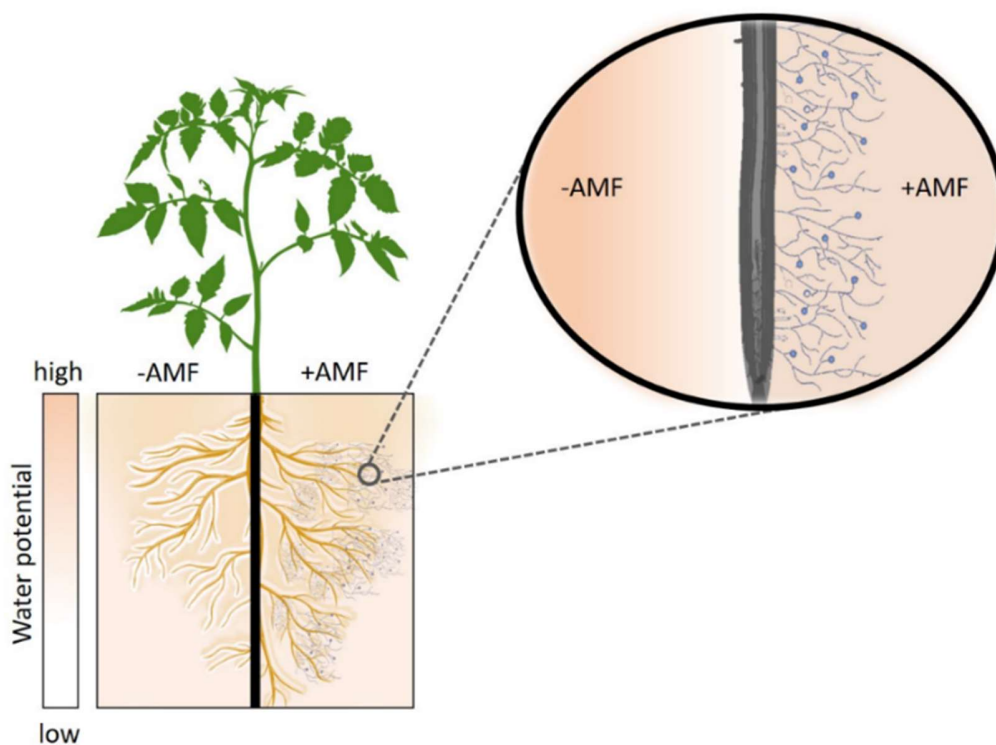

Figure 6.1 *Hypothetical role of Arbuscular Mycorrhiza Fungi (AMF) in enhancing plant water status and soil–plant hydraulic conductance. During soil drying, AMF increase the root-soil contact and extend the effective root radius hereby reducing the water fluxes at the root-soil interface and softening the drop in matric potential across the rhizosphere. The follow-up hypothesis is that AMF enhance soil–plant hydraulic conductance and plant water status during soil drying. Plants without AMF symbiosis (-AMF) require larger gradients in matric potential around their roots to sustain similar transpiration rates.*

6.3 MATERIALS AND METHODS

6.3.1 Plant preparation

We used two tomato genotypes (*Solanum lycopersicum* L.): a mutant with highly reduced AMF symbiosis (RMC) and its wild-type counterpart (WT) (Barker *et al.*, 1998). Growth was shown to be very similar in both genotypes, suggesting no pleiotropic effects of the mutation (Cavagnaro *et al.*, 2004). Seeds were sterilized in 30 % H_2O_2 for 90 seconds and thereafter washed and germinated on Petri dishes. The seeds were then planted in PVC columns of 30 cm in height and 9 cm in diameter. The columns had small five holes on the side, which were used for soil water content measurements during the experiment. The columns were filled with sandy soil through a 1-mm sieve. The hydraulic properties and fertilization of the soil are reported in Vetterlein *et al.* (2021) and in supplementary information (Figure S1). To potentially upsurge AMF colonization of the WT, the soil was inoculated with commercial *Rhizophagus irregularis* spores (BIOFA AG, Münstingen, Germany) in a ratio of 50 spore kg^{-1}.

6.3.2 Growth conditions

Twenty plants (10 per genotype) were placed in a climate-controlled chamber with a day/night temperature of 29/19 °C, a day/night relative humidity of 51/79 %, 14 hours of photoperiod, and light intensity of 1000 $\mu mol\ m^{-2}\ s^{-1}$. Plants were randomized inside the chamber. The soil surface was covered with polyolefin to prevent evaporation. We measured shoot fresh weight at the end of the experiment.

6.3.3 Transpiration rate

Plants were placed onto wireless balances that automatically recorded the changes in weight every 10 minutes. Transpiration rate was obtained gravimetrically by calculating the difference in weight over time. We extracted the transpiration rate for predawn (no light and low VPD) and midday. Plants were irrigated daily until the start of measurements.

6.3.4 Leaf water potential measurements

After withholding irrigation, leaf water potential was measured on daily basis at midday. A leaflet was covered with a plastic bag and lined with aluminum foil for at least 20 minutes before measurement. Covered leaves were cut and placed inside a Scholander-type pressure chamber (MODEL 3115, Soil Moisture Equipment Corp, Santa Barbara, CA, USA) to obtain stem water potential, which was used as a proxy for leaf water potential (One leaflet was measured per plant).

6.3.5 Soil dryness assessment

Soil water content (θ) was measured daily using time-domain refractometer (TDR) that encompasses two rods (spacing: 0.5 cm, length: 6 cm) connected to a data logger (E-Test, Lublin, Poland). Soil water potential was computed from the soil water content using the soil water retention curve (Supplementary Figure S1).

6.3.6 Soil–plant hydraulic conductance

During soil drying, soil–plant hydraulic conductances of RMC and WT were obtained using eq. 1 as follow:

$$Ksp = {E}/{\Delta\psi} \qquad (1)$$

where K_{sp} is soil–plant hydraulic conductance (cm^3 s^{-1} MPa^{-1}), E is transpiration rate (cm^3 s^{-1}), and $\Delta\psi$ is the difference between absolute values of leaf and soil water potentials (MPa).

6.3.7 AMF abundance assessment

Roots were collected at the end of the experiments and stored in 60 % ethanol. Root samples of both genotypes were washed with distilled water, cleared with 5 % KOH and stained in 5 % ink-vinegar solution to visualize AMF colonization in roots (after Vierheilig *et al.* (1998)). The percentage of colonized root length was determined by recording 150 root-intersects per sample using the light microscopy (Olympus BX40) and the attached digital camera (Olympus SC50).

6.3.8 Statistical analysis

Analysis of variance (ANOVA) was used to identify significant differences in transpiration rates, leaf water potential and soil plant hydraulic conductance of WT and RMC. T-test was applied to evaluate the differences in root colonization between the WT and RMC mutant. MATLAB (R2019) was used to perform the statistical analysis.

6.4 RESULTS AND DISCUSSION

We investigated the impact of AMF on plant water status and soil–plant hydraulic conductance in two tomato genotypes, reduced mycorrhiza colonization (RMC) and its wild type (WT) counterpart. Plant biomass of both genotypes were similar (Figure S2). Shoot fresh weight was 30.2 ±8.2 g and 28.4 ±7.9 g for the WT and RMC, respectively (Figure S2). The root colonization of the WT was four times higher than RMC ($p\text{-value} < 0.05$; Figure 6.2). This finding is consistent with results of Zhou *et al*. (2020), who assessed AMF root colonization in same tomato genotypes and observed significantly higher AMF abundance in roots of WT compared to RMC.
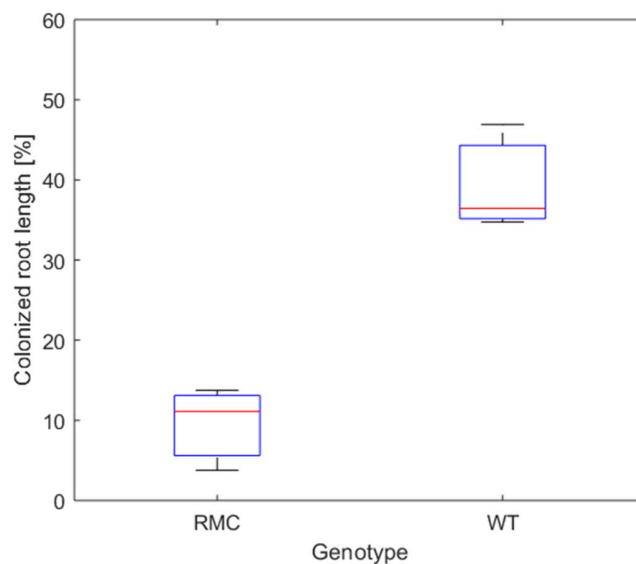

Figure 6.2 *AMF abundance assessment in roots of reduced mycorrhiza colonization (RMC) and wild type counterpart (WT). AMF root colonization was four times higher in WT compare to RMC (p-value < 0.05).*

Leaf water potential of the WT plants did not drop below -0.8 MPa six days after withholding irrigation, while leaf water potential of the RMC dropped below -1.0 MPa already after four days (*p-value* < 0.01; Figure 6.3; Supplementary Table S1). These results are in line with previous findings in maize, soybean and barley (Subramanian *et al.*, 1997; Porcel, 2004; Khalvati *et al.*, 2005). The authors showed that, under water deficit, plants with AMF colonization exhibited higher (less negative) leaf water potential compared to plants without AMF.
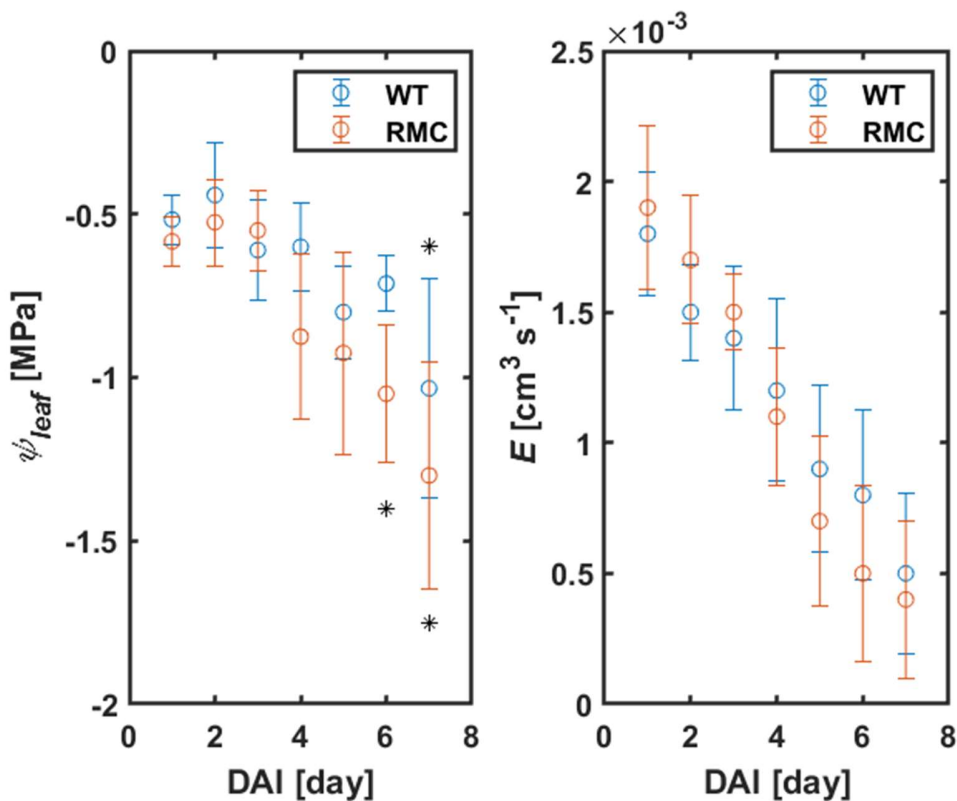

Figure 6.3 *Leaf water potential (ψ_{leaf}) and transpiration rate (E) of reduced mycorrhiza colonization (RMC) and wild type (WT) tomato during soil drying. ψ_{leaf} declined markedly in the absence of AMF, which nicely support our initial hypothesis. Asterisks denote s significance decline of ψ_{leaf} (p-value < 0.01), on top for WT and bottom for RMC. DAI: day after last irrigation. n = 10.*

Transpiration declined in both treatments as a consequence of water deficit (Figure 6.3). During soil drying, we observed, surprisingly, no differences in transpiration rate between the two genotypes (*p-value* = 0.5, Supplementary Table S2). These results are in line with the findings of Chitarra *et al.* (2016), who reported similar stomatal conductance of tomato

inoculated with different AMF species and the control (see Figure 1b in Chitarra *et al.* (2016)). Despite the absence of difference in transpiration rate, the authors compared the water use efficiency and demonstrated that AMF improved tomato performance under water deficit (Chitarra *et al.*, 2016). Similar transpiration rate was also observed in inoculated and not inoculated common bean (Aroca *et al.*, 2007). On the other hand, Bitterlich *et al.* (2018b) showed that, in tomato, AMF facilitate higher transpiration in dry soil. Similarly, Hallett *et al.* (2009) used the same genotypes and reported a significant increase in transpiration of the wild-type compared to RMC mutant. These apparently contradicting findings on the impact of AMF on transpiration rate clearly suggest that the role of AMF on transpiration (and stomatal conductance) is soil, species, and environment specific. Hence, the impact of AMF on transpiration on some of these studies might have been masked out as a result of species x environment interactions, which is well known to impact transpiration (Vadez *et al.*, 2013, 2021). Indeed, an improved performance of AMF treatment was shown in field experiments compare to greenhouse and climate-controlled experiments (where normally plants are grown in pots) (Poorter *et al.*, 2012; Augé *et al.*, 2015). The fact that the two genotypes exhibited no significant difference in transpiration in the present study could be explained by the limited soil volume. Hence, plants and AMF had to share a limited amount of water (and nutrients) within the pot (Chitarra *et al.*, 2016). Moreover, this explanation can potentially justify the drop in leaf water potential in both genotypes on the seventh day after withholding irrigation (Figure 6.3).

In previous studies, simultaneous measurements of transpiration rate and leaf water potential with high temporal resolution revealed that leaf water potential drops rapidly when a critical transpiration rate is reached at a given soil water potential (Carminati *et al.*, 2017; Abdalla *et al.*, 2021; Cai *et al.*, 2021). In other words, at a specific transpiration rate, leaf water potential can vary based on below-ground hydraulic conductance (see Cai et al. (2021)). In this study, we observed a decoupling in the relation between transpiration and leaf water potential (Figure 6.3). We explain this by the fact that RMC plants require larger gradients in soil water potential at the root-soil interface to sustaining a similar transpiration rate to the WT. The underlying mechanisms is that AMF extends the root surface active in water uptake, which reduces the flow velocity and attenuate the drop in matric potential at the root surface (see Figure 6.1). Hence, RMC plants exhibited more negative leaf water potential to sustain a similar

transpiration rate as in WT. This would explain why RMC plants displayed more negative leaf water potential while maintaining similar transpiration rate as WT plants. These results demonstrate that the relation between transpiration rate and leaf water potential is not unique and depends on below-ground hydraulics. Moreover, our data show that AMF clearly affect this relation. More work would be needed to test the impact of AMF on this relation among diverse plant species, contrasting soil types and climatic conditions.

Another possible explanation for similar transpiration rate is that AMF colonization might influence the stomatal density. Chitarra *et al*. (2016) demonstrated that inoculation with *Rizuphagus interaradices* induced two times stomatal density compared to un-inoculated tomato plants or inoculated with *Funneliformis mosseae*. However, a different AMF species was used in this study, namely *Rhizophagus irregularis*, and its influences on stomatal density in tomato is yet to be explored. Nevertheless, our data on leaf water potential suggest that AMF could contribute positively, allowing tomato plants to mitigate water stress conditions.

During soil drying, the relation between transpiration and leaf water potential was affected by AMF colonization (Figure 6.4). In wet conditions, i.e., day one, both genotypes showed high transpiration and leaf water potential (Figure 6.4). As soil progressively dried, RMC showed relatively lower transpiration and more negative leaf water potential than the WT (Figure 6.4). Soil–plant hydraulic conductance (*Ksp*) was obtained from the relation between transpiration rate and leaf water potential at a given soil water potential (Figure 6.5). Figure 6.5 shows that, during soil drying, WT plants exhibited a higher *Ksp* compared to RMC (Figure 6.5; *p-value* = 0.06; supplementary table S3). Note that *Ksp* is highly dependent on both transpiration rate and leaf water potential (see equation 1). The marginal difference in *Ksp* is a reflection of the similar transpiration rate and the significantly different leaf water potential between the two genotypes. This finding supports our hypothesis that AMF maintain soil-root hydraulic conductance. Further, *Ksp* of RMC plants declined at less negative soil water potential compare to WT (Figure 6.5). The absence of AMF in the reduced mycorrhiza colonization (RMC) plants entailed a severe reduction in leaf water potential as soil water potential declined, possibly due to loss of contact between root and soil (Carminati *et al.*, 2009, 2013). On the other hand, AMF presence in the wild type (WT) facilitated higher leaf water potential despite declining soil water potential (Figure 6.3). AMF could play a central role in sustaining the hydraulic

continuity between root and soil, as it not only improves the unsaturated hydraulic conductivity (Bitterlich *et al.*, 2018a; Pauwels *et al.*, 2020), but also avoids excessive drop of soil water potential around roots.
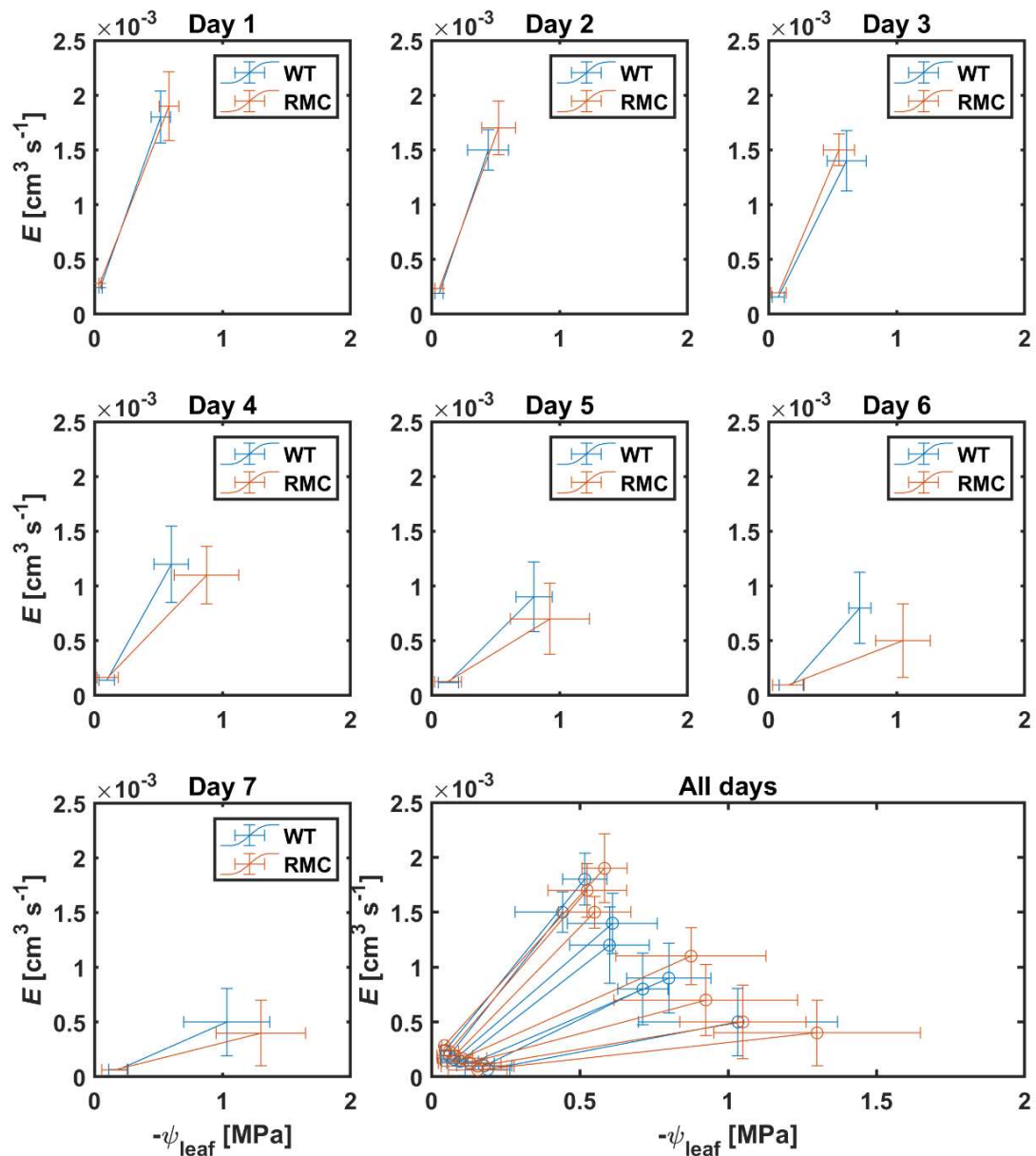

Figure 6.4 *Relation between transpiration rate (E) and leaf water potential (ψ_{leaf}) during soil drying. Subplots show the relation on daily basis after last irrigation. As soil progressively dried, the reduced mycorrhiza colonization (RMC) plants showed lower E and more negative ψ_{leaf} on the same day compare to wild type (WT). n = 10.*
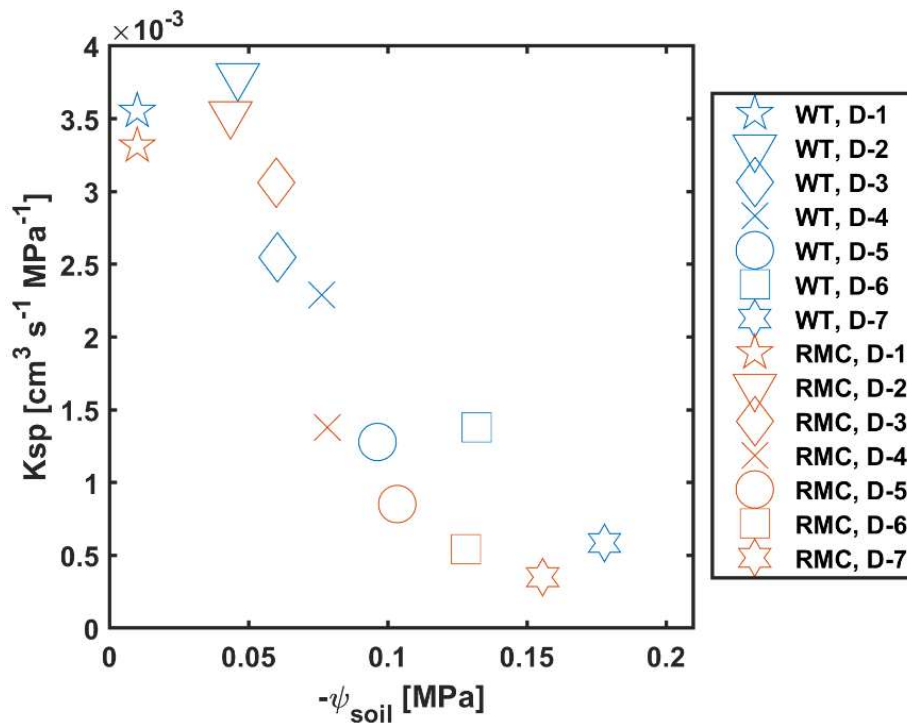
Figure 6.5 *Soil–plant hydraulic conductance (Ksp) decreases as soil water potential (ψ_{soil}) declines. Plants with mycorrhiza symbiosis (WT) show higher Ksp during soil drying (similar symbols, diverse colors) compare to reduced mycorrhiza colonization mutants (RMC). D: day after last irrigation. n= 10.*

Taken together, we have demonstrated the direct influence of AMF on soil–plant hydraulic conductance and plant water status during soil drying. WT plants exhibited higher soil–plant hydraulic conductance and leaf water potential compared to RMC plants during soil drying. We conclude that AMF extended the effective root radius hereby reducing the water fluxes at the root-soil interface and softening the drop in matric potential across the rhizosphere. This would result in an enhanced soil–plant hydraulic conductance and plant water status in drying soil. Further research is needed to directly measure the effects of AMF on water fluxes under contrasting soil textures and nutrient availabilities. The latter could be achieved using the combination of isotopes and neutron imaging (Ahmed *et al.*, 2016, 2018b). Our data suggest that AMF could play an essential role in achieving sustainable agricultural production with greater importance in regions faced by water scarcity conditions worldwide.

Author contributions:

MA and MAA designed the study. MA conducted the experiments and analyzed the data. MA and MAA wrote the manuscript.

6.5 REFERENCES

Abdalla, M., Carminati, A., Cai, G., Javaux, M., and Ahmed, M. A. (2021). Stomatal closure of tomato under drought is driven by an increase in soil–root hydraulic resistance. *Plant, Cell & Environment* 44, 425–431. doi:https://doi.org/10.1111/pce.13939.

Ahmed, M. A., Kroener, E., Holz, M., Zarebanadkouki, M., and Carminati, A. (2014). Mucilage exudation facilitates root water uptake in dry soils. *Functional Plant Biol.* 41, 1129. doi:10.1071/FP13330.

Ahmed, M. A., Passioura, J., and Carminati, A. (2018a). Hydraulic processes in roots and the rhizosphere pertinent to increasing yield of water-limited grain crops: a critical review. *J Exp Bot* 69, 3255–3265. doi:10.1093/jxb/ery183.

Ahmed, M. A., Zarebanadkouki, M., Kaestner, A., and Carminati, A. (2016). Measurements of water uptake of maize roots: the key function of lateral roots. *Plant Soil* 398, 59–77. doi:10.1007/s11104-015-2639-6.

Ahmed, M. A., Zarebanadkouki, M., Meunier, F., Javaux, M., Kaestner, A., and Carminati, A. (2018b). Root type matters: measurement of water uptake by seminal, crown, and lateral roots in maize. *Journal of Experimental Botany* 69, 1199–1206. doi:10.1093/jxb/erx439.

Aroca, R., Porcel, R., and Ruiz-Lozano, J. M. (2007). How does arbuscular mycorrhizal symbiosis regulate root hydraulic properties and plasma membrane aquaporins in Phaseolus vulgaris under drought, cold or salinity stresses? *New Phytologist* 173, 808–816. doi:https://doi.org/10.1111/j.1469-8137.2006.01961.x.

Augé, R. M. (2001). Water relations, drought and vesicular-arbuscular mycorrhizal symbiosis. *Mycorrhiza* 11, 3–42. doi:10.1007/s005720100097.

Augé, R. M., Toler, H. D., and Saxton, A. M. (2015). Arbuscular mycorrhizal symbiosis alters stomatal conductance of host plants more under drought than under amply watered conditions: a meta-analysis. *Mycorrhiza* 25, 13–24. doi:10.1007/s00572-014-0585-4.

Barker, S. J., Stummer, B., Gao, L., Dispain, I., O'Connor, P. J., and Smith, S. E. (1998). A mutant in Lycopersicon esculentum Mill. with highly reduced VA mycorrhizal colonization: isolation and preliminary characterisation. *The Plant Journal* 15, 791–797. doi:https://doi.org/10.1046/j.1365-313X.1998.00252.x.

Bitterlich, M., Franken, P., and Graefe, J. (2018a). Arbuscular Mycorrhiza Improves Substrate Hydraulic Conductivity in the Plant Available Moisture Range Under Root Growth Exclusion. *Front. Plant Sci.* 9. doi:10.3389/fpls.2018.00301.

Bitterlich, M., Sandmann, M., and Graefe, J. (2018b). Arbuscular Mycorrhiza Alleviates Restrictions to Substrate Water Flow and Delays Transpiration Limitation to Stronger Drought in Tomato. *Front. Plant Sci.* 9, 154. doi:10.3389/fpls.2018.00154.

Bourbia, I., Pritzkow, C., and Brodribb, T. J. (2021). Herb and conifer roots show similar high sensitivity to water deficit. *Plant Physiology*. doi:10.1093/plphys/kiab207.

Brodribb, T. J., Powers, J., Cochard, H., and Choat, B. (2020). Hanging by a thread? Forests and drought. *Science* 368, 261–266. doi:10.1126/science.aat7631.

Cai, G., Carminati, A., Abdalla, M., and Ahmed, M. A. (2021). Soil textures rather than root hairs dominate water uptake and soil-plant hydraulics under drought. *Plant Physiology*. doi:10.1093/plphys/kiab271.

Carminati, A., Ahmed, M. A., Zarebanadkouki, M., Cai, G., Lovric, G., and Javaux, M. (2020). Stomatal closure prevents the drop in soil water potential around roots. *New Phytologist* 226, 1541–1543. doi:10.1111/nph.16451.

Carminati, A., and Javaux, M. (2020). Soil Rather Than Xylem Vulnerability Controls Stomatal Response to Drought. *Trends in Plant Science* 25, 868–880. doi:10.1016/j.tplants.2020.04.003.

Carminati, A., Passioura, J. B., Zarebanadkouki, M., Ahmed, M. A., Ryan, P. R., Watt, M., et al. (2017). Root hairs enable high transpiration rates in drying soils. *New Phytologist* 216, 771–781. doi:10.1111/nph.14715.

Carminati, A., Vetterlein, D., Koebernick, N., Blaser, S., Weller, U., and Vogel, H.-J. (2013). Do roots mind the gap? *Plant Soil* 367, 651–661. doi:10.1007/s11104-012-1496-9.

Carminati, A., Vetterlein, D., Weller, U., Vogel, H.-J., and Oswald, S. E. (2009). When Roots Lose Contact. *Vadose Zone Journal* 8, 805–809. doi:10.2136/vzj2008.0147.

Carminati, A., Zarebanadkouki, M., Kroener, E., Ahmed, M. A., and Holz, M. (2016). Biophysical rhizosphere processes affecting root water uptake. *Ann Bot* 118, 561–571. doi:10.1093/aob/mcw113.

Cavagnaro, T. R., Smith, F. A., Hay, G., Carne-Cavagnaro, V. L., and Smith, S. E. (2004). Inoculum type does not affect overall resistance of an arbuscular mycorrhiza-defective tomato mutant to colonisation but inoculation does change competitive interactions with wild-type tomato. *New Phytologist* 161, 485–494. doi:https://doi.org/10.1111/j.1469-8137.2004.00967.x.

Chitarra, W., Pagliarani, C., Maserti, B., Lumini, E., Siciliano, I., Cascone, P., et al. (2016). Insights on the Impact of Arbuscular Mycorrhizal Symbiosis on Tomato Tolerance to Water Stress. *Plant Physiology* 171, 1009–1023. doi:10.1104/pp.16.00307.

Draye, X., Kim, Y., Lobet, G., and Javaux, M. (2010). Model-assisted integration of physiological and environmental constraints affecting the dynamic and spatial patterns of root water uptake from soils. *Journal of Experimental Botany* 61, 2145–2155. doi:10.1093/jxb/erq077.

Hallett, P. D., Feeney, D. S., Bengough, A. G., Rillig, M. C., Scrimgeour, C. M., and Young, I. M. (2009). Disentangling the impact of AM fungi versus roots on soil structure and water transport. *Plant Soil* 314, 183–196. doi:10.1007/s11104-008-9717-y.

Hayat, F., Ahmed, M. A., Zarebanadkouki, M., Javaux, M., Cai, G., and Carminati, A. (2020). Transpiration Reduction in Maize (Zea mays L) in Response to Soil Drying. *Front. Plant Sci.* 10. doi:10.3389/fpls.2019.01695.

Khalvati, M. A., Hu, Y., Mozafar, A., and Schmidhalter, U. (2005). Quantification of Water Uptake by Arbuscular Mycorrhizal Hyphae and its Significance for Leaf Growth, Water Relations, and Gas Exchange of Barley Subjected to Drought Stress. *Plant Biology* 7, 706–712. doi:https://doi.org/10.1055/s-2005-872893.

168

Liu, L., Gudmundsson, L., Hauser, M., Qin, D., Li, S., and Seneviratne, S. I. (2020). Soil moisture dominates dryness stress on ecosystem production globally. *Nature Communications* 11, 4892. doi:10.1038/s41467-020-18631-1.

Madadgar, S., AghaKouchak, A., Farahmand, A., and Davis, S. J. (2017). Probabilistic estimates of drought impacts on agricultural production. *Geophysical Research Letters* 44, 7799–7807. doi:https://doi.org/10.1002/2017GL073606.

Marin, M., Feeney, D. S., Brown, L. K., Naveed, M., Ruiz, S., Koebernick, N., et al. (2020). Significance of root hairs for plant performance under contrasting field conditions and water deficit. *Annals of Botany*. doi:10.1093/aob/mcaa181.

Ouledali, S., Ennajeh, M., Zrig, A., Gianinazzi, S., and Khemira, H. (2018). Estimating the contribution of arbuscular mycorrhizal fungi to drought tolerance of potted olive trees (Olea europaea). *Acta Physiol Plant* 40, 81. doi:10.1007/s11738-018-2656-1.

Passioura, J. B. (1980). The Transport of Water from Soil to Shoot in Wheat Seedlings. *J Exp Bot* 31, 333–345. doi:10.1093/jxb/31.1.333.

Pauwels, R., Jansa, J., Püschel, D., Müller, A., Graefe, J., Kolb, S., et al. (2020). Root growth and presence of Rhizophagus irregularis distinctly alter substrate hydraulic properties in a model system with Medicago truncatula. *Plant Soil* 457, 131–151. doi:10.1007/s11104-020-04723-w.

Poorter, H., Bühler, J., Dusschoten, D. van, Climent, J., Postma, J. A., Poorter, H., et al. (2012). Pot size matters: a meta-analysis of the effects of rooting volume on plant growth. *Functional Plant Biol.* 39, 839–850. doi:10.1071/FP12049.

Porcel, R. (2004). Arbuscular mycorrhizal influence on leaf water potential, solute accumulation, and oxidative stress in soybean plants subjected to drought stress. *Journal of Experimental Botany* 55, 1743–1750. doi:10.1093/jxb/erh188.

Quiroga, G., Erice, G., Ding, L., Chaumont, F., Aroca, R., and Ruiz-Lozano, J. M. (2019). The arbuscular mycorrhizal symbiosis regulates aquaporins activity and improves root cell water permeability in maize plants subjected to water stress. *Plant Cell Environ* 42, 2274–2290. doi:10.1111/pce.13551.

Rodriguez-Dominguez, C. M., and Brodribb, T. J. (2020). Declining root water transport drives stomatal closure in olive under moderate water stress. *New Phytologist* 225, 126–134. doi:10.1111/nph.16177.

Sperry, J. S., and Love, D. M. (2015). What plant hydraulics can tell us about responses to climate-change droughts. *New Phytologist* 207, 14–27. doi:10.1111/nph.13354.

Subramanian, K. S., Charest, C., Dwyer, L. M., and Hamilton, R. I. (1997). Effects of arbuscular mycorrhizae on leaf water potential, sugar content, and P content during drought and recovery of maize. 75, 10.

Trivedi, P., Leach, J. E., Tringe, S. G., Sa, T., and Singh, B. K. (2020). Plant–microbiome interactions: from community assembly to plant health. *Nature Reviews Microbiology* 18, 607–621. doi:10.1038/s41579-020-0412-1.

Vadez, V., Choudhary, S., Kholová, J., Hash, C. T., Srivastava, R., Kumar, A. A., et al. (2021). Transpiration efficiency: insights from comparisons of C4 cereal species. *Journal of Experimental Botany* 72, 5221–5234. doi:10.1093/jxb/erab251.

Vadez, V., Kholova, J., Zaman-Allah, M., and Belko, N. (2013). Water: the most important 'molecular' component of water stress tolerance research. *Functional Plant Biol.* 40, 1310–1322. doi:10.1071/FP13149.

Vetterlein, D., Lippold, E., Schreiter, S., Phalempin, M., Fahrenkampf, T., Hochholdinger, F., et al. (2021). Experimental platforms for the investigation of spatiotemporal patterns in the rhizosphere—Laboratory and field scale. *Journal of Plant Nutrition and Soil Science* 184, 35–50. doi:https://doi.org/10.1002/jpln.202000079.

Vierheilig, H., Coughlan, A. P., Wyss, U., and Piché, Y. (1998). Ink and Vinegar, a Simple Staining Technique for Arbuscular-Mycorrhizal Fungi. *Appl. Environ. Microbiol.* 64, 5004–5007. doi:10.1128/AEM.64.12.5004-5007.1998.

Zhou, J., Zang, H., Loeppmann, S., Gube, M., Kuzyakov, Y., and Pausch, J. (2020). Arbuscular mycorrhiza enhances rhizodeposition and reduces the rhizosphere priming effect on the decomposition of soil organic matter. *Soil Biology and Biochemistry* 140, 107641. doi:10.1016/j.soilbio.2019.107641.

6.6 Supplementary information

Table S1. Analysis of variance to identify the significant difference in leaf water potential between different treatments.

Source	d.f. ¶	Sum Sq.	Mean Sq.	F	Prob>F
AMF	1	0.38514	0.38413	9.46	0.0033
DAI	6	3.18522	0.53087	13.07	<<0.0001
AMF * DAI	6	0.26388	0.04398	1.08	0.3848
Error	52	5.93955	0.04061		

¶ **d.f.**: degree of freedom. **Sum. Sq**: Sum of squares, **Mean Sq**: Mean Sum of Squares, **F**: F-statistic value. **DAI**: day after irrigation.

Table S2. Analysis of variance to identify the significant difference in transpiration rate between different treatments.

Source	d.f. ¶	Sum Sq.	Mean Sq.	F	Prob>F
AMF	1	3.23e-8	3.23e-8	0.39	0.5
DAI	6	1.58e-5	2.65e-6	32.1	<<0.0001
AMF * DAI	6	4.45e-7	7.42e-8	0.9	0.5016
Error	56	4.62e-6	8.24e-8		

¶ **d.f.**: degree of freedom. **Sum. Sq**: Sum of squares, **Mean Sq**: Mean Sum of Squares, **F**: F-statistic value. **DAI**: day after irrigation.
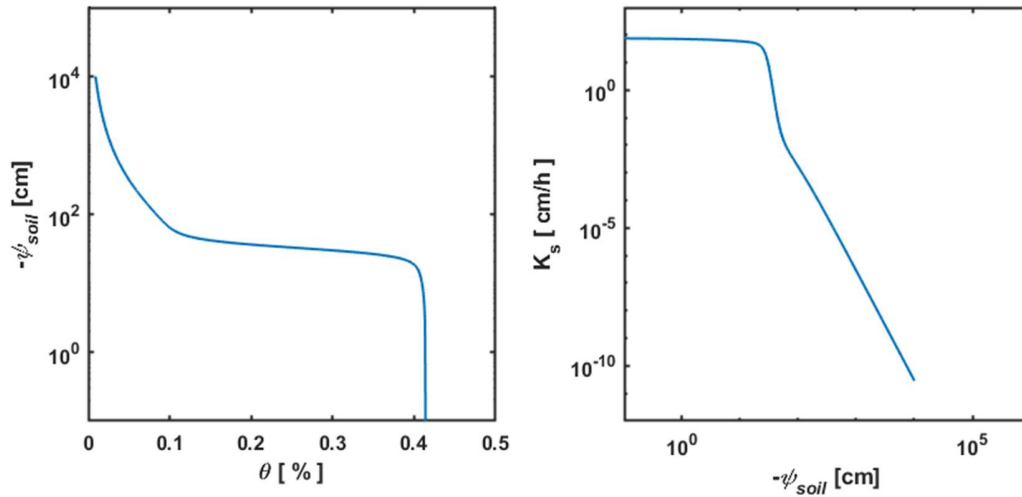
Figure S1: (**a**) Soil water retention curve, and (**b**) soil hydraulic conductivity curve of sandy soil used in this experiment.
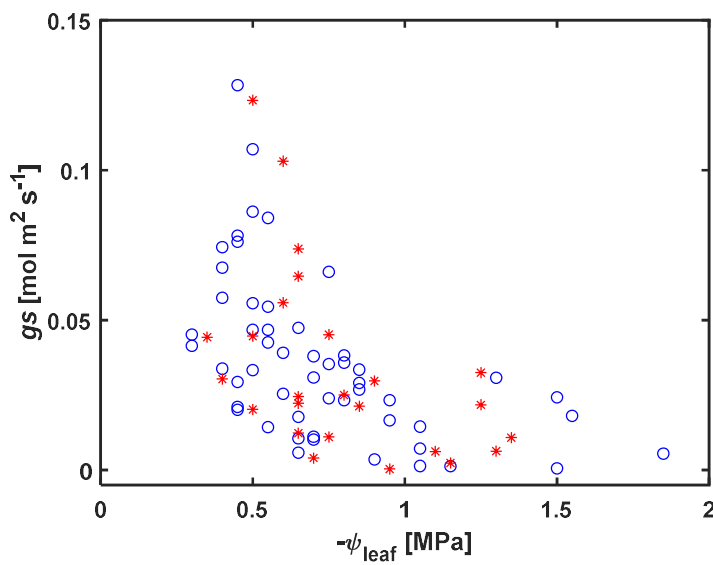

Figure S2: Relation between stomatal conductance (*gs*) and leaf water potential (ψ_{leaf}) during soil dying, of reduced mycorrhiza colonization (RMC; red asterisk) and wild type (WT; blue open symbol) tomato plants (*n* = 10).
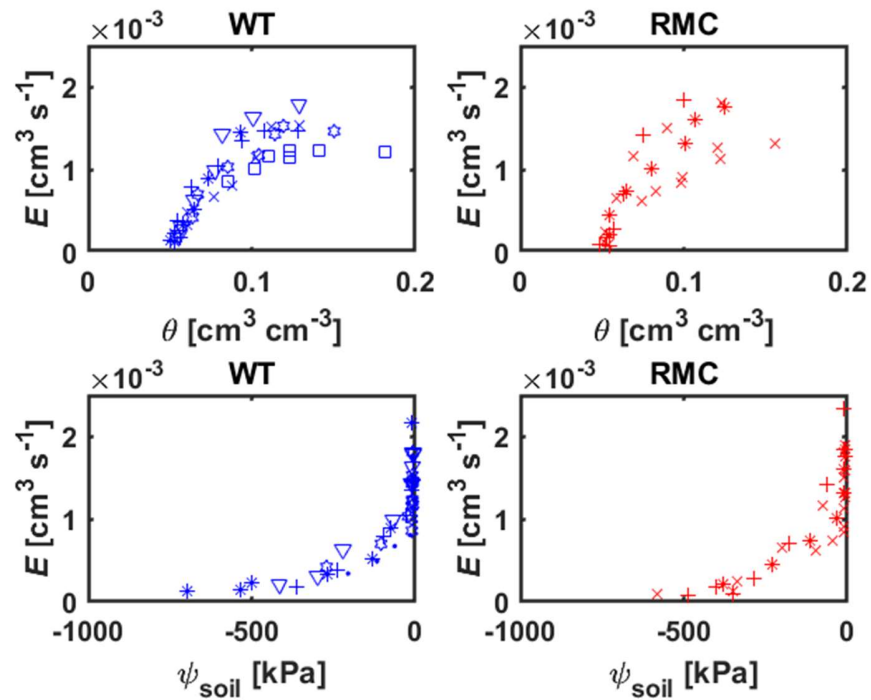
Figure S3: Transpiration rate (*E*) as function of soil water content (*θ*) and soil water potential (ψ_{soil}) in reduced mycorrhiza colonization (RMC; red) and wild type (WT; blue) plants. *E* declined gradually as *θ* decreased, while it cannot be sustained as soon as ψ_{soil} starts to decrease. *n* = 10. Different symbols for individuals.

(Eidesstattliche) Versicherungen und Erklärungen

Hiermit versichere ich eidesstattlich, dass ich die Arbeit selbstständig verfasst und keine anderen als die von mir angegebenen Quellen und Hilfsmittel benutzt habe (vgl. Art. 64 Abs. 1 Satz 6 BayHSchG). (§ 9 Satz 2 Nr. 3 PromO BayNAT).

Hiermit erkläre ich, dass ich die Dissertation nicht bereits zur Erlangung eines akademischen Grades eingereicht habe und dass ich nicht bereits diese oder eine gleichartige Doktorprüfung endgültig nicht bestanden habe. (§ 9 Satz 2 Nr. 3 PromO BayNAT).

Hiermit erkläre ich, dass ich Hilfe von gewerblichen Promotionsberatern bzw. -vermittlern oder ähnlichen Dienstleistern weder bisher in Anspruch genommen habe noch künftig in Anspruch nehmen werde. (§ 9 Satz 2 Nr. 4 PromO BayNAT)

Hiermit erkläre ich mein Einverständnis, dass die elektronische Fassung meiner Dissertation unter Wahrung meiner Urheberrechte und des Datenschutzes einer gesonderten Überprüfung unterzogen werden kann. (§ 9 Satz 2 Nr. 7 PromO BayNAT).

Hiermit erkläre ich mein Einverständnis, dass bei Verdacht wissenschaftlichen Fehlverhaltens Ermittlungen durch universitätsinterne Organe der wissenschaftlichen Selbstkontrolle stattfinden können. (§ 9 Satz 2 Nr. 8 PromO BayNAT).

....

Ort, Datum, Unterschrift